Republic of Iraq

Ministry of Higher Education and

Scientific Research

University of Babylon

Faculty of Materials Engineering

Department of Metallurgical Engineering

The Effect of Nickel Additions on the Flux of Submerged Arc AISI 5147 Steel Welds

A Dissertation

Submitted to the Council of the Faculty of Materials Engineering/University of Babylon in Partial Fulfillment of the Requirements for the Master Degree in Materials Engineering/Metallurgical Engineering

by

Doaa Kamil Yousif Hammady

Supervised by

Assist. Prof. Abdul Sameea J. A. Z. Jilabi (Ph.D)

2021 A.D **1442 A.H**

بِسْمِ اللَّهِ الرَّحْمَٰنِ الرَّحِيمِ

﴿وَأَنزَلْنَا الْحَدِيدَ فِيهِ بَأْسٌ شَدِيدٌ وَمَنَافِعُ لِلنَّاسِ﴾

صدق الله العلي العظيم

(سورة الرعد اية 25)

Dedication

This dissertation is lovingly dedicated to

my homeland,

my family and

to every individual who inspired me, guide me and helped me in my endeavors.

☼ ☼ ☼ ☼ ☼

Acknowledgements

Foremost, I am profusely thankful to ALLAH for the blessings of age, mind and health He bestowed upon me and the determination and patience with which I challenged the difficulties I encountered during the completion of this research.

It is really a pleasure to express my deep sense of thanks and gratitude to my supervisor and guide, **Asst. Prof Dr. Abdul Sameea Jasim Abdul Zehra**. His sincerity and keen interest on me at every stage of my study, with all his great attitude to help his students had been mainly responsible for finishing my work. His constant scholarly advice, meticulous scrutiny and scientific approach have enabled me to a great extent to complete my dissertation.

The application of the welding process was carried out in the Heavy Engineering Equipment State Company-Baghdad, I thank extremely all the staff working there especially whom at the equipment and technology departments for their kind help and cooperation throughout my work period. Many thanks go to the staff in the warehouse department for providing me with the material I needed, despite the difficulties. I would like to express my gratitude to the staff at the milling workshop for preparing the samples. Thanks are also due to the machine operator, **Mr**. **Abbas Jasim Atiya** who has willingly helped me out with his abilities.

I am also thankful to the staff of my department, Metallurgical Engineering, Faculty of Materials Engineering, for their help whenever I needed.

Finally, I extend my thanks and appreciation to my family, parents, husband and all friends for their material and moral support throughout the study period, and my lovable boys, ABBAS and HUSSEIN who served as my inspiration to pursue this endeavor.

Supervisor Certificate

I certify that this dissertation entitled **"The Effect of Nickel Additions on Submerged Arc Low Alloy Steel Welds**" is prepared by **(Doaa Kamil Yousif Albhate)** under my supervision at the Department of Metallurgical Engineering/ Faculty of Materials Engineering/University of Babylon in partial fulfillment of the requirements for the Master Degree in Material's Engineering/Metallurgical Engineering.

Signature:

Name of Supervisor:

Assist. Prof. Dr. Abdul Sameea J. A. Z. Jilabi

Date: / / 2021

ABSTRACT

Low alloy steels are particularly used in the manufacture of several products such as storage tanks, oil and gas pipelines, industrial equipment and many agricultural and construction machinery parts that may experience service failure, and thus may require repair through welding processes. Submerged arc welding (SAW) is considered one of the most widely used processes for welding many engineering industries. SAW of low alloy steels is however associated with some defects; hot cracks are typically considered the most significant and dangerous defects. The weldability of steel is determined by its susceptibility to cracking, which can be prohibited by using certain welding procedures, which are often costly and difficult to use. SAW of AISI 5147 low alloy steel was implemented, firstly without nickel additives, followed by adding pure nickel powder to flux with different weight percentages (10, 20, 30, 40 and 50). The study mainly aims to investigate the influence of nickel content on the properties of submerged arc low alloy steel welds. It also aims to study the effect of nickel in decreasing hot cracks in these welds, and thus increasing the efficiency of the weld joints. Several examinations were carried out to evaluate the resulting welds, involve X-ray radiography, fractography, microscopy, energy dispersive spectrometry and mechanical tests. The results revealed that the tensile strength and weld joint efficiency reached (845 MPa) and (112 %) respectively when 20 wt. % of nickel powder was added to the flux, where the microstructure was a fine acicular ferrite. The maximum hardness across the welds was at the coarse grained heat affected zone, whereas the minimum hardness was observed in the inter-critical zone, where the pearlite was partially spheroidized. X-ray radiography and microscopy showed that the greater the wt.% of Ni powder added to the flux, the more inclusions and porosity defects. Fractography however showed that the fracture behavior changed from brittle to ductile, as the structure of the weld center generally appeared to be austenitic with a 50 wt.% of Ni powder added to the flux.

List of Tables

Table of Figures

Table of Abbreviations

SAW	Submerged Arc Welding
AWS	American Welding Society
DC	Direct Current
AC	Alternating Current
DCSP	Direct Current Straight Polarity
DCEP	Direct Current Electrode Positive
DCRP	Direct Current Reverse Polarity
DCEN	Direct Current Electrode Negative
CE	Carbon Equivalent
HAZ	Heat Affected Zone
CGHAZ	Coarse Grained Heat Affected Zone
RGHAZ	Refine Grained Heat Affected Zone
ICHAZ	Inter Critical Heat Affected Zone
SC-HAZ	Sub Critical Heat Affected Zone
Ms	Martensite starting
FZ	Fusion Zone
HSLA	High Strength Low Alloy Steel
OM	Optical Microscopy
SEM	Scanning Electron Microscopy
ANOVA	Analysis of Variance
ASTM	American Society for Testing and Materials
EDS	Energy Dispersive Spectrometer
AISI	American Iron and Steel Institute

Table of Contents

CHAPTER ONE:

INTRODUCTION

CHAPTER ONE: INTRODUCTION

1.1 General Review

Alloy steels have been produced for many reasons, one of the most significant of them is to avoid the limitations of using carbon steels. Obtaining a tensile strength more than (700N/mm^2) cannot be achieved when using carbon steels if ductility and toughness are also required. Carbon steels also exhibit poor corrosion resistance [1,2]. In general, alloy steels are stronger and own thermal and corrosion resistance more than carbon steels, in addition to other properties, such as machinability, hardenability and ductility. This is because alloying elements are added to steels in different amounts [3,4]. Alloy steels have a wide range of applications. The most common of them are rails, door beams, rocker panels, and bumpers [5].

This decade, low alloy steels entered promisingly in vehicle structural applications and then ended it as the preferred material. Mass reduction potential of these steels has been clearly demonstrated in the theoretical literature, experimental applications and industrial equipment [5].

Arc welding processes are generally the most common worldwide. submerged arc welding (SAW) is one of the most widely used [6].

Unfortunately, welding of low alloy steels by SAW is associated with several defects; porosity is the most common, whereas cracking, particularly hot cracks are considered the most significant and serious defects [7].

Hot cracks typically arise due to the existence of segregated constituents of relatively low solidification temperatures at the grain boundaries. These constituents have low ductility and also have low strength at elevated temperatures. A rupture along the grain boundaries will therefore occur under the effect of shrinkage stresses [8].

After literature survey, a lot of researches, which dealt with decreasing or controlling hot cracks in a variety of alloy welds and various controlling methods were found. Several researches dealt with the control of hot cracking in austenitic stainless steel welds. Moreover, some of the researches dealt with the influence of nickel content in decreasing hot cracks in SAW steel welds, but mainly of mild steel and austenitic stainless steels.

1.2 The Goals of this Work

1. The main aim of this study is to investigate the influence of nickel content on properties of submerged arc low alloy steel welds.
2. It also aims to study the effect of nickel in decreasing hot cracks in these welds.

1.3 View of the Current Work

The thesis consists of five chapters. The present chapter deals with a general introduction in addition to the objectives of this study.

Chapter two provides important details about the material being used as a parent metal (low alloy steels) and the reason behind using them, their applications, effects of alloying elements and the SAW process. The advantages and limitations of this process were explained, in addition to the accompanied defects, specifically hot cracks. A literature survey also given in this chapter. Chapter three precisely describes the experimental section, where low alloy steels were used as raw material. Pure nickel powder was also used. Manufacturing the samples and preparing them for physical and mechanical testing were described as well. In chapter four, the results of the experimental work on low alloy steel welds were analyzed and discussed. Lastly, chapter five

deals with the most significant conclusions in addition to the future recommendations for other researchers.

CHAPTER TWO:

THEORETICAL PART &

LITERATURE REVIEW

CHAPTER TWO: THEORETICAL PART AND LITERATURE REVIEW

2.1 Introduction

This chapter explains low alloy steels and their weldability, particularly by using the submerged arc welding (SAW) process; the principle work of this process in addition to wires and fluxes used with SAW of low alloy steels. Additional details about implemented heat treatments, the metallurgical impacts of the thermal cycle of the welds, and the defects accompanied with SAW of low alloy steels, particularly hot cracking will be dealt with. The influence of nickel content on hot cracks will also be explained. Literature survey for studies about the current work will be highlighted.

2.2 Low Alloy Steels

Alloy steels can be defined as steels that acquire their improved characteristics due to the existence of one or more specific elements or to considerable amounts of elements like manganese and silicon more than usually present in carbon steels [3].

Alloy steels have been developed to achieve the needs of the engineering industry so as to overcome the restrictions caused by using of carbon steels, where [1,2]:

1- It is difficult to get a tensile strength of more than 700 N/mm^2 while keeping reasonable ductility and toughness.

2- There is an exposure to the resultant risk of cracking while severe quenching by water necessary to achieve full hardening.

3- Plain carbon steels are susceptible to “mass effect”, which makes it difficult to harden large sections effectively.

4- Plain carbon steels are susceptible to corrosion and oxidation at high temperatures.

Alloy steels can be categorized to three parts: low, medium and high alloy steels [9]. The addition of alloying elements like nickel, chromium, and molybdenum to low alloy steels gives them superior properties relative to plain carbon steels. The most important function of alloying elements, for many low alloy steels, is to improve the hardenability so as to optimize the toughness and strength as a result of heat treatments. In some cases, yet, additives are used to decrease environmental degradation under particular conditions [3,4].

Low alloy steels are possibly categorized based on [10]:

1- The chemical composition of steels, such as Ni steels, Mo steels, Ni–Cr steels, Cr-Mo steels, and so on, based on the main additives present.
2- Heat treatments like annealed steels, normalized and tempered steels, quenched and tempered steels and so on.
3- The weldability.

Bridges, towers of power transmissions, industrial equipment, light poles, oil and gas pipelines, storage tanks, off-road and heavy-duty high way vehicles, passenger car components, farm and construction machinery, building beams and panels, mine and railroad cars, and lawn mowers, the automotive, aerospace, heavy equipment etc., are all considered applications of low alloy steels [11,12].

2.2.1 Alloying Elements

Alloying elements are commonly added to steels for several important purposes. Among them are [13,14]:

- Corrosion resistance
- Increasing hardenability
- Greater strength
- Grain size control
- Improving machinability
- Improving ductility
- Improving mechanical properties at both high and low temperatures

The most common alloying elements added to steels are as follows [10]:

1. Carbon: influences hardness, machinability, tensile strength and the melting point.
2. Manganese: noticeably contributes in the increase of hardness and strength. It also decreases both ductility and weldability when presents in high weight percentage with high content of carbon in steels.
3. Silicon: improves the resistance of oxidation and increases the strength of low alloy steels.
4. Nickel: increases toughness and impact resistance. A high percentage of it enhances corrosion resistance.
5. Chromium: is added to acquire deep hardenability with improved abrasion resistance. It also helps avoiding corrosion and oxidation.
6. Molybdenum: increases the hardenability of steels, makes them fine grained in addition to increasing creep and tensile strengths at elevated temperatures. It also decreases temper brittleness in Ni-Cr steels.

7. Vanadium: enhances fine grains in steels and raises strength while keeping ductility.
8. Tungsten: when added to steels, it gives higher hardness and strength at elevated temperatures, resists heat and enhances fine grains.
9. Cobalt: participates in getting red-hardness via hardening ferrite.
10. Copper: when (0.2-0.5%) added to steels, raises atmosphere corrosion resistance and plays a role as a strengthening factor.
11. Aluminum: causes a fine austenitic grain size and plays as a deoxidizer.
12. Sulphur: increases machinability but decreases ductility and weldability at the same time.
13. Boron: (0.001-0.003%) is a strong hardening factor.
14. Titanium: lowers martensitic hardness in Cr steels.

2.3 Welding of Low Alloy Steels

Low alloy steels can generally be welded by all common welding processes. The most common ones are [6]:

1. Oxy- acetylene Welding

The type of metal used as a filler rod depends on the desired mechanical properties. The filler rod made of high tensile steel will prove its effectiveness. There must be a match between the weld metal and the parent metal.

2. **Flux- Shielded Metal Arc Welding**
    - Electrodes made of mild steels work effectively with steels containing carbon content below 0.14%. Weld acquires tensile strength as high as 80,000 psi (5600 kg/cm^2) as a result of alloy picked-up from the parent steel.
    - Electrodes made of low alloy steels may be required where higher strength with better ductility is desirable.
    - It might be desirable to use core wires of the same composition of the parent steel where the resistance of corrosion is a factor.

3. **Submerged Arc Welding**

Both classes of low alloy steels (hot rolled and heat treated) are welded by using a method comparable to that used in welding of carbon steels.

4. **Thermite welding**

Low alloy steels can be readily thermite-welded. Metallic alloying elements are usually added to the thermite mixture to acquire a composition similar to that of the parent metal.

5. **Resistance Spot Welding**

Spot welding can be achieved adequately. Special heat treatments like preheating, grain refinement and tempering may be combined with the welding cycle for alloys having higher hardenability.

6. **Other welding processes include:**
    - Gas Metal Arc Welding
    - Resistance Seam Welding
    - Atomic Hydrogen Welding

2.4 Submerged Arc Welding of Low Alloy Steels

2.4.1 Submerged Arc Welding Process

Submerged arc welding (SAW) is a process that melts and joins metals by heating them with an electrical arc initiated between a consumable uncovered wire and the workpiece [15]. The arc, wire and weld pool are all hidden and invisible for being under a layer of granular material known as flux [16]. The uncovered wire continuously fed acts as a filler metal. No pressure is required to complete the welding process. This process is one of the most widely used processes for welding thick plates and pipes, pressure vessels [17]. This wide spread of application is due to the high productivity, good strength and good surface appearance of the weld. The SAW process is commercially suitable for welding low alloy steels [6].

2.4.1.1 Principle Work

Granular fluxes and uncovered wires are typically used in SAW process instead of coated electrodes. An arc forms between the wire and the workpiece, which is submerged under the flux, is the heat source required for welding. This process might be automatic or semi-automatic [18,19]. In semi-automatic welding, the welding head is manually moved along the joint, whereas in automatic welding, either the welding head is moved automatically along the fixed workpiece or the workpiece moves (or rotates) under the fixed welding head. Backing plates made of steel or copper may be used to control penetration and support larger amounts of molten metal accompanying the process [6]. Figure (2.1) shows the principle work of this process.

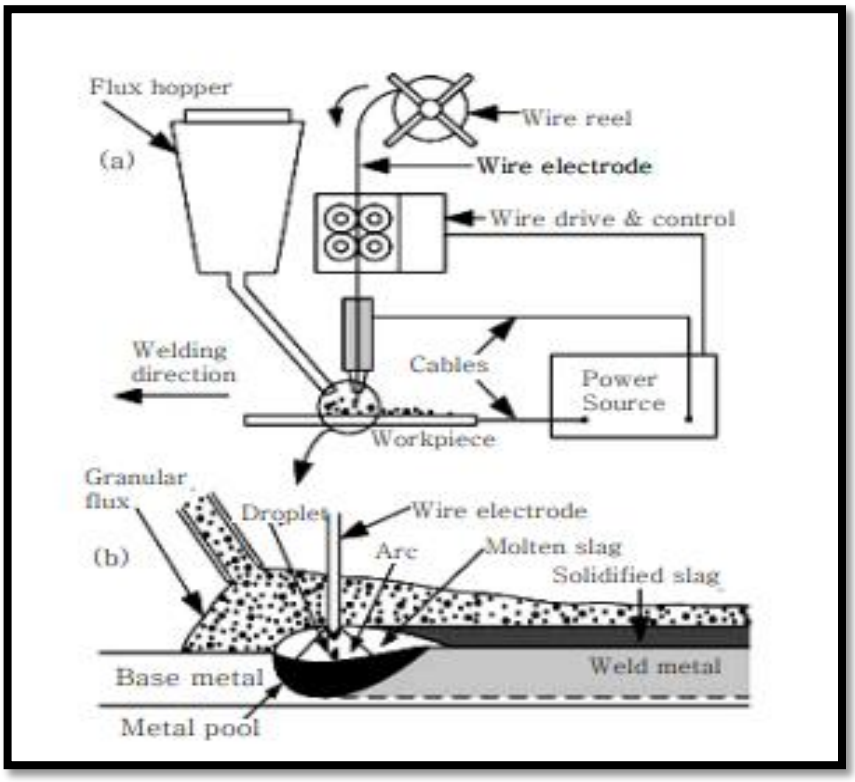

Figure (2.1): The principle work of SAW process [20].

2.4.1.2 Equipment

Equipment of SAW basically consists of [18]:

1. Welding Head, feeds the weld joint with the flux and the filler wire.

2. Flux Hoper, stores the flux and controls the its deposition rate on the joint.

3. Power Supply, supplies continuous or alternating current up to (1500 A) [21].

4. Flux, is selected depending on the type of the metal to be welded and the required mechanical properties.

5. Welding Wires, the chemical composition of the wire used depends also on the type of the metal to be welded. Alloying elements may be added to the weld joint by the welding wire depending on the mechanical properties required.

2.4.1.3 Polarity

There are two types of current used for welding: direct current (DC) and alternating current (AC). SAW process can be carried out using DC or AC [22]. When welding using direct current, the welding arc is relatively smooth and stable because the DC flows in one direction during the cycle of welding. The AC, however, collects the straight and reverse polarity (direction of the current flow) alternatively in regular cycles. These cycles are repeated periodically during welding, as the polarity frequents (100) times per one second in (50) cycles. These frequencies result in an extremely fast pulsating arc, causing roughness and less stability to some extent compared to the DC arc.

Polarity is a significant factor when welding with direct current. Choosing the kind of polarity depends on several significant factors: the type of flux used, the type of penetration desired and the type of metal being welded [8].

- **Straight Polarity:**

Direct current straight polarity (DCSP) is the direct current used with this polarity. In straight polarity, the current flows from the work piece, which is connected with the positive terminal of the power supply to the wire, which is negatively charged. Therefore, this polarity is also called direct current electrode negative (DCEN) [23]. Nearly, two-thirds of the total heat energy is concentrated on the wire. Therefore, in comparison with the case of utilizing the direct current reverse polarity (DCRP), higher melting rate and thus higher deposition rate of the wire are obtained. Consequently, the welding speed is higher, the shrinkage stresses resulted are less severe and hence the work piece is less prone to distortion. The penetration, for the same reason, will be shallow and narrower [20,24].

• Reverse Polarity:

With this polarity, the current flows from the wire, which is connected with the positive terminal of the power supply to the work piece, which is negatively charged. Therefore, this polarity is also called direct current electrode positive (DCEP) [23]. Nearly, two-thirds of the total heat energy is concentrated on the negative work piece. Therefore, the use of the DCRP results in a deeper penetration compared with the use of the DCSP or the AC for the same welding current value (Figure 2.2). The amount of the welding current is however considered the main determinant of the extent of penetration [5].

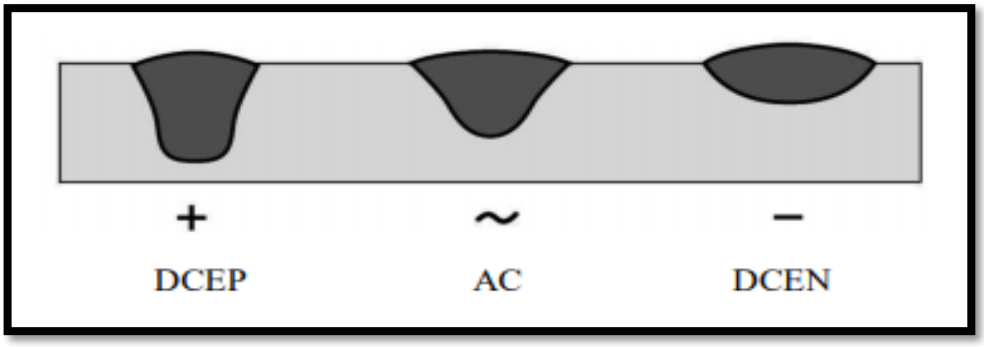

Figure (2.2): welding profile as a function of polarity [25].

2.4.1.4 Advantages & Limitations of SAW Process

Submerged arc welding process has several advantages, the most important of them are [8,26]:

1. The molten flux provides very suitable conditions to flow high welding current values. High thermal intensity can be generated and concentrated to weld thicker sections with deep penetration [27].
2. Higher welding speed can be used because of the high thermal concentration.

3. Due to the high thermal concentration and high welding speed, the distortion is much less.
4. High deposition rates can be obtained. Thick sheets can also be welded with a single pass and conventional equipment [28].
5. The welding process is carried out without spark, smoke or spatter [3].
6. A very clean and smooth weld appearance can be obtained.
7. The welding process can be used outdoors where a relatively high winds.
8. It is not necessary to make the edge preparation for the parent metal with a thickness of less than (12 mm).

Submerged arc welding process however has some limitations such as [8,29]:

1. The operator cannot adjust the welding progress precisely because the weld cannot be seen during the process. Therefore, attachments may be used such as guides, fixtures, etc. to ensure a proper welding of the joint.
2. This process requires the flux to be deposited in advance, which is sometimes not possible.
3. The SAW process can be used with the flat position only, and for a metal thickness of more than (4.8mm), as for the small thickness, the joint is likely to burn-off.
4. The edge preparation and fit-up of the joint have to be carried out precisely, otherwise, the flux may drop out through the gap, and the arc may burn-off the edges of the workpiece.

2.4.2 Flux Used with SAW of Low Alloy Steels

Flux plays a vital role in SAW process. It has several benefits, and the most important of them are [17]:

1. prevents the weld pool from atmospheric contamination.

2. controls mechanical properties and quality of the deposited weld.

3. increases the arc stability.

4. influences the weld metal physically, chemically and metallurgically. It physically influences the weld bead geometry, which in turn affects the load-carrying capacity of the weldment. Chemically, flux affects the weld metal chemistry, which further influences the mechanical properties of the weld metal.

2.4.3 Wires Used with SAW of Low Alloy Steels

The chemical composition of the wire used depends on the type of the metal to be welded. Alloying elements may be added to the weld joint via welding wire. Welding wires are generally covered with copper in order to prevent rust and to increase the electrical conductivity. The wire diameters used in SAW range from (1.6-6.4 mm) [6].

2.4.4 Classification of the Wires and Fluxes Used with the SAW of Low Alloy Steels

The classification below shows how to determine the type of wires and fluxes used with the low alloy steels according to American Welding Society (AWS) [30].

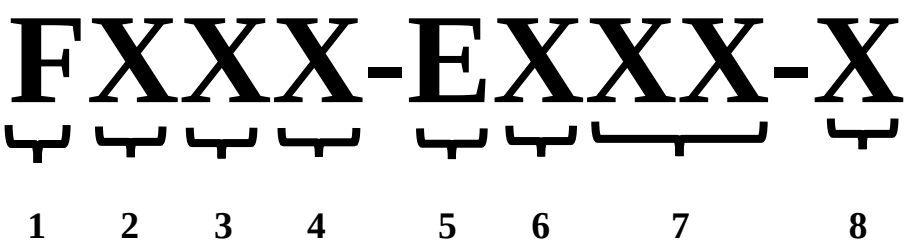

1. F: a letter refers to the submerged arc flux.
2. One (or sometimes two) numbers indicates the minimum tensile strength (in increments of 10 000 psi) of weld metal deposited with the flux. If they are (70) for example, this means that the minimum tensile strength of the weld metal is 70000 psi, and so on.
3. Designates the condition of heat treatment in which the tests were conducted: "A" is for as-welded and "P" for postweld heat treated.
4. Indicates the temperature in °F at or above which the impact strength of the weld metal referred to above meets or exceeds 20 ft.lbf.
5. E: a letter refers to the word of electrode (wire).
6. Chemical composition of the electrode:

   Ni = Nickel.

   M = carbon steel, medium Mn solid electrode.
7. Number (or letter if needed) that makes up a part of the electrode classification. For example: EM12K.

   12: the nominal carbon content is 0.12.

   K: the electrode is made from a killed steel [31].
8. Indicates the chemical composition of the weld metal resulted from the flux and the electrode. Two or more letters and/or digits are used.

   A = C-Mo weld metal.

Here is a brief overview of some of these wires and fluxes [30,32]:

EM12K: is a killed medium Mn-alloyed, Cu-coated steel wire for SAW of medium and high strength structural steels and low alloy steels; contains 0.12 C, 0.3 Si and 1.0 Mn.

EA2: is a Cu-coated, Mo-alloyed wire for SAW of non-alloy and low alloy steels with impact strength requirements higher than those obtainable with mild steel filler wires; contains 0.1 C, 0.1 Si, 1.0 Mn and 0.5 Mo.

EB3: is a low alloyed, non-coppered wire designed for SAW of creep resistant steel of the 2.25Cr1Mo type; contains 0.11 C, 0.2 Si, 0.7 Mn, 2.5 Cr &1.0 Mo.

ENi2: is a Cu-coated, low alloyed, 2%Ni electrode for SAW of low alloyed and low temperature steels (in the offshore industry application, for example); contains 0.1 C, 0.1 Si, 1.0 Mn and 2.5 Ni.

F8A4-EC-G: is designed for single and multi-pass butt welding of mild and medium tensile strength steels. It is typically used with pressure vessel manufacturing, shipbuilding applications with impact strength requirements down to -40°C.

F7P2-EA2-A2: is designed for the single wire, multi-run butt welding of mild, medium and high tensile steels with impact strength requirements down to -40/-60 °C. It can be used on DC.

F8P8-EB3-B3: is a high basic agglomerated all-mineral non-alloying flux designed primarily for the multi-pass welding of creep resistant steels in combination with low alloy Cr-Mo wires. The very low impurity level of the flux helps to produce an exceptionally clean weld metal, with high impact properties, even after step cooling treatment.

F7A5-EM12K: is a basic agglomerated, slightly Si and Mn alloying, specially designed for fillet welding and for single and multi-pass butt welding of mild, medium and high tensile steels. It can be used particularly for narrow gaps.

2.5 Weldability of Low Alloy Steels by SAW

The weldability of low alloy steels depends primarily on its hardenability, which in turn, depends largely on its chemical composition, mainly the carbon content. Other alloying elements such as manganese, molybdenum, chromium, vanadium, nickel and silicon also have effects on the hardenability of low alloy steels, but with a much less extent [33]. Thickness and weld pool design are also important factors when considering weldability. Alloying elements, along with carbon, are all generally expressed as a single value called carbon equivalent (CE) [34]. The higher the carbon equivalent, the higher the hardenability which is closely related to the weldability, the more difficult the steel is to weld and the steel becomes more prone to cracking [35]. Care and caution in addition to using special welding procedures should also be taken [36-37].

Low alloy steels can be welded by the SAW process, however, high hardness and brittleness may occur in the weld zone and the heat effected zone. The welding conditions should be low in hydrogen as well to obtain the best possible results when using this process [8].

In order to have a high toughness in the weld zone when welding these steels, the austenitic stainless steel wires are sometimes used, however, the heat affected zone (HAZ) might remain hard and brittle. Therefore, it is important to use the preheating and the postheating for avoiding the high hardness and brittleness of these zones [8].

The need for preheating or/and post heating can be determined approximately for each type of steels via calculating the carbon equivalent, which is typically defined by several formulas. The following formula is usually used in most ASME applications:

$$CE = C + (Mn+Si)/6 + (Cr + Mo + V)/5 + (Ni + Cu)/15 \ldots\ldots \text{Eq. (1)} \quad [35]$$

According to this formula, if the CE value is of 0.45 or less, steels can be welded without any preheating or postheating of the joint. The welding conditions should also be low in hydrogen. With higher CE values, steels may require either preheating or postheating treatment in order to relief stresses and hence to avoid weld cracking [35]. The CE is an approximate value since it is only related to the chemical composition of the steel, as other factors like section thickness and joint constraints, which have a higher or equal effect on the weldability, are not taken into consideration.

The cooling rate and thus the possibility of welding cracks can be reduced by some developments, which are carried out through the welding procedures. For example, a large V-shaped weld joint design with the utilize of a multi-pass welding process, in which the weld metal of the latest pass is deposited, surrounded by the weld metal of the previous passes from both sides. The heating of the subsequence pass will act as a tempering treatment to the HAZ resulting from the weld bead deposition of the pervious pass.

2.5.1 Preheating

Essentially, preheating is used to prevent cracks in the weld zone or in the HAZ. It slows down the cooling rate and thus leads to decrease the hardness of the HAZ. Residual stresses and distortion will also be reduced [29].

When welding low alloy steels, the preheating temperature should always be above that of the martensite formation, which is called Ms (martensite starting) in the S.S diagram. The reason behind this is to prevent the formation of the hard and brittle martensite, and thus avoiding or reducing associated cracking [5,38]. The preheating value depends on the carbon content and all other alloying elements, in addition to variables related to the weld joint design, particularly the thickness [39]. Preheating is the easiest and most effective way to prevent cracks caused by welding in cold weather (especially below the room temperature) [40].

The size of the weld bead affects the preheating value, where the cooling rate of small beads is greater than that of large beads. A larger bead size, which can be obtained by reducing the travel speed for instance, increases the heat input, and thus decreases the cooling rate. Consequently, martensite and hence hardness will be less in the HAZ [41]. The need for preheating is eliminated in some applications by controlling the weld bead size.

The need for preheating can also be reduced or sometimes eliminated by using the multi-pass welding. Multi-passes in specific applications can prevent cracking that may occur while using one welding pass without preheating. The previous welding pass acts as a preheating mean for the subsequent welding pass and each welding pass will act as a postheating for the previous passes. In multi-pass welding, if the preheating is required, the temperature between passes should be under control to be, at least, equal to the preheating temperature [5].

The preheating process is ideally implemented by furnaces, otherwise, the furnaces may not always be available, or the weldment might not be of a size or a shape that can be heated in the furnaces. In this case, a gas torch is typically used to preheat the joint through heating one side of the joint, and then

measuring the temperature of the opposite side to ensure that the joint has been heated to the desired temperature. Induction heating devices can also be used when welding pipes [41].

Preheating has however other benefits; it dries out moisture from the surfaces of the work piece being welded and burns any grease or oils [8].

2.5.2 Postheating

Tempering or stress relief heat treatment after welding of low alloy steels is desired, while it is necessary in some applications. As it is for preheating, the choice of stress relieving temperature is influenced by the thickness of the parent metal and the carbon content [42]. The restraint severity of the welded joint also determines the need for such treatment. This treatment is typically carried out for alloy steel welds through heating them (550-650 °C) for an hour for every (25.4 mm) of thickness (this is the shortest time for this treatment, and it should not exceed eight hours at all). The weld joint is preferred to be heated in the furnace before it cools to a temperature below that of preheating and/or intermittent between passes, despite this is not always applicable and is not often considered mandatory. The aim of this is to prevent the martensite formation, and thus preventing the associated cracks [5].

The purpose of postheating treatment is to restore ductility and to reduce residual stresses and distortion of the weldment [43]. Sometimes, the normalizing treatment is carried out on the weld joint immediately after the welding process to achieve high ductility and tensile strength. The weldment is however preferred to be heated and cooled in furnaces gradually in order to decrease the thermal gradient through the thickness of the section [8].

Welds should be supported adequately during stress relief treatment to avoid the excessive distortion caused by the degradation or removal of these stresses. The localized heating of the weldments softens the hardened regions, as heating the entire weldments by furnaces does. It may not decrease the residual stresses, but may increase them if it is incorrectly used. The thermal gradients of the welds should therefore be under control and its restraints should be reduced [8].

2.6 Metallurgical Effects of the Weld Thermal Cycle Associated with the SAW Process

2.6.1 Transformations in the Weld Metal

Solidification is the first transformation that occurs in the weld metal. The solidification mechanism of metals is summarized through nucleation and grain growth, as in the case of solidification that occurs in castings. In fusion welding, the formation of nuclei, usually, does not occur. This is because the molten metal (which its volume rarely exceeds 1 cubic inch) will solidify within a few seconds owing to very rapid cooling rate of the weld pool caused by the heat absorbed by the cold, relatively large sized parent metal. The heat lost due to convection to the atmosphere is really another cause. This rapid cooling leads the weld metal to grow from the adjacent, incompletely melted grains of the parent metal. Therefore, the growth mechanism in welding is important, whereas the nucleation is not. [6,44]. The incompletely melted parent metal grains serve as the ideal base from which the molten weld metal crystalizes. Hence, the grains of the molten weld metal will grow directly from the incompletely melted grains of the parent metal, so that the grain boundaries of both become continuous across the fusion line, as shown in Figure (2.3). Moreover, these grains are identical in the orientation of atoms.

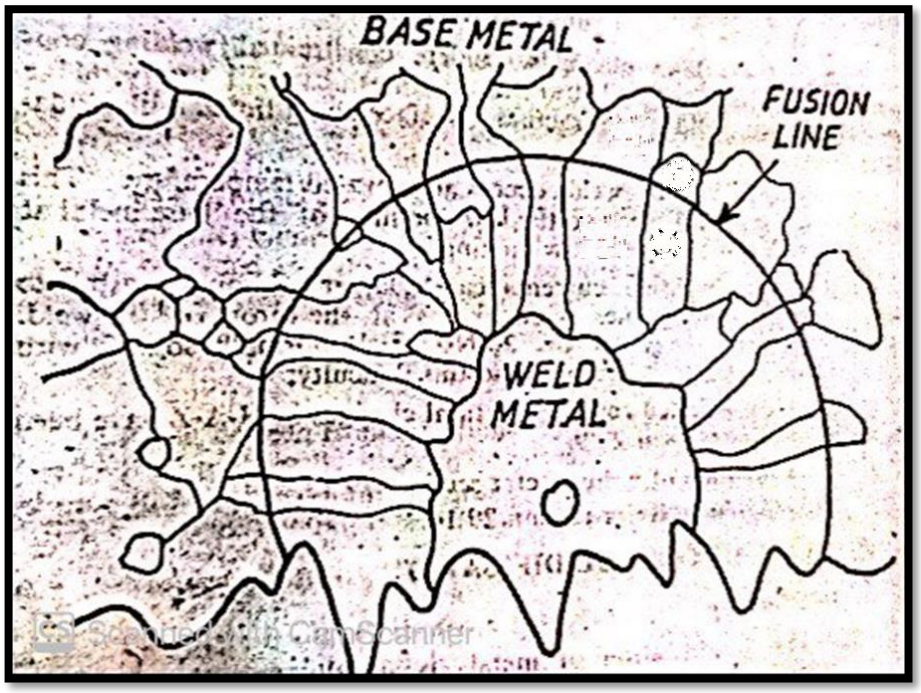

Figure (2.3): Weld metal growth [6].

In fusion welding, the existence of solid grains at the liquid-solid interface works as ready nuclei from which the granular growth releases [6]. In steels, the weld metal solidifies forming a solid solution of C, Mn and some other elements with iron. Based on cooling speed, the resulting grains might be dendritic or columnar. Heat typically flows from the weld zone towards the colder metal adjacent to this zone. The weld metal therefore, has columnar grains with right angles to the fusion line. This is what distinguishes grains resulting from single-pass welding. With multi-pass welding, and due to repeated heating, these grains transform into equiaxid grains, where each welding pass reheats the previous pass. This reduces the particle size of the formed grains, consequently improving the mechanical properties of the weld zone [45].

The weld metal, as mentioned previously, is a mixture of the filler metal with the molten parent metal. The mixing of a portion of the parent metal with the deposited filler metal is known as dilution process, which can be expressed as [46]:

$$\text{Dilution ratio (D) \%} = \frac{\text{weight of the molten parent metal}}{\text{total weight of the molten metal}} * 100$$

The maximum dilution occurs in thin section butt-welding without beveling the edges with one-pass. Less dilution happens in the case of multi-pass welding, with edge preparation, as shown in Figure (2.4):

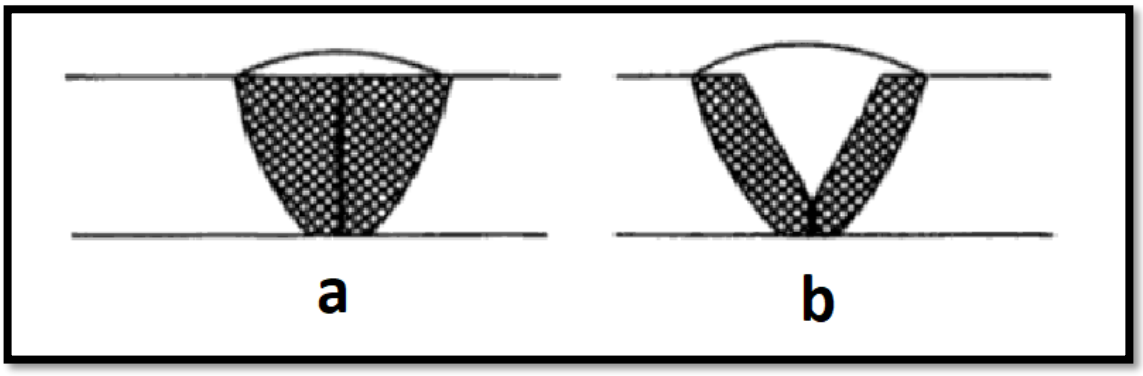

Figure (2.4): Dilution of the (a): one pass Square butt joint weld (b): multi-pass Single-V butt joint weld [51].

It is worth mentioning that the first bead in the case of multi-pass welding, which is called root bead, smelts a large proportion of the parent metal in comparison with the subsequent beads. Cracks possibly occur in the root bead, as this bead exhibits high hardness and brittleness due to the high dilution ratio, and excessive cooling caused by heat absorbing from this small-sized bead by the large size of the cold parent metal. The large strain caused by shrinkage stresses also promotes the development of these cracks. Therefore, caution should be considered when welding the root pass, particularly in high carbon steels, to avoid cracks in this bead [47].

Dilution is more prominent when welding dissimilar metals. It however can be decreased via depositing one or a number of weld layers on the edges of the joint being welded before the start of the welding process. This is called the buttering process, and in some cases, specific alloys can be used for this purpose [46]. Increasing the carbon content does not increase the weld metal strength as it does, e.g., with the wrought steel, because such an increase causes segregation of carbon during the solidification. This leads to the formation of cementite during the subsequent solid-state transformation of austenite, decreasing the toughness of the weld metal. Therefore, the carbon content in the weld metal should be kept low as (0.1%) as a maximum. This ratio should therefore not be exceeded in the welding electrodes, whatever the strength desired of the weld metal, or the carbon content in the parent metal. When the carbon content of the weld metal is maintained low, the microstructure will mostly be a mixture of ferrite and carbides with a very small proportion of bainite or martensite. The microstructure of the parent metal however varies from ferrite to martensite, based on the percentage of carbon and alloying elements in steels [48].

2.6.2 Thermal Effects of SAW on the Parent Metal and its Mechanical Properties

The parent metal adjacent to the weld zone is typically divided into two zones:- the heat affected zone (HAZ), and unaffected parent metal [6].

2.6.2.1 Heat Affected Zone

It is the region just adjacent to the weld zone which represents the parent metal that is not melted by the welding heat, except that it is heated to a temperature and for a period sufficient for the occurrence of grain growth in it. This region undergoes to a complicated thermal cycles representing by sudden

heating to different temperatures, ranged between melting temperature and that of the unaffected parent metal. Subsequently, the heating is followed by rapid cooling due to the nearby cold metal and the surrounding atmosphere. This heating and cooling cycle serves as a different heat treatment for each region of the HAZ. This zone therefore consists of a series of structures gradient and different in their mechanical properties.

In low alloy steels, these structures might vary from the hard martensite to the coarse pearlite. The HAZ width in arc welds doesn't exceed a few millimeters. When welding low alloy steels with a single pass by SAW process, three different metallurgical regions can be observed [6]:

A. Grain growth region B. Grain refined region C. Transition region

A. Grain Growth Region: it is exactly adjacent to the fusion boundary (weld zone). In this region, the parent metal is heated to temperatures in a range between above the upper critical temperature (A_3) and melting temperature (Figure 2.5). This resulted in coarsening the structure or grain growth [6]. The largest grain growth region and the maximum grain size occur as the cooling rate decreases. The cooling rate depends upon the amount of heat utilized during welding, initial temperature of the parent metal, thickness of the welds in addition to the design of the weld zone. The high initial temperature of parent metals and weld heat causes slow cooling rates, whereas the large weldment thicknesses result in rapid cooling rates. Generally, the cooling rate of this region is greater than those in the other regions of the heat effected zone, because of the severe thermal drop from the temperature of this region to that of the cold parent metal [6,44]. This region is therefore the hardest of the HAZ in weldments of low carbon steels [48].

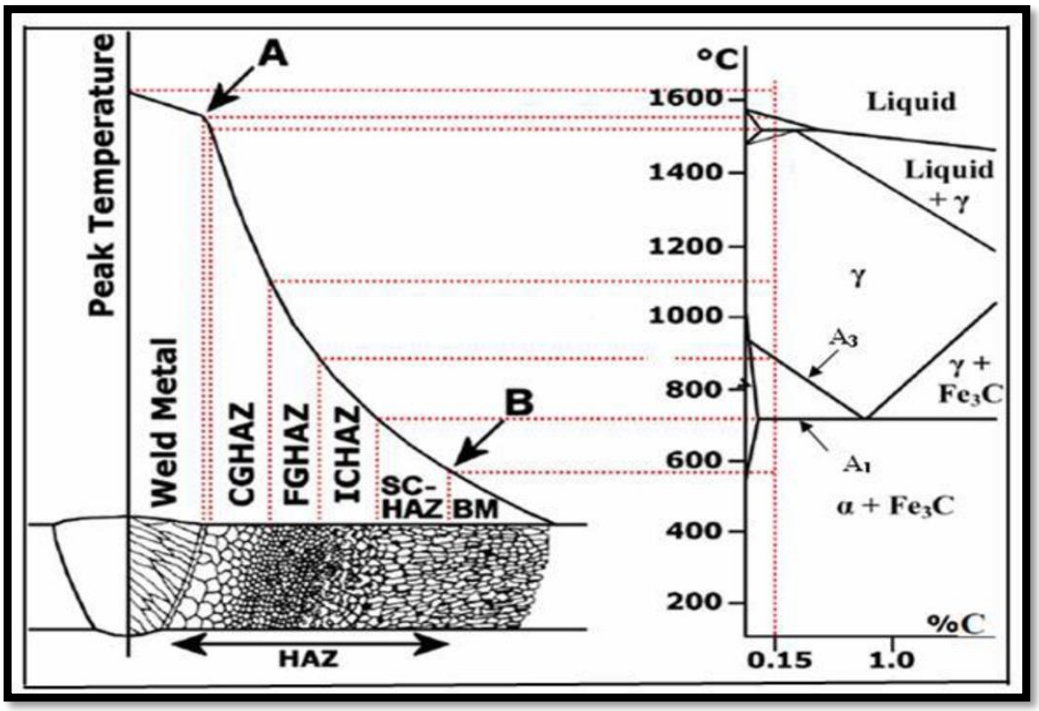

Figure (2.5): Fe-C phase diagram [49].

The microstructure in this region based on the percentage of carbon and alloying elements, grain size and the cooling rate. In weldments of low carbon steels, the structure in the grain growth region is pro-eutectoid ferrite at the grain boundaries of the prior austenite, whereas the grains themselves are usually ferrite with pearlite, or ferrite with bainite. With the increase of the cooling rate or increasing the content of carbon and alloying elements, the grains of ferrite disappeared. The austenite grains then transform into bainite upper or lower, martensite or a mixture of these microstructures [50].

The resulting grain size depends on the grain size of the austenite. If the austenitic grains were large, the resulting structure will be coarse [50]. Generally, the metal in this region losses some of its ductility particularly the impact strength. Figure (2.6) shows the structure of this zone.

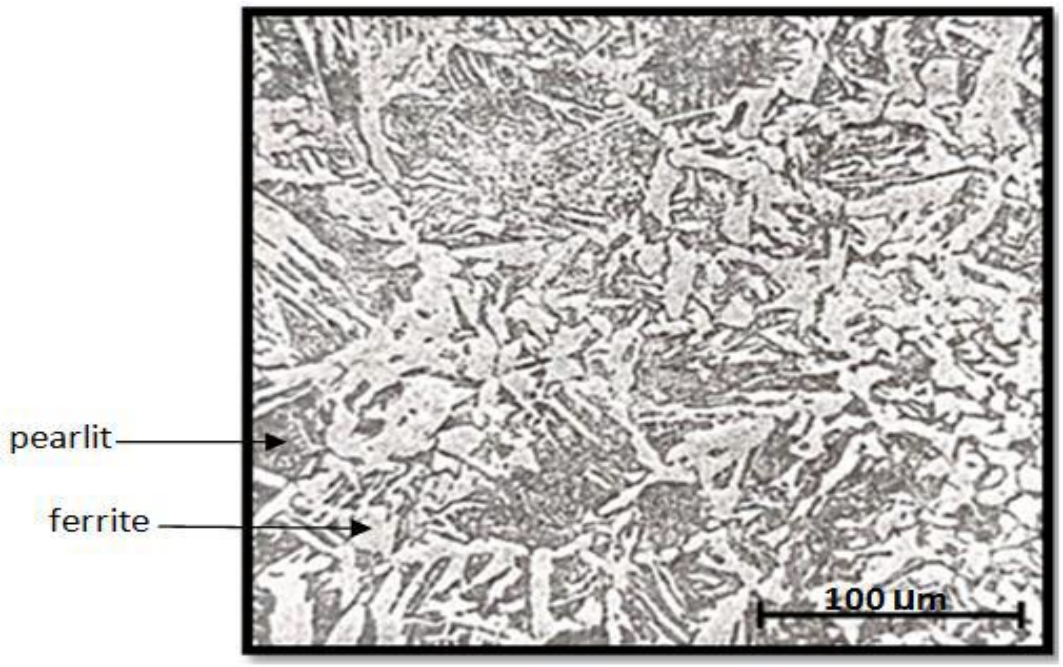

Figure (2.6): Grain growth region [6].

B. Grain Refined Region: it is the region adjacent to that of grain growth, at which the metal is heated to a temperature directly above the high critical temperature (A_3) [6]. The metal in this zone completely transforms to a new, fine-grained austenitic structure, where the heating time isn't long enough for the growth of the austenite grains. Therefore, moderate cooling will form fine pearlitic grains. This is identical to the normalizing heat treatment implemented on carbon steels, which include heating to this temperature and then cooling with still air [42]. This region has relatively high strength and toughness, the same features and properties of normalized steels. Figure (2.7) shows the structure of this region, where dark areas indicate pearlite and light areas indicate ferrite.

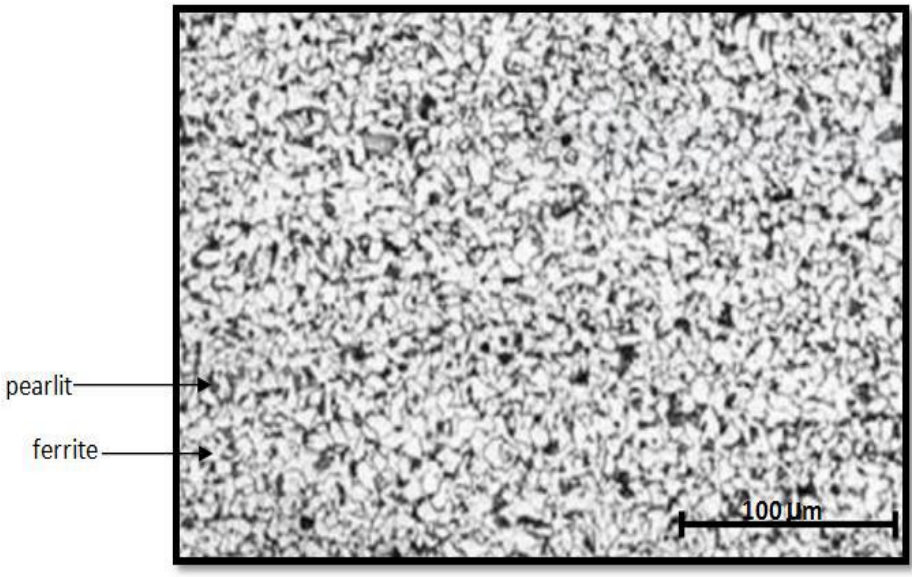

Figure (2.7): Grain refined region [6].

C. Transition Region: during welding, this region is exposed to temperatures ranging between higher critical temperature (A_3) and lower (A_1) [6]. This heating works on transforming pearlite grains (at least partially) into fine austenite grains, but it is not sufficient to transform ferrite grains [44]. A partial allotropic recrystallization occurs in this region. Upon cooling, the fine austenite grains transform into fine pearlite. Obviously, in this case, the pearlite grains are reduced while the ferrite grains remain the same [6]. Figure (2.8) represents the microstructure of this region.

For alloy steels, this region is of particular interest, as the same cooling rate might be enough to convert the fine grains of austenite to martensite, resulting in high hardness and brittleness in this region. This exposes these kinds of steels to hydrogen cracks. Consequently, care must be followed while welding these steels to avoid such cracks. It should be noted that the main reason for the formation of martensite in this region is carbon, as with the increase in the percentage of carbon and other alloying elements, the hardenability of steels increases as mentioned early.

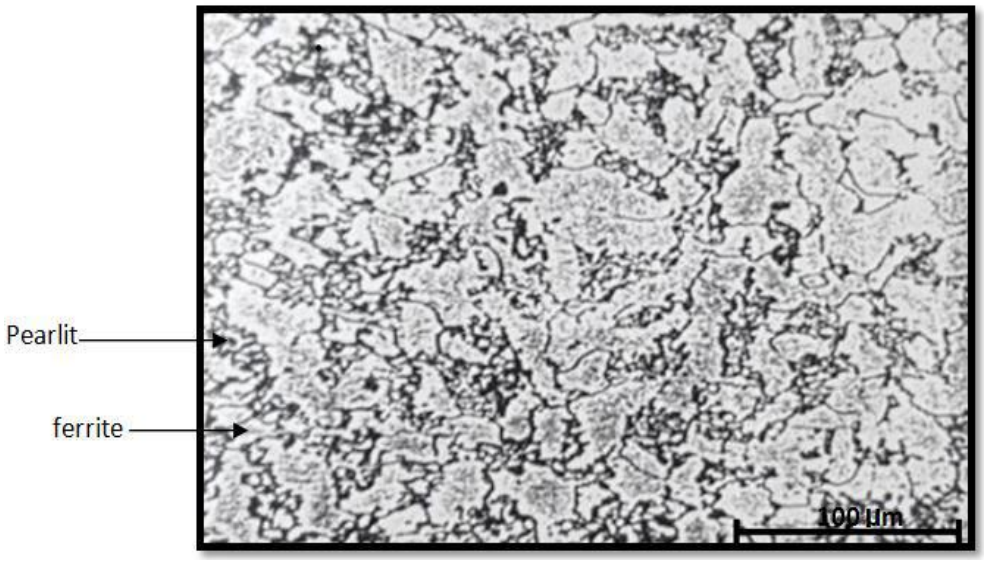

Figure (2.8): Transition region [6].

2.6.2.2 Unaffected Parent Metal

The parent metal that is heated upon welding to temperatures insufficient to make change in its structure, comes directly after the HAZ [6]. Figure (2.9) shows the microstructure of the parent metal of low carbon steel unaffected by welding heat.

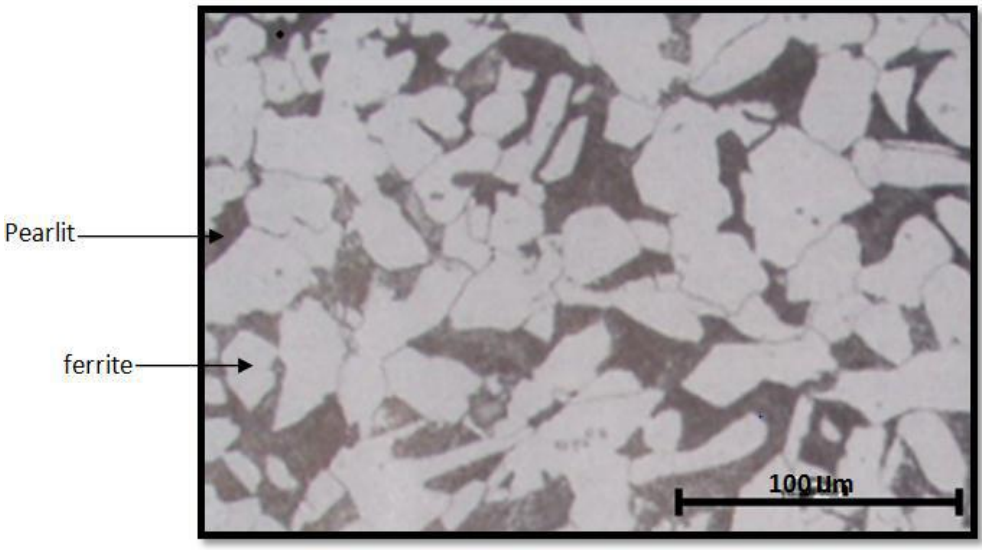

Figure (2.9): Unaffected parent metal [6].

2.7 Defects Associated with the SAW of Low Alloy Steels

Submerged arc welding of low alloy steels is usually associated with many defects that occur in the weld zone and HAZ.

The weldment that has defects might fail during service causing economic and human loses, so studies of welding defects and analysis of welding defects are necessary [5].

The most common weld defects include [7]:

- Hydrogen embrittlement
- Hot cracking
- Porosity
- Poor impact strength
- Undercut
- Slag inclusions
- Uneven weld beads

2.7.1 Hot cracking

They are cracks that happen at elevated temperatures; in general, after the weld metal starts to solidify instantly, so they are called hot cracks [52]. Solidification of the weld metal begins from the fusion line towards the center of the weld that is at the highest temperature and solidifies lastly [53]. During solidification, liquid and solid phases might vary greatly in chemical compositions; crystals initiated firstly or dendrites that have high solidification temperatures differ from the residual molten metal that consists of some

alloying elements and impurities of low solidification temperatures [50]. The residual molten metal is driven towards crystals growth until dendrite interlocking at the last solidification stages, leaving constituents of relatively low solidification temperatures on the grain boundaries [6], and this is called *segregation*. The chemical composition of these phases can be modified by *diffusion*. Because the solidification occurs at a relatively fast rate, there will not be sufficient time for the desired diffusion, and as a result, the metal is poor in homogeneity. It is possible to distribute this segregation by post weld heat treatments, but the elements may respond differently to these treatments. As the metal impurities increase, the probability of segregation increases [50].

Hot cracking occurs due to the existence of the constituents of relatively low solidification temperatures at the grain boundaries. These constituents have low strength and low ductility at elevated temperatures resulting in a rupture along grain boundaries due to the effect of thermal shrinkage stresses. Therefore, these cracks are sometimes called intercrystalline cracking [54].

Intercrystalline cracking occurs before the solidification is completed while the metal is though in the plastic state. Microscopy usually shows a thin oxide layer covering these cracks as an evidence that they are created at elevated temperatures. These cracks range between micro-fissures and readily visual cracks based on the amount of the strain [55].

In steels, the residual constituents on the grain boundaries are typically either elements or compounds like phosphides and sulfides [54]. The elements that segregate in steels are usually carbon, phosphorus, sulfur and manganese, but the carbon is of the most significant and segregated elements. The resulting microstructure however appears regions rich with carbon (like cementite) and others are poor with carbon [50].

2.7.1.1 Hot cracking reasons

Hot cracking is attributed to many causes, the most significant of them are:

1. Large grain size, where longitudinal grains might create due to rapid cooling of the weld pool. These grains are similar to those created while molten metal is poured into a cold metallic mold. These grains might cause weak planes as a result of hot cracks occurring through them [45].
2. Impurities that promote the creation of thin liquid layers of low solidification temperatures, such as sulfur, which participates in the creation of the brittle iron sulfide film of low solidification temperature on the grain boundaries. The amount of impurities in the weld pool is based on the initial impurity content in steels and on the dilution ratio [53].
3. High content of carbon in steels, where carbon (as mentioned previously) is one of the elements which segregate in the weld pool, and contributes in cementite formation, through the subsequent solid state transformation of austenite [54].
4. High rigidity of the pieces being welded or severe restraints of the joint that concentrate shrinkage stresses in the weld deposit [54].
5. Rapid cooling, which causes high shrinkage stresses in the weld deposit [54].
6. The very small root bead. During cooling, when the weld zone and the HAZ begin to shrink, the larger mass of the parent metal absorbs the heat rapidly from the small weld bead, thus cooling the root bead quickly, exposing it to higher thermal shrinkage stresses [56]. Hot cracks frequently extend from the root bead through the subsequent good layers, but they might not extend to the weld surface [6]. In addition to the previous causes, high ratio of carbon and other impurities in the root bead are among factors that encourage the root cracking because of the severe dilution in this region, mainly when welding high carbon steels as mentioned previously [47].

7. Incorrect preparation of the weld joints participates to hot cracks occurrence by decreasing the effective surface area of the weld zone. Incomplete penetration and poor fit-up of the joint, for instance, weaken these joints and therefore easily expose them to hot cracks. Hot cracks can initiate due to the narrow root opening of the weld joint when weld metal penetration is deep, particularly for the large ratio between penetration and width of the bead.

2.7.1.2 Hot cracking remedies

Hot cracks can be avoided or decreased by several ways, the most significant of which are:

1. Precisely controlling the impurities that promote the creation of the thin liquid films of low solidification temperatures by obstructing the effect of detrimental elements in steels by a specific way [53]. For instance, the additive of manganese to the weld pool, which containing sulfur to create the soft manganese sulfides of a high solidification temperature decreases the possibility of hot cracking [57]. This solution might have a little influence when welding of high carbon steels [8], as shown in Figure (2.10).
2. Minimizing the dilution ratio by several means, such as avoiding the usage of too high current densities and choosing the suitable weld joint design [5].
3. Permitting the ends of the weldment to move freely as possible while welding, and developing of welding procedures to decrease the effect of high rigidity of the pieces being welded [5].
4. Preheating the pieces being welded decreases the strain causing by the shrinkage thermal stresses [5].
5. Making sure that the weld bead has sufficient resistance to the stresses, which might arise because of the welding heat. Avery small size weld bead between

two heavy pieces should not be used, as it must be ensured that the weld beads have appropriate size in all weld joints [56].

6. Drying fluxes to decrease the moisture content and cleaning surfaces of the pieces being welded from moisture, grease, oils and other contaminants [55].

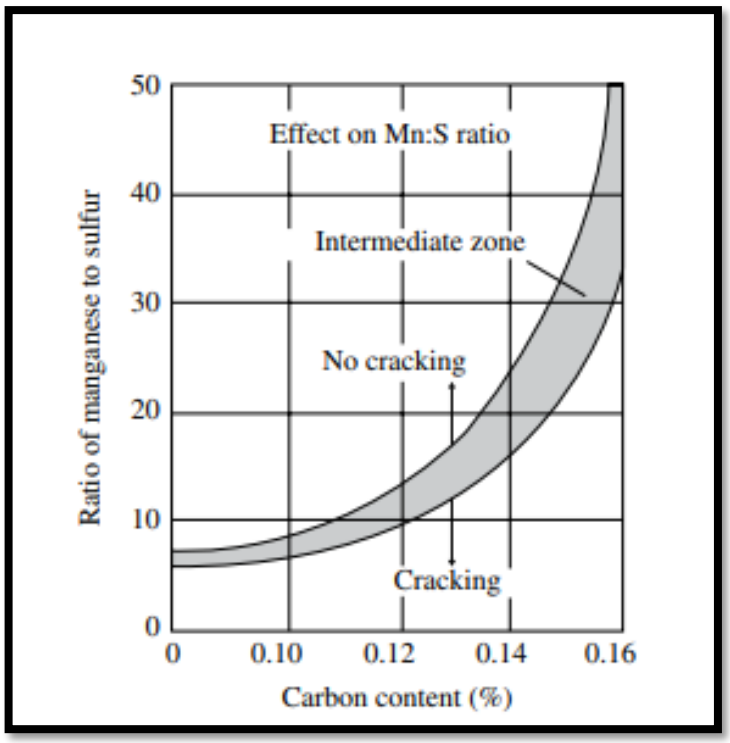

Figure (2.10): Influence of the Mn:S ratio with the C content on the susceptibility of carbon steel weld metals to hot cracking **[58]**.

There is a type of cracks happen in the crater formed at the starting or end of the weld or when the welding process is stopped for any reason [59]. These cracks are called as crater cracks. The craters are caused by the high forces of the arc, hence the surface of the weld retracts into a concave (crater) shape when the weld pool solidifies after extinguishing of the arc. When a concave weld zone is cooled, stresses are usually concentrated in the cross section of the lowest thickness and the highest temperature of the weld. The crater therefore provides ideal conditions for hot cracks occurrence. The crater generally solidifies from all sides towards the weld center. So, the crack begins from the

top surface inward [60]. The crater cracks might be star, transverse or serve as a start out for longitudinal cracks [61], as shown in Figure (2.11) below.

The crater cracks can result in failure, so they have to be avoided. A common way to achieve this is to place steel plates of the same parent metal (to hinder the dilution between them) at the starting and end of the weld. The craters will remain in the added steel plates, which are finally separated from the weld joint after the welding process is completed [58,61].

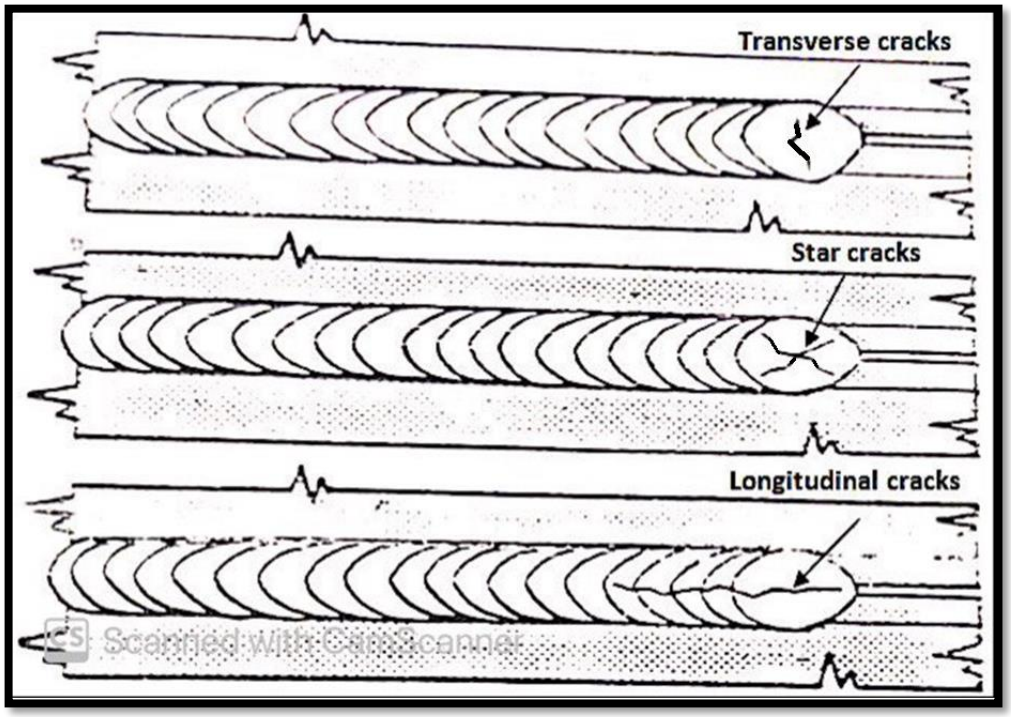

Figure (2.11): Crater cracks caused by hot shrinkages [5].

Submerged arc steel welds are generally more susceptible to a risk of solidification cracking due to the deep penetration and considerable melting of the workpiece material associated with this process. Consequently, more constituents of low melting temperature will segregate. In a deep and narrow joint, the weld metal solidifies in such a way as to leave these weak segregated constituents in the middle of the weld, which then breaks due to longitudinal

cracks occur under the influence of thermal shrinkage stresses [7], as shown in Figure (2.12) below.

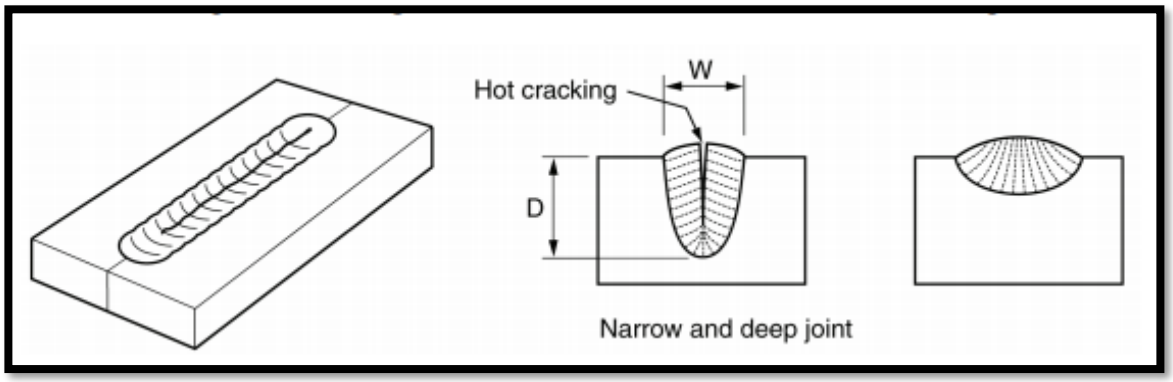

Figure (2.12): Solidification cracks may appear when the weld is deep and narrow [7].

2.8 Effect of Nickel on Steel Welds

Nickel is a silver-white metal that is extremely shiny and capable to take a high polish. It can be forged, machined, welded and rolled into sheets or wires. It is also ductile, relatively strong and has high resistant to corrosion in many conditions. Nickel has a relatively high melting point (1455 C°), and can withstand extremely high and low temperatures. It also can retain its strength at elevated temperatures in addition to both ductility and strength at sub-zero temperatures [62]. These characteristics make it a very important material and main alloying element in ferrous metals. Nickel exists as plates, strips, wires and also powder. In its commercially pure form (99.5 %), it has enormous and significant industrial applications. Fabricated nickel has mechanical properties comparable to those of low carbon steels. It is, however, unlike steel, resistant to corrosion, and this fact, together with the fact that it is non-toxic, makes it suitable to the use in the plant manufacturing for food and pharmaceutical processing [45].

Nickel has a marked strengthening effect on the steel, since it goes into solid solution and decreases the carbon content of the eutectoid [45]. Unfortunately, Ni does not combine chemically with carbon, and, worse still, tends to make cementite decompose and thus release free graphite. Consequently, nickel steels are always low carbon steels, or, alternatively, medium carbon steels with very small amount of nickel. However, because of their shortcomings due to carbide instability, they have been almost entirely replaced in recent years by other new low alloy steels [63]. Nickel lowers the critical cooling rate, thereby increasing the hardenability of the steel. It also lowers the critical range, thus stabilizing austenite [45]. Additions of nickel are frequently used to improve the toughness at low temperatures, due to the fact that increasing nickel has a great effect on the acicular ferrite content [64,65]. The toughness improvement is also attributed to the grain size refinement and reduction of the stalking fault energy of the ferrite in such a way that plastic deformation at lower temperatures is facilitated [66]. Other than making steels more hardenable, the presence of nickel in steel causes no difficulty in welding [64].

The main influences of nickel on steel welds can be briefed as follows:

1- Prevent the creation of hard and brittle micro constituents in the fusion zone (FZ) [67].

2- Mechanical strength and impact toughness of steel weld are higher due to refining microstructure by limiting grain growth. The improvement of these properties is also attributed to high percentage of acicular ferrite in steel weld. The impact toughness of the steel weld in fusion welding is directly proportional to the nickel content in the weld metal [63,68]. Nickel improves the toughness when it is added alone, but when it is co-present with a high amount of manganese, it affects mechanical properties in complicated ways because the

microstructure become martensite which susceptible predominantly to intergranular brittle crack propagation [68].

3- The high ductility of the Ni-based FZ can play a significant role in the absorption of tensile stresses initiated during welding. This participates in decreasing the crack susceptibility of the weld joint [5].

4- The Ni-based FZ presents good machinability [5,69].

2.9 Literature Review

The literature survey gives comprehensive information on researches, which discuss the influence of Ni content on properties of SAW steel welds.

In 2000, Kang et al. [70] evaluated the mechanical properties of mild steel welds with different additives of Ni and Mn using metal-cored wires and shielding gas (Ar–2% O_2). It was found that the hardness of the weld metals increased linearly with these additives that was attributed mostly to strengthening of the solid solution and partially to hard phases formation. With a low Mn content (0.5%), Ni additives increased hardness without decreasing the impact toughness, while with a high Mn and Ni contents (1.6 and 7.45 wt.% respectively), the impact toughness deteriorated seriously even at room temperature, leading to intercrystaline fracture. The fracture was at prior austenite grain boundaries because no δ-ferrite phase created during solidification. Therefore, these boundaries were prone to cracking under cyclic loading. Depending on hardness and impact resistance, the best amounts of Mn and Ni were suggested to be in the ranges (0.5–1%) and (4–5%), respectively.

Eroglu et al. (2002) [71] investigated the effect of nickel contents (1.0, 2.0, 2.9, 4.1, and 5.2 wt.%) besides different amounts of heat input (0.5, 1.0, and 2.0

kJ/mm) on the mechanical properties and microstructure of the HAZ of submerged arc mild steel welds. The results showed that the combination of 2.9-5.2 wt.% nickel content with 0.5 kJ/mm heat input resulted in creation of martensite structure, hence giving lower toughness values. The toughness, hardness, and microstructure of the HAZ showed good results with 0.5 kJ/mm and 1.0 wt.% nickel, and with 1.0 kJ/mm heat input and 2.0-5.2 wt.% nickel.

Bhole et al. studied **in 2005 [72]** the effects of Ni and Mo powder, which added individually and together, on the impact toughness of submerged arc API HSLA-70 steel welds. The results showed that the Ni additions (2.03–3.75 wt.%) decreased the impact toughness and increased fracture appearance transition temperature in the welds. This is because the increase in nickel content restrained the formation of acicular ferrite. In contrast, the combined effect of Ni and Mo in the weld metal reduced the volume fractions of ferrite at grain boundaries and promoted the high toughness acicular ferrite formation. The optimal impact toughness was obtained (at -45 ◦ C) with Mo additives of (0.881 wt.%) in the weld metal, where the microstructure was 77% acicular ferrite and 20% granular bainite.

In 2007 Trindade et al. [73] studied the effect of nickel content (0.50 - 3.11 wt.%) on the microstructure and toughness of A36 steel welds, as-welded state and after post weld heat treatment, using SAW process. Optical microscopy (OM) and scanning electron microscopy (SEM) were used to observe the microstructures. The charpy impact test was carried out on samples cut perpendicular to the weld bead to evaluate the toughness. The results showed that the nickel content up to 1.0 wt.% increases the toughness due to the increase of the acicular ferrite content and to microstructural refinement. On the other hand, more nickel contents have a reverse effect on the toughness as a result of the existence of the micro-constituents martensite-austenite in the weld metal.

The postheating treatment had an insufficient improvement in toughness of the weld metal, even if these constituents had decomposed into ferrite and carbides. This might be due to the precipitation of carbides along the ferrite boundaries.

In 2014 Sham et al. [74] studied using a variety of advanced analytical techniques the effect of nickel (1.0, 2.0, 3.0, 4.0, 5.0 wt. %) on toughness and strength particularly for submerged arc multi-pass HSLA steel welds in the as-welded condition. Mechanical testing showed that nickel content ≥ 3.0 wt. %, in the as-welded condition achieved the aimed mechanical properties (yield strength ≥ 586 Mpa, ultimate tensile strength ≥ 724 Mpa and nil ductility temperature ≤ -96℃). From 1.0-5.0 wt. % Ni content, during the primary solidification, the structure varied from primary delta-ferrite to primary austenite, and the thickness of dendrite/cellular was refined. With increasing Ni content, austenite transformation temperatures were also reduced to refine grain size of the effective ferrite. Dislocation density and strain therefore increased. At 5.0 wt. % Ni, precipitates (in the form of $FeNi_3$ or $MnNi_3$) appeared in both inter and intergranular regions, which resulted in enhancing strength and toughness by reducing the grain size of ferrite and precipitation strengthening.

Sharma et al. (2014) [75] investigated the effect of 10 and 20 % nickel powder added in AUTOMELT B31 flux, to improve the impact strength of submerged arc IS 2062 mild steel welds. The analysis of variance (ANOVA) used to analyze the effect of all the input parameters on the output responses. Taguchi technique was used to design the experiments. The results showed that the joint welded with 20% Ni using voltage 34 V and travel speed 200 mm/min had maximum value of impact strength and tensile strength of 295 Mpa.

Lijun et al. (2015) [76] studied the effect of Ni and Mn amounts on the impact toughness and microstructure of the submerged arc high strength low alloy steel welds. The results showed that both Ni and Mn increased acicular ferrite at the

expense of pro-eutectoid ferrite. Depending on the property of impact resistance, the optimum contents of Ni and Mn were suggested to be in the ranges of 2.5-3.5% and 0.6-0.9% respectively. Additions beyond these ranges will promote segregation structures that may be detrimental to the toughness of the weld metal.

Verma et al. studied **in 2015 [77]** the influence of flux on the microstructure, tensile strength and microhardness of submerged arc mild steel (IS 2062) welds. The analysis of variance (ANOVA) used to analyze the effect of all the input parameters on the output responses. Strength of the weld joint was 580 N/mm^2 after nickel powder addition 20% in comparing with the typical joint strength (505 N/mm^2) when welding with a single pass using 10 m/hr welding speed and voltage of 34 V. Voltage has an important effect on the tensile strength with the contribute of 61.69 %, while travel speed and flux have unimportant effect on the tensile strength with the contribute of 10.28 % and 25.87 % respectively. Flux and voltage have important effect on the hardness with the contribute of 55.59 % and 25.37% respectively, while travel speed has unimportant effect with the contribute of 17.72 %.

WU et al. (2015) [78] investigated the effect of 0.3 and 0.5 wt.% Ni additions to SANi03 and H08MnMoTiB wires on microstructure, toughness and hardness of both sides submerged arc K65 gas pipeline high strength steel welds using the post-weld heat treatment. The results showed that a high Ni content decreased the ferrite transformation temperature and increased the proportion of acicular ferrite. The high Ni content also induced more martensite/austenite constituents after reheating, which resulted in more and coarser cementite particles after tempering heat treatment. More acicular ferrite in this weld resulted in relatively high density of large angle grain boundary that improved the impact toughness despite the negative effect of cementite.

Mei et al. (2017) [79] studied the influence of nickel on properties of submerged arc SA-508 Gr.3 Cl.1 steel welds by using two kinds of filler metal, with 0.67 wt.% Ni (AWS classification F8P4-EGN-F2N) and without Ni (F8P4-EA3N-A3N), which have been mainly used in the manufacture of the reactor pressure vessel. The results showed similar mechanical properties for both weld metals, except that the weld metal with Ni has better Charpy V-notch impact property than that without Ni. The microstructures of both weld metals were ferrite base with granular bainite, except the columnar grain size of the weld metal with Ni was smaller, which resulting in better impact property.

In 2018, Wang et al. [80] investigated the influence of different Ni contents (0.93, 1.19, 1.45 wt. %) on the mechanical properties and microstructure development of submerged arc K65 oil and gas pipeline steel welds. The strength and impact toughness at −40 and −60 °C were significantly improved with the increase of Ni content, which stabilizes the austenite grain and decreases the ferrite transformation temperature, subsequently promotes the creation of predominant acicular ferrite, at the expense of grain boundary ferrite. The Ni content determines the completion degree of transformation, and then changes the volume fraction of grain boundary ferrite and the status of martensite/austenite constituents. This is, in samples containing 0.93 and 1.19 wt.%. Ni, a higher fraction of grain boundary ferrite and martensite/austenite constituents with larger size were due to the relatively incomplete transformation. In sample containing 1.45 wt.% Ni, the complete transformation significantly lowered the fraction of grain boundary ferrite and martensite/austenite constituents, and martensite/austenite size. Consequently, this Ni addition enhanced the toughness of the weld metal.

Mao et al. (2018) [81] used different powder flux-cored wires to investigate the influence of Ni (2.0, 4.0, 6.0 wt.%) on the toughness and microstructure of Q345

HSLA steel welds. The results showed that with increasing Ni, more martensite transformation happens and the ductile-brittle transition temperature drops as well. Welding wires with Ni content of 4.0 wt.% achieved best results where the microstructure was mainly lower bianite, grain boundary ferrite and acicular ferrite.

In 2020, Jilabi and Talib [82] studied the effect of Ni on properties of shielded metal arc LAHSS (65Γ) welds by using an economical technique involves coiling pure Ni wires with different diameters around and along a cheap welding electrode (E6013). The results showed that the tensile strength and efficiency of the weld joint were 198 MPa and 22% respectively when the cheap electrode (E6013) was used. The tensile strength increased to 475MPa and the weld joint efficiency to 54% as a result of coiling a 0.8 mm diameter pure Ni wire (36 wt.% Ni deposited in the weld) around the (E6013) electrode, while 56% efficiency reached by the use of an expensive electrode (E8018-C3).

2.9.1 Summary

The Table (2.1) below summarizes the most reviewed literature related to the current research.

I	Researchers	Year	Welding Type	Parent Metal Type	Ni Additions	Major Results
1	Sharma et al.	2014	SAW	IS 2062 mild steel (ASTM A36)	10-20 wt.%	With 20% Ni, the weld joint had maximum value of impact strength and tensile strength of 295 Mpa.
2	Bhole et al.	2005	SAW	HSLA-70 steel (ASTM A513)	2.03-3.75 wt.%	Ni additives in this range decreased the impact toughness and increased fracture appearance transition temperature in the welds.
3	Trindade et al.	2007	SAW	ASTM A36 steel	0.50-3.11 wt.%	The nickel content up to 1.0 wt.% increased the toughness.
4	Verma et al.	2015	SAW	IS 2062 mild steel (ASTM A36)	10-20 wt.%	Strength of the weld joint was best (580 Mpa) after nickel powder addition 20% in comparing with the typical joint strength when welding with a single pass.
5	Jilabi and Talib	2020	SMAW	65 Γ (ASTM A29)	0.4, 0.6, 0.8, 1.0, 1.4 mm dia. wire	The tensile strength increased to 475MPa and the weld joint efficiency to 54% as a result of coiling a 0.8 mm diameter pure Ni wire around the (E6013) electrode.

It is clearly noted from the review of previous literatures and the above table that there are some researches that dealt with the effect of nickel content on submerged arc steel welds. Most of them were however on low carbon steels and a few on high strength low alloy steels. At the time of writing this research, it has not been found any research dealing with the effect of nickel content on low alloy steel welds using the SAW process. Moreover, previous literatures that dealt with the study of the effect of nickel content were confined to limited ratios and there was not any comprehensive study that includes a wide range of nickel ratios and their effects on the properties of low alloy steel welds and in reducing hot cracks in these welds.

CHAPTER THREE:

EXPERIMENTAL PART

CHAPTER THREE: EXPERIMENTAL PART

3.1 Introduction

This chapter presents a vision on the experimental work and describes all the conditions under which the tests have been carried out. It includes materials, equipment and experimental procedures used in this study which involve welding of low alloy steel plates using the SAW process. Mechanical properties of the weld joint were investigated by micro hardness and tensile tests. The changes in microstructure of the weld joint were evaluated by the optical microscope, scanning electron microscope (SEM) and energy dispersive spectrometer (EDS). Internal defects of the weld joint were detected by the X-ray radiography, in addition to the visual inspection after the samples of the tensile test were fractured.

3.2 Program of the Current Study

Figure (3.1) shows the overall program outline used in the current work**.**

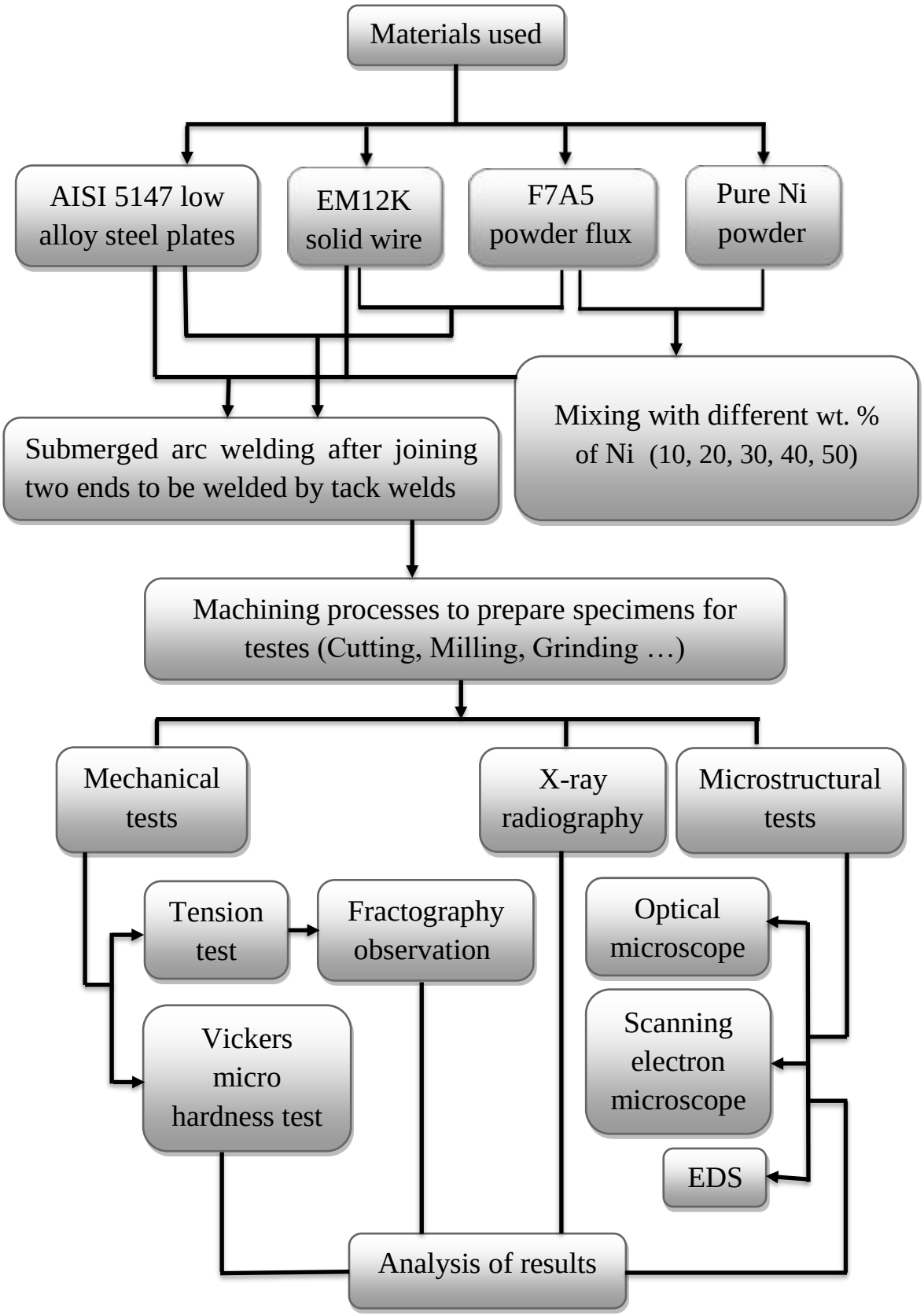

Figure (3.1): Program of the current work.

3.3 Materials and their Specifications

Basic materials used in this study and their specifications are shown in the Table (3.1).

Table (3.1): Materials used in the current study.

Matreials	Specifications
Low alloy steel plates	American Iron and Steel Institute (AISI)
welding wire EM12K	American Welding Society (AWS)
Flux F7A5	American Welding Society (AWS)
Pure nickel powder	Ni-powder of 99.3% purity (Oerlikon)

3.3.1 The alloy used in this study

Specifications of low alloy steel plates used in this study according to the American Iron and Steel Institute (AISI) [83] is shown in the Table (3.2), knowing that the raw material is in the annealed condition.

Table (3.2): Specifications of the alloy used in the research [83].

Alloy	**Chemical composition**						**Spec. symbol**	**Shape and raw material cross section (mm)**	**Min. tensile strength (MPa)**
Low alloy steel	C%.	Mn%	Si%.	Cr%.	P% max.	S% max.			
	0.46-0.51	0.70-0.95	0.20-0.35	0.85-1.15	0.035	0.040	5147	Plate (9*100)	680

The following procedures have been performed:

1- Preparation of pieces to be welded from the raw material, where the length of each piece was (100mm).

2- Chemical composition analysis for the raw material was carried out by using Spectro Max Metal Analyzer in the State Company for Engineering Rehabilitation and Testing–Baghdad (Figure 3.2). Table (3.3) shows the chemical composition (average of three readings) of the raw material used as a parent metal. It is within the range of the chemical composition according to AISI shown in the table (3.2).

Figure (3.2): Chemical composition analyzer.

Table (3.3): Chemical composition of the parent metal.

Parent metal	**Chemical composition (wt.%)**				
Low alloy steels	**C**	**Mn**	**Si**	**Cr**	**Ni**
	0.461	0.855	0.385	0.963	0.087
	Mo	**Al**	**Cu**	**S**	**P**
	0.013	0.092	0.104	0.026	0.012

3.3.2 Solid wire used in this work

Table (3.4) shows specifications of the SAW wire used as a filler metal according to American Welding Society (AWS) [32,84].

Table (3.4): Solid wire specifications.

Copper coated steel wire	Wire metal type	Wire size (mm)	Typical properties all weld metal			Wire composition (wt.%)			
			Tensile strength (MPa)	Yield stress (MPa)	El. (%)	C	Mn	Si	Fe
EM12K	Killed medium manganese alloyed	3.2	450-540	370-450	25-30	0.1	1.0	0.2	Balance

3.3.3 Flux used in this work

Table (3.5) presents specifications of the powder flux used in combination with the solid wire above, according to AWS [32].

Table (3.5): Powder flux specifications.

Powder flux	Flux type	Typical properties all weld metal		Typical all weld metal composition (wt.%)			
		Tensile strength (MPa)	Yield stress (MPa)	C	Mn	Si	Fe
F7A5	Basic agglomerated, slightly Si and Mn alloying	520	425	0.07	1.3	0.5	Balance

3.3.4 Pure nickel powder used

Table (3.6) shows specifications of the pure nickel powder, according to Oerlikon Metco LTD. Chobham, Woking, England [85].

Table (3.6): Powder nickel specifications.

Product	Chemical composition (wt.%) min.	Nominal particle size distribution (µm)	Manufacturing method
Metco 56C-NS	99.3	-75 +45	Precipitated

3.4 Submerged Arc Welding of Low Alloy Steels

The following procedures have been carefully carried out before start of the welding; Figure (3.3) shows the weld joint design (square butt joint), and dimensions of plates to be welded on one side according to the AWS.

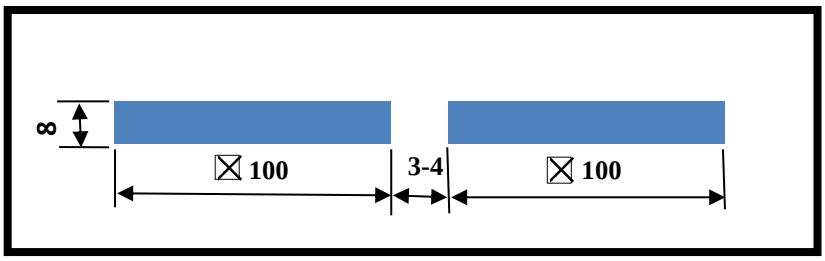

Figure (3.3): Dimensions (in mm) of the plates to be joined.

1- Removing rust from the piece surfaces using a face milling machine by (0.5 mm) from each surface, then cleaning the pieces from oils, grease and the residues of chips and other impurities.

2- Fixing the two pieces to be welded and fit-up the distance between them on (3-4 mm). Steel plates were tack welded to the pieces at the starting and end of the weld (Figure 3.4), so that the craters will remain in the added steel plates, which are finally separated from the weld joint after the welding process is completed. Another advantage was to restrain distortion.

3- Submerged arc welding of the tack welded pieces was implemented with the use of flux backing. Table (3.7) shows SAW of low alloy steel plates and some welding conditions. The procedures above in addition to the welding process were completely carried out in the Heavy Engineering Equipment State Company-Baghdad.

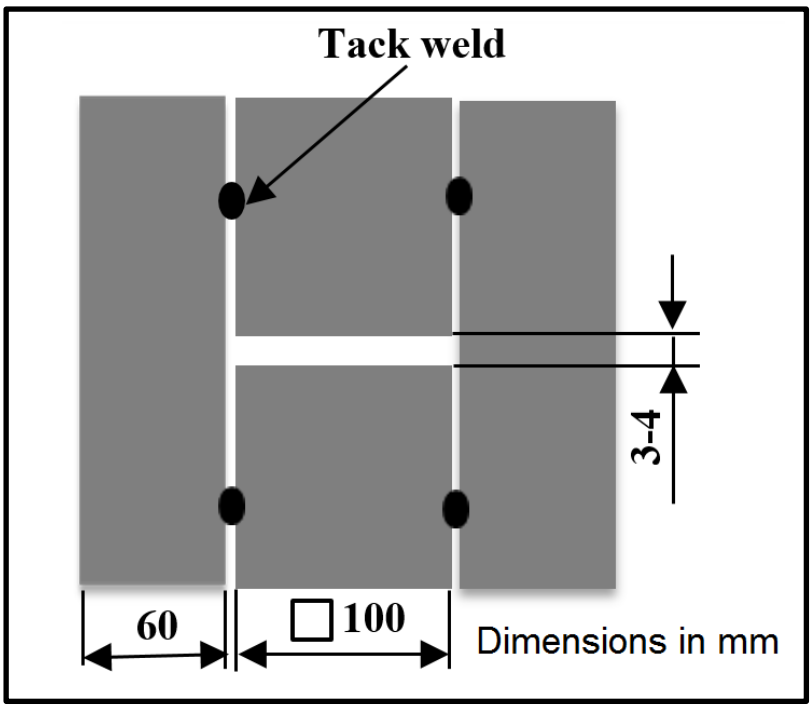

Figure (3.4): Steel plates tack welded to the pieces.

Table (3.7): Submerged arc welding conditions of low alloy steel plates.

Welding by the use of / Welding conditions	EM12K solid wire combined with the F7A5 powder flux	EM12K wire combined with mixed of F7A5 flux and pure Ni powder of ratios (%)				
		10	20	30	40	50
Current value (A)	330	330	350	400	400	400
Travel speed (mm/min)	325	250	265	265	360	380
Voltage value (V)	33-34					
Wire size (mm)	3.2					
Current type	DCRP					
Position	Flat					

3.5 Manufacturing of Test Specimens

After SAW of low alloy steel plates mentioned in the previous paragraph, specimens were prepared from the weldments (Figure 3.5) for tensile, microhardness, micrography (optical and SEM), EDS and X-ray radiography tests, according to ASTM. Below the most important steps to prepare the test specimens.

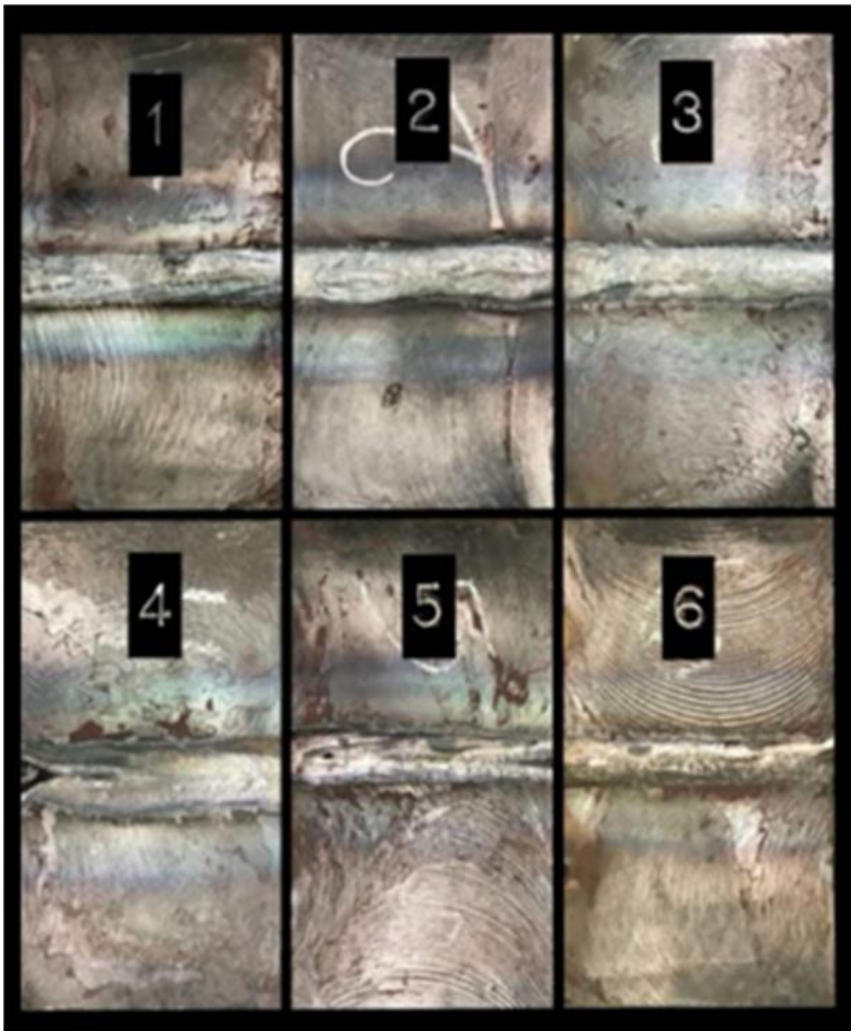

Figure (3.5): The weldments before manufacturing of test specimens.

1- Straightening the weld zone (weld line), roughly, with the weldment surface, by a fixed head grinding machine, to facilitate weldments installing on the milling machine.

2- Milling the top and bottom surfaces of the weldments.

3- Grinding the weldment surfaces by the surface grinding machine so that the weldment can be easily clamped during subsequent stages of machining processes.

4- Marking the dimensions of the required specimens on one of the two grinded surfaces.

5- Cutting the weldments according to the marking using the universal milling machine with a saw cutter with (3 mm) thickness for the prepare of specimens.

3.6 X-ray Radiography

The aim of this test is to identify the type, size and location of the possible internal defects of the welds (cracks, porosity, slag inclusions, etc.), where such defects cannot be observed in microscopic examination. Top and bottom surfaces of the weldments were milling machined before carrying out this test. The test was implemented at the Heavy Engineering Equipment State Company-Baghdad by the use of the XXG-2005 X-ray control unit device -China shown in Figure (3.6).

Figure (3.6): X-ray radiography device.

3.7 Microscopy

3.7.1 Optical Microscopic Inspection

Specimens for microstructure analysis were prepared according to the standard metallographic techniques which involve the following steps.

1- Specimens were cut to an appropriate size to facilitate handling and detect the microstructure variations in different zones.

2- The wet grinding process was carried out by exposing the specimen surface to the rotary disk using emery papers of (SiC) with different grades in sequence (400, 600, 800, 1000, 1200 and 1500). The specimen was then washed with water and dried with hot air.

3- Mechanical Polishing: Diamond particle pastes were used to remove the new finer scratches introduced by the grinding step. Polishing was achieved using 6, 1 and 0.25μm pastes sequentially; the polishing was applied on special clothes fixed on electrically powered rotary discs.

4- Etching: Nital (2% HNO_3 + 98% Ethanol) was used as an etchant to reveal the phases by its chemical effect on the different phases in variable levels. Following the etching, the prepared surface to be examined was cleaned with ethanol.

An optical microscope was then used to define microstructure and topography of different regions on the prepared specimen surfaces across the centerline of the welds (weld zone, HAZ and the parent metal). It also used to observe and determine the type, size and location of the possible surface defects across the welds. This inspection was done at the labs of the Metallurgical Department-Faculty of Materials Engineering-University of Babylon.

3.7.2 Scanning Electron Microscope (SEM)

Microstructural examinations and chemical composition analysis were carried out using the Scanning Electron Microscope (**SEM)** at Alkhora Company/Baghdad and Energy Dispersive Spectrometer detector **(EDS)** at the University of Kufa (Figure 3.7). SEM images were taken for all prepared specimens in order to clearly investigate the microstructure with high accuracy. The specimens were prepared with suitable grinding papers, polished and then etched by nital solution with the same steps as in the optical microscopic inspection for welds. Three regions across the weld centerline were studied; the weld zone, HAZ and the parent metal. The EDS was performed in order to obtain the elemental analysis especially the nickel content in the weld zone.

Figure (3.7): SEM and EDS device.

3.8 Mechanical Tests

3.8.1 Microhardness test

Micro hardness test was carried out using digital Vickers micro hardness tester type (HVS-1000) according to ASTM E92–-17. Measurements were done across the weld centerline on both sides of the welds (weld zone, HAZ and unaffected parent metal) after grinding process of the surfaces to be measured. This test was done with load of 500 g and loading time of 10 seconds. The measurement point distribution was by 1.0 mm intervals across the welds, with two measurements per point. This test was done at the labs of the Metallurgical Department-Faculty of Materials Engineering-University of Babylon.

3.8.2 Tension test

Figure (3.8) shows the shape and dimensions of the tensile test specimen used. The specimens manufactured by milling and grinding processes were as shown in Figure (3.9). Centerline of the weld was in the mid specimen and the tensile strength value was an average of three. All test specimens were notched in the weld zone with a radius of 2.5 mm to ensure that the fracture occurs in this zone. The test was carried out via universal type device WAW-200 China (Figure 3.10) according to (ATSM E8/E8M−13a) with a speed of 1 mm/min. at the labs of the Metallurgical Department-Faculty of Materials Engineering-University of Babylon.

G=50, W=12.5, T=6, L=200, A=64, B=64, C=20, R=13 (mm).

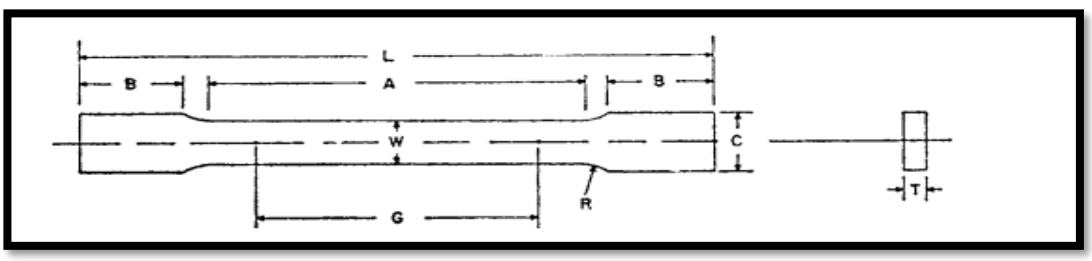

Figure (3.8): Tensile Test Specimen.

Figure (3.9): Shape of the manufactured tensile test specimens.

Figure (3.10): Tensile test device.

3.9 Fractography Observation

This test was performed on tensile specimens after fracture. The aim of this test is to determine the type, size and location of possible defects (including slag inclusions and cracks) which can be easily seen by the naked eye as photographed.

CHAPTER FOUR:

RESULTS & DISCUSSION

CHAPTER FOUR: RESULTS and DISCUSSION

4.1 Introduction

In this chapter, the results of experimental part will be introduced and discussed. Microscopy and microanalysis of low alloy steel welds will be studied using the optical microscope, SEM with the help of the EDS. Results of mechanical tests for these welds such as Vickers micro hardness and tensile strength will also be discussed. In addition, interior defects of these welds will be explored through the X-Ray radiography.

4.2 Materials and Welding Parameters

AISI-5147 steel has been chosen as a parent metal for being one of the most widely used low alloy steel types in industries. It has a wide range of applications for agricultural implements, transportation equipment, industrial machine structures, boilers, pressure vessels, marine engineering, chemical processing plants, nuclear power plants, furnaces and gas turbines [86-88]. In addition, it is considered a difficult steel to weld owing to its hardenability related to its contents of carbon and alloying elements [6,89].

EM12K solid wire - F7A5 flux is one of the most common combination used in SAW of low alloy steels [32], which is adopted in the Heavy Engineering Equipment State Company-Baghdad, the site in which the research was implemented.

It is clearly evident from Table (3.7) that in the second welding (Ni powder added with a weight percentage of 10%), the travel speed (welding speed) was reduced to 250 mm/min with the welding current value fixed at 330 A. The aim is to avoid or at least reduce the incomplete penetration that occurred in the first weld (without adding Ni powder to the flux). It is well known that the weld penetration increases with decreasing the travel speed [8]. In the

third welding (Ni powder added with wt. 20%), the value of the welding current was increased to 350 A in order to smelt the nickel well. Increasing both the welding current value and the added nickel percentage, however increases the deposition rates (the amount of metal deposited during a unit time). To counteract these high deposition rates, the travel speed was increased to 265 mm/min. This speed was fixed in the fourth welding with increasing the value of the welding current to 400 A to smelt the relatively high proportion of Ni powder added in this weld (30%). In the fifth and sixth welding, the current value was fixed at 400 A, but the travel speed was increased to 360 and 380 mm/min, respectively, in order to counteract the increased deposition rates due to the increased percentage of the added nickel (40% and 50% respectively).

4.3 X-Ray Radiography

The X-Ray radiography was performed on six weldments, the first one was with no nickel added to the weld. The other weldments were however welded with adding pure nickel powder to the flux in various weight ratios (10, 20, 30, 40 and 50 wt.%).

This test showed a small longitudinal crack at the weld center of the second weldment (Figure 4.1b), although nickel powder with a weight ratio of 10% was added to the flux, and the relatively low cooling rate of this weldment because the travel speed was slower (Table 3.7), and thus the amount of heat input was greater. It may be a hot crack attributed to segregation of micro-ingredients with relatively low solidification temperatures at the grain boundaries of the weld zone. These ingredients have low ductility and low strength at elevated temperatures causing rupture along the grain boundaries under the effect of thermal shrinkage stresses [54].

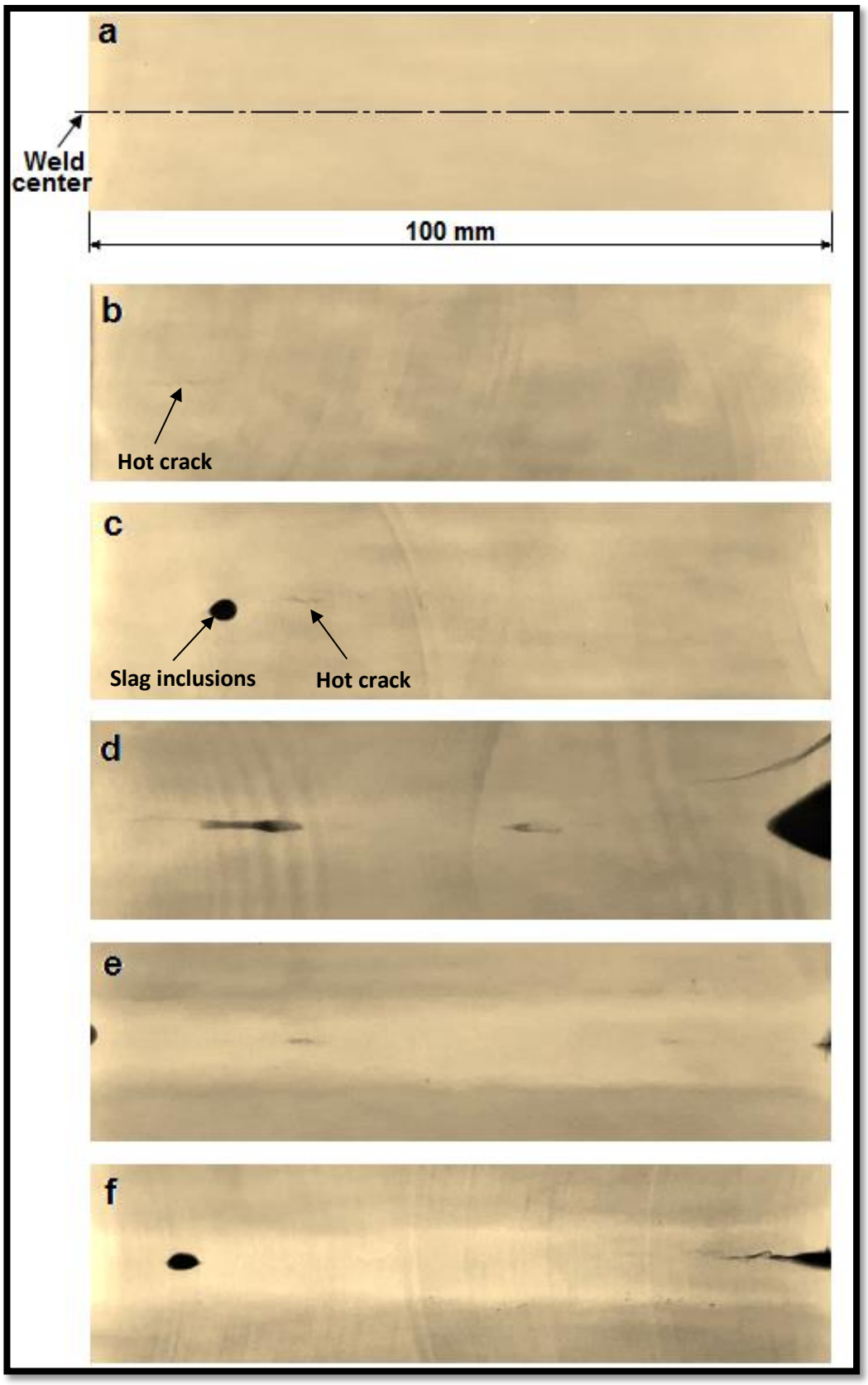

Figure (4.1): X- ray radiographic inspection: (a) for a weldment submerged arc welded with no nickel powder added to the flux, (b), (c), (d), (e) and (f) for weldments welded with adding nickel powder of different wt.% (10, 20, 30, 40 and 50) respectively.

The crack which appeared in the third weldment (Figure 4.1c) is smaller, and this might be due to the influence of nickel in the weld where the formation of hard and brittle micro-ingredients is prohibited [67]; the nickel element has a greater affinity for sulfur and phosphorus. This could increase the weld zone resistance to hot cracking [5]. The high ductility of nickel can play a significant role in absorbing tensile stresses created during welding, and thus contribute to decreasing the weld joint susceptibility to cracks [5]. The presence of few slag inclusions in the third weld could be attributed to the fact that with increasing the travel speed, the cooling rate increases due to decreasing the amount of heat input and thus leads to insufficient duration for slag to float on the surface of the weld [8]. The increased cooling rate could be the main cause of slag inclusions (with associated cracks sometimes) which appeared with various sizes and shapes in the weld center of the fourth, fifth and sixth weldments (Figure 4.1d, e and f respectively). No slag inclusions or cracks were observed in the first weld (Figure 4.1a).

4.4 Microstructural Results

Microscopy showed variations in the microstructures of the heat affected zone (HAZ) starting from the region adjacent to the weld zone (the grain growth region) to those unaffected by the weld temperature, passing through the grain refined and transition regions. These variations are attributed to large thermal gradients to which the HAZ is subjected from the melting temperature to that of the parent metal that is unaffected by the heat. This is typically followed by a rapid cooling rate resulting from the nearby, relatively cold parent metal and atmosphere. This heating and cooling cycle is ordinarily considered different heat treatments for each HAZ region. As is well known, the difference in the nature of the microstructures is reflected as differences in properties and thus differences in performance [6].

4.4.1 The First Sample

Microscopy of the AISI-5147 low alloy steel weld joined by the SAW process with no Ni added to the weld presented three regions: weld zone (WZ), heat affected zone (HAZ) and unaffected parent metal (PM).

4.4.1.1 Weld Zone

Figure (4.2) exhibits that the microstructure of the weld center predominantly was acicular ferrite and a small amount of pearlite colonies with ferrite at the grain boundaries. This is in agreement with that obtained by Trindade et al. (2007). The SEM microstructure of this zone with two different magnifications is presented in Figure (4.3).

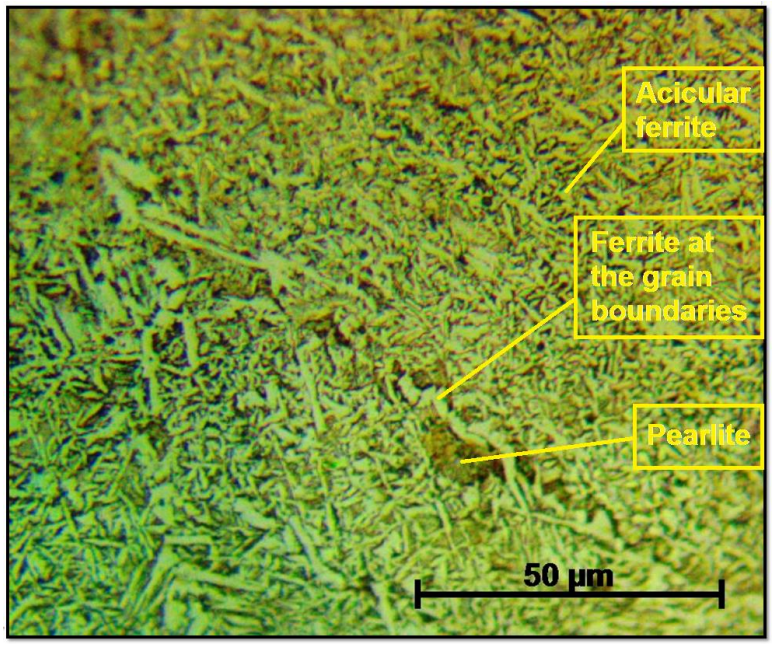

Figure (4.2): Optical microscopy of the weld center with no Ni added to the weld.

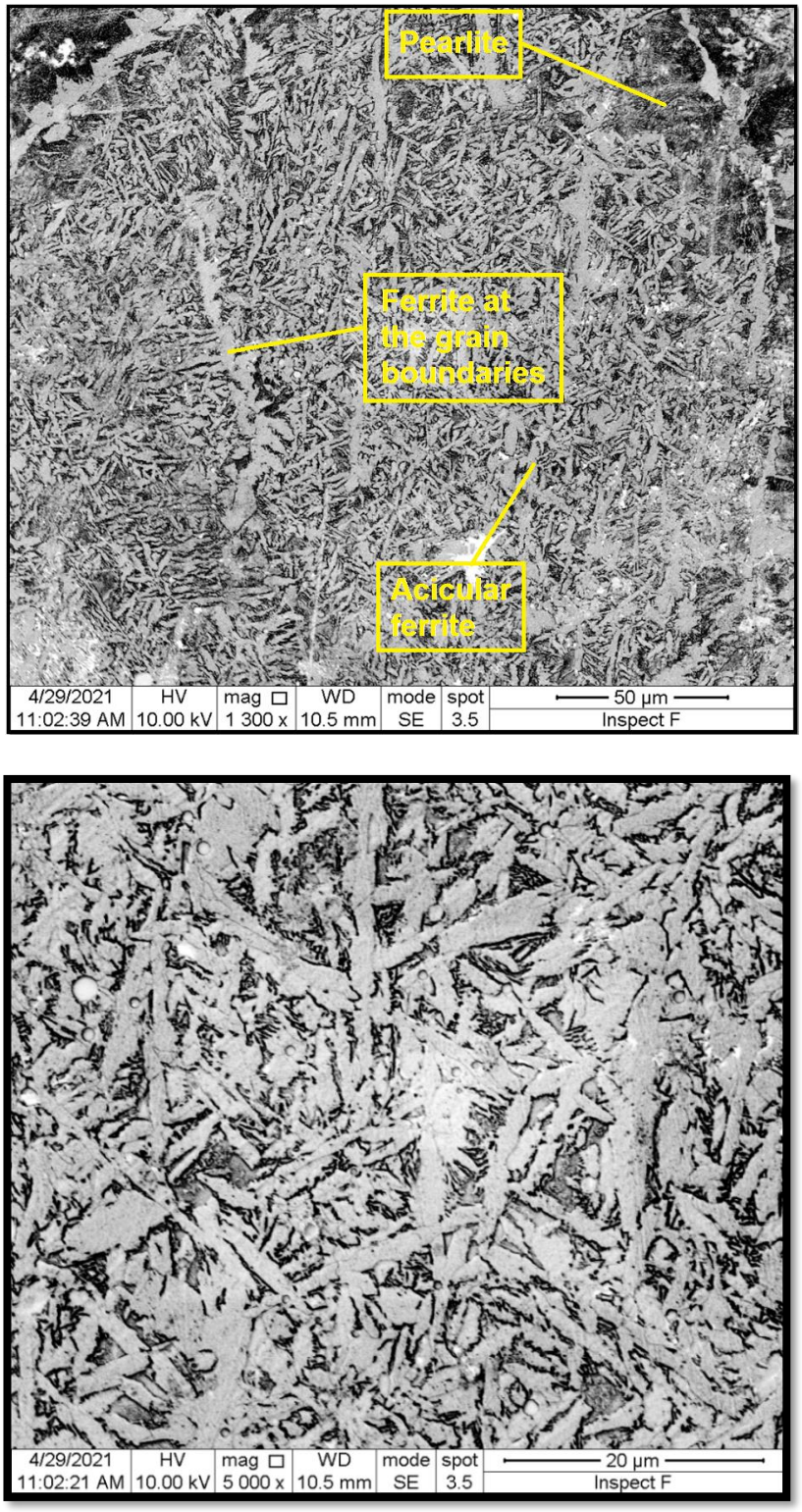

Figure (4.3): Microstructure of the weld center without adding Ni to the weld using an SEM with two magnifications.

While advancing from the weld center towards the HAZ, the pearlite colonies increase (Figure 4.4) due to the influence of dilution (paragraph 2.6.1).

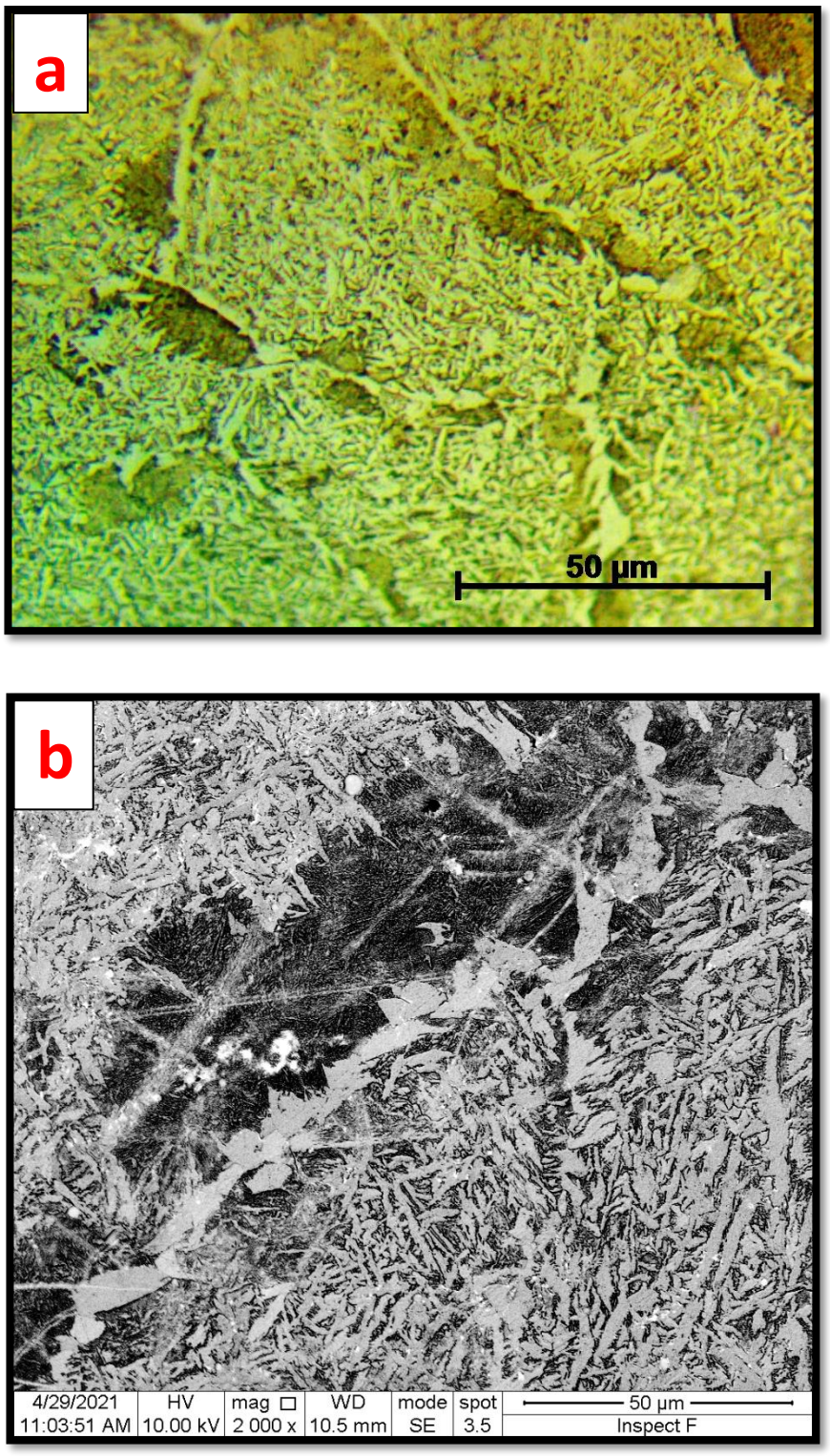

Figure (4.4): Micrography of the weld zone without adding Ni, using an (a): OM (b): SEM.

4.4.1.2 Heat Affected Zone

The microstructure of the HAZ varies within three regions as follows:

Coarse grain growth region (CGHAZ): it is the region immediate vicinity of the weld zone which is exposed to a higher temperature compared to other regions in the HAZ, so this region contains coarse grains. The microstructure of this region is very fine pro-eutectoid ferrite at the prior austenite grain boundaries, while the grains are coarse pearlitic and even coarser than those of the parent metal (Figure 4.5a). The resulting particle size of pearlite depends on the grain size of the austenite [50]. Accompanying with these structures, the figure also shows a structure looks like martensite or lower bainite or a mixture of them. Figure (4.5b) shows the SEM microstructure of this region. Moving towards the parent metal, the grain size of the coarse grained zone gradually decreases up to the FGHAZ.

Grain refined region (FGHAZ): it is the region vicinity of the grain growth region where the region just above A3 in the Fe-Fe$_3$C phase diagram is exposed to a temperature so that the grain growth is slight and the grains remain fine. The microstructure of this region shows a grain size smaller than that of the parent metal (Figure 4.6).

Transition region (Inter-critical HAZ): Figure (4.7) illustrates the microstructure of this region; the region vicinity of the FGHAZ (between A1 and A3). The finest grain size across the weld can be noticed in this region, in which the pearlite is partially spheroidized. The SEM presents that the microstructure of this region has partially spheroidized cementite in a ferrite matrix (Figure 4.8). Moving towards the parent metal, a sharp change in the grain size could be clearly observed while transition from the inter-critical to sub-critical zone (Figure 2.5). The structure of the sub-critical zone seems similar to that of the parent metal, in terms of the phase and grain size.

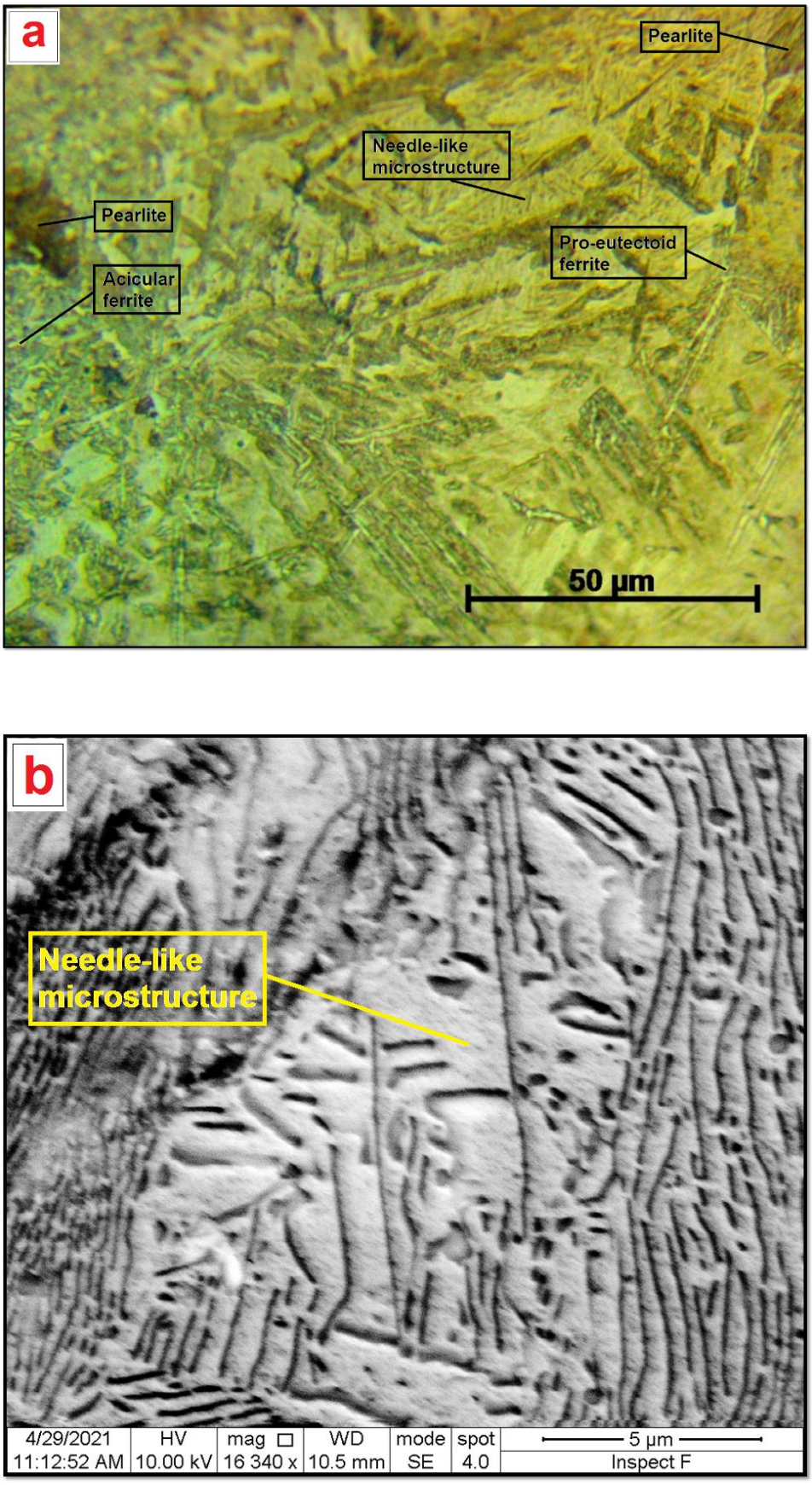

Figure (4.5): Microstructure of the CGHAZ of the 1st sample using an (a): OM and (b): SEM.

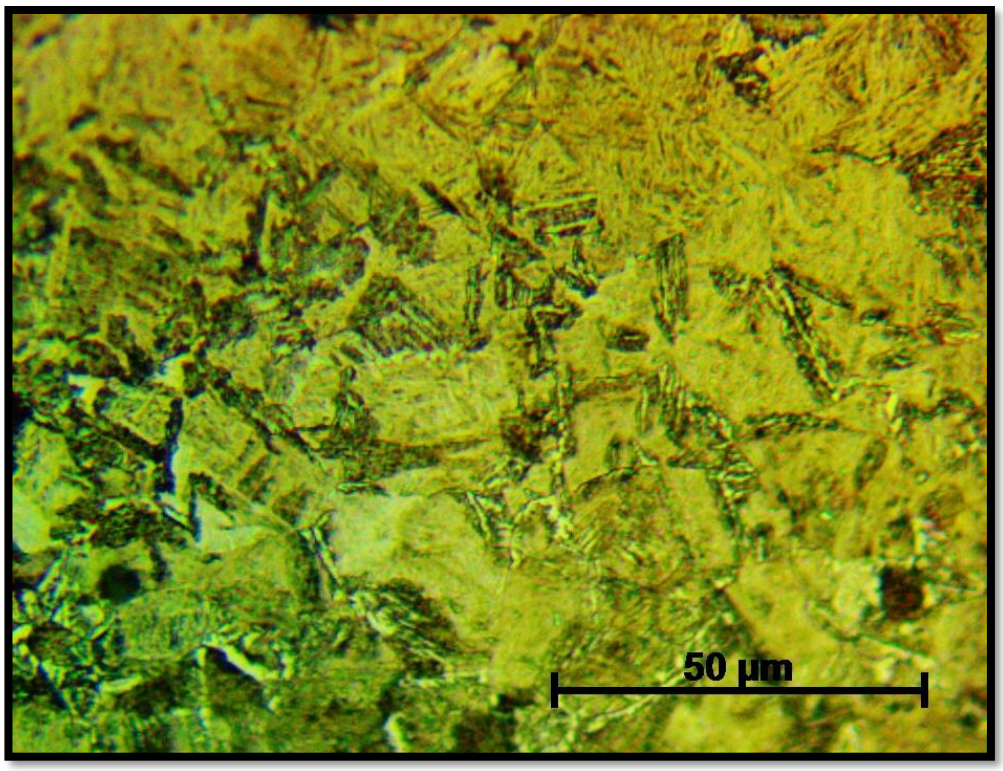

Figure (4.6): Optical microstructure of the FGHAZ of the 1st sample.

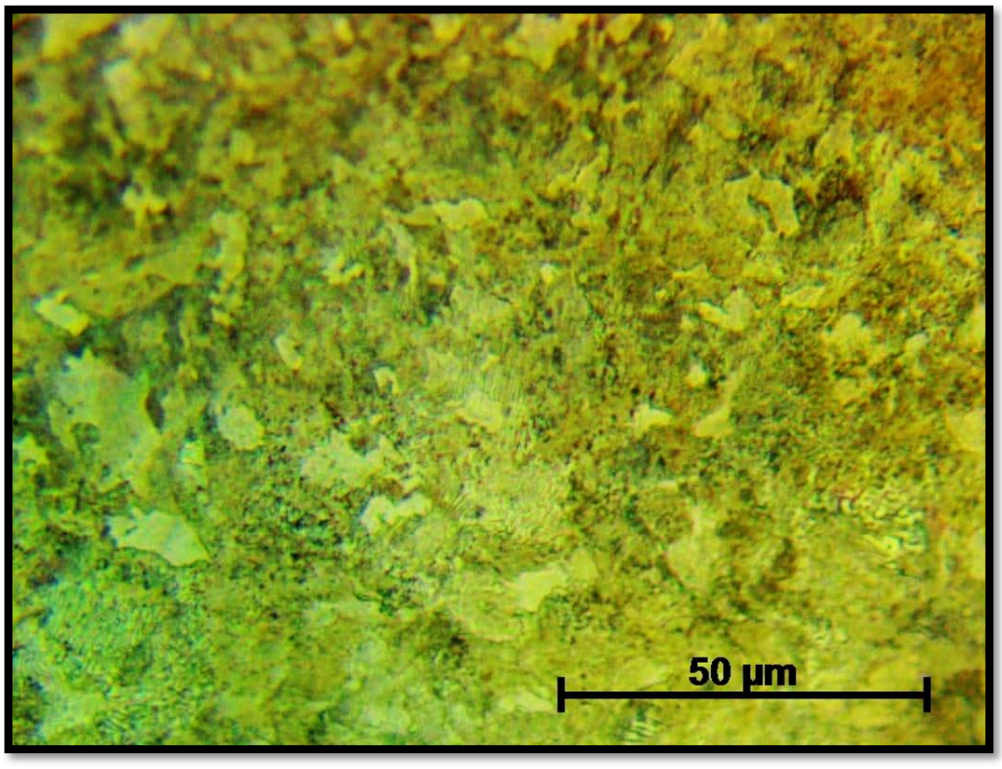

Figure (4.7): Optical microstructure of the Inter-critical HAZ of the 1st sample.

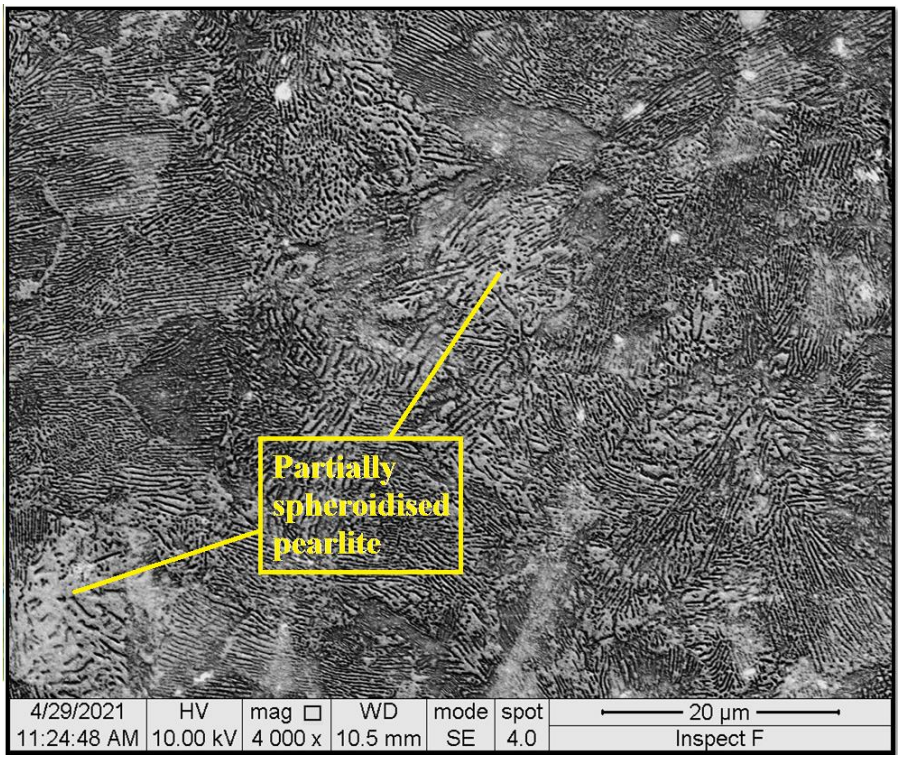

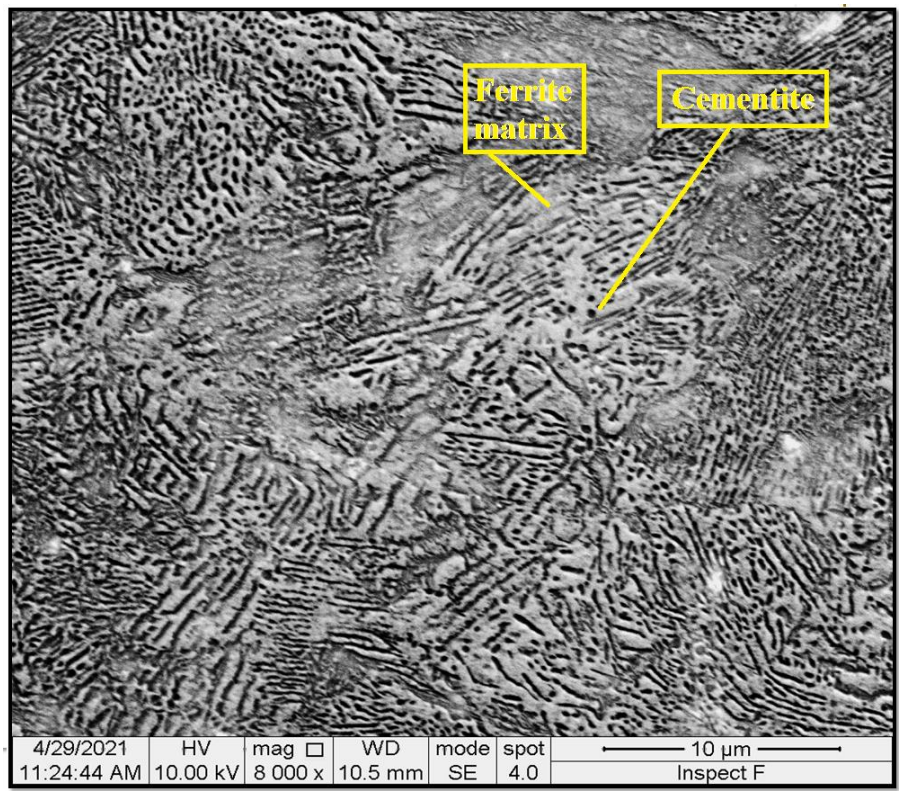

Figure (4.8): Micrography of the inter-critical HAZ of the 1st sample using an SEM with two magnifications.

4.4.1.3 Unaffected Parent Metal

This part of the parent metal comes immediately after the HAZ, where the microstructure exhibits a very small amount of pro-eutectoid ferrite with lamellar pearlite which has alternating lamellae of ferrite and cementite (Figure 4.9a). The SEM structure of the parent metal of the low alloy steel welds is shown in figure (4.9b).

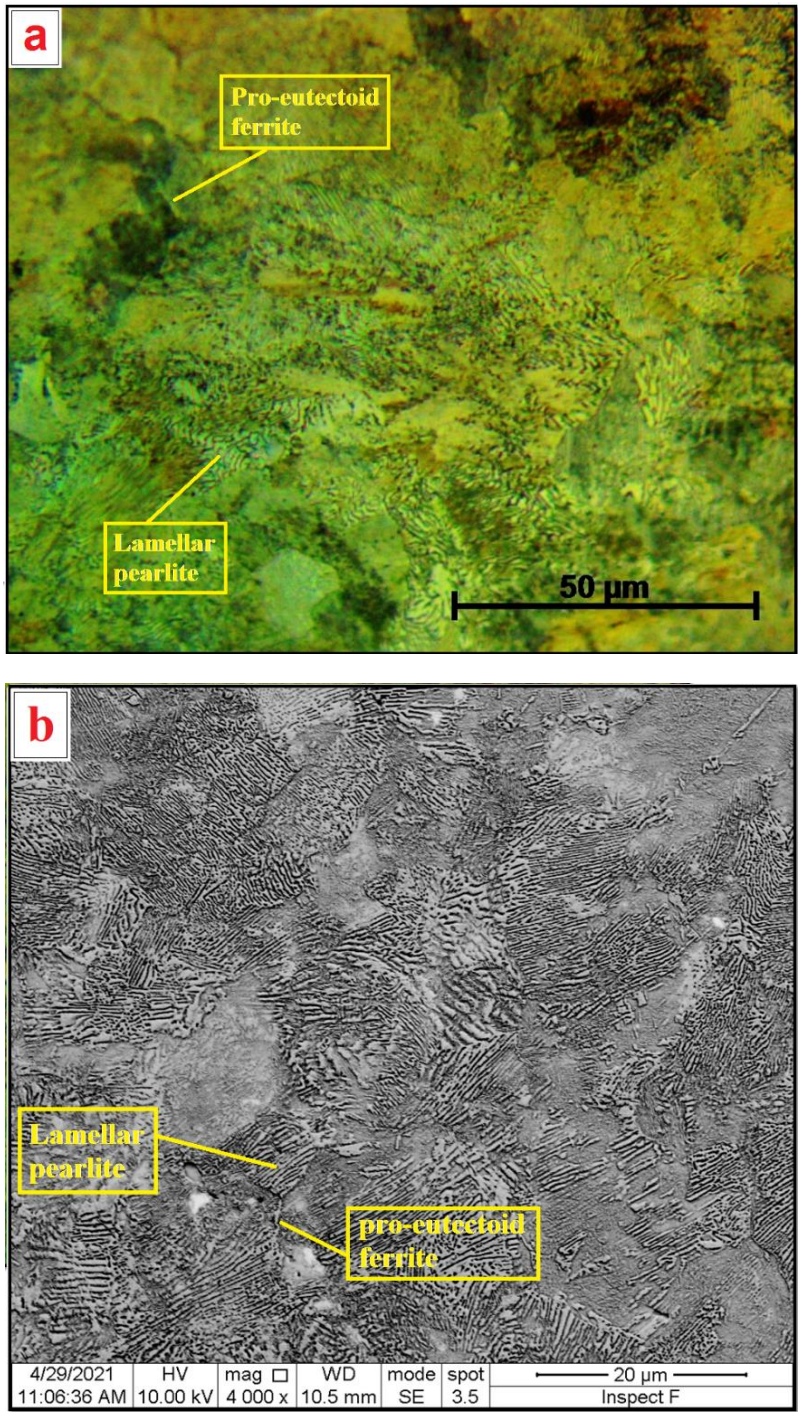

Figure (4.9): Unaffected parent metal microstructure by using an (a): OM and (b): SEM.

4.4.2 Samples Welded by Adding Nickel to the Flux

4.4.2.1 Weld Zones

The optical microscopy of the weld center for the 2nd sample which submerged arc welded with a 10 wt.% Ni added to the flux is shown in the Figure (4.10). The structure of the weld center was similar to that revealed in the 1st sample. It was mainly acicular ferrite and pearlite colonies with ferrite at the grain boundaries. Despite the fact that the Ni added to the weld refines the structure of the acicular ferrite [73], the figure shows that the acicular ferrite has a coarser structure. This could be attributed to the fact that the welding speed used with this sample was less than that used with the 1st sample (Table 3.7). This leads to an increase in the amount of heat input, which causes coarsening the structure. The SEM microstructure of the weld center with two different magnifications is shown in Figure (4.11). Similar to the 1st sample, the pearlite colonies increase while advancing from the weld center towards the HAZ (Figure 4.12).

Microscopic examination also presented no cracks, although the X-ray radiographic examination exhibited a slight crack in the weld center (Figure 4.1b) and this can be attributed to the fact that the crack was internal and not in the surface layer where the microscopy was performed.

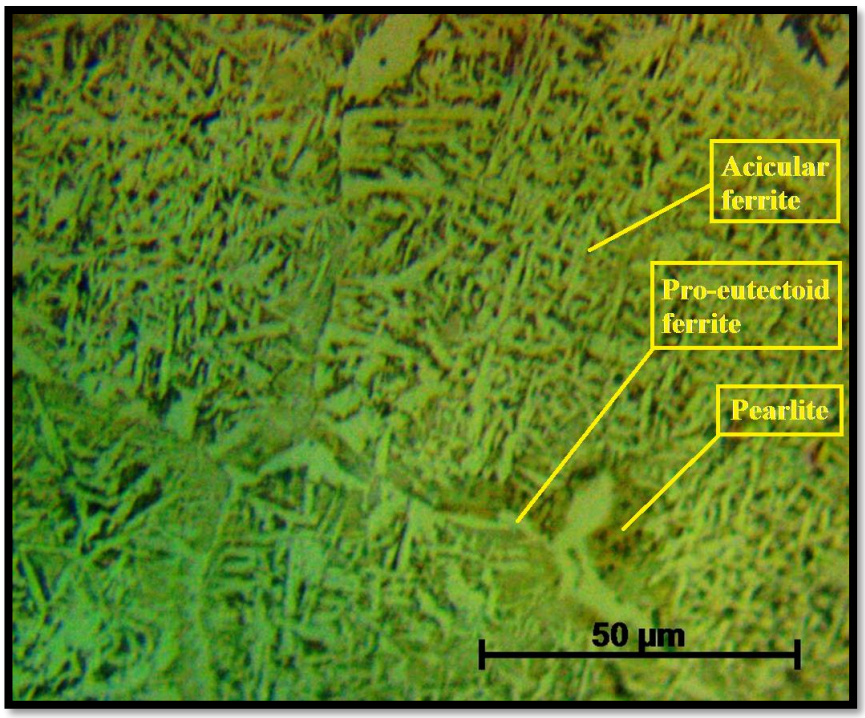

Figure (4.10): Optical microscopy of the weld center with a 10 wt.% Ni added to the flux.

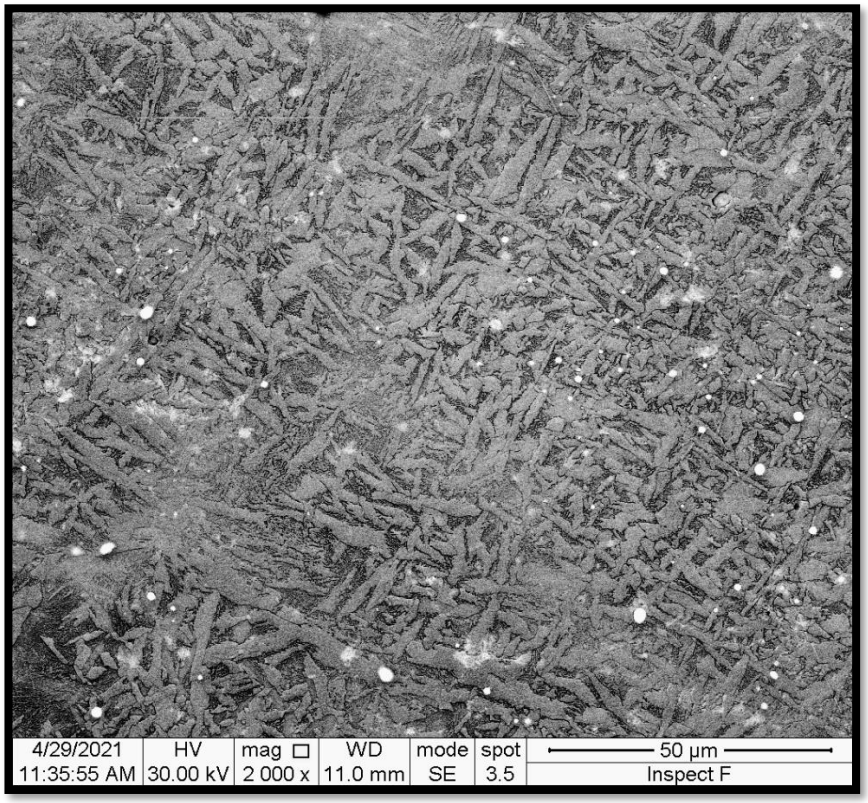

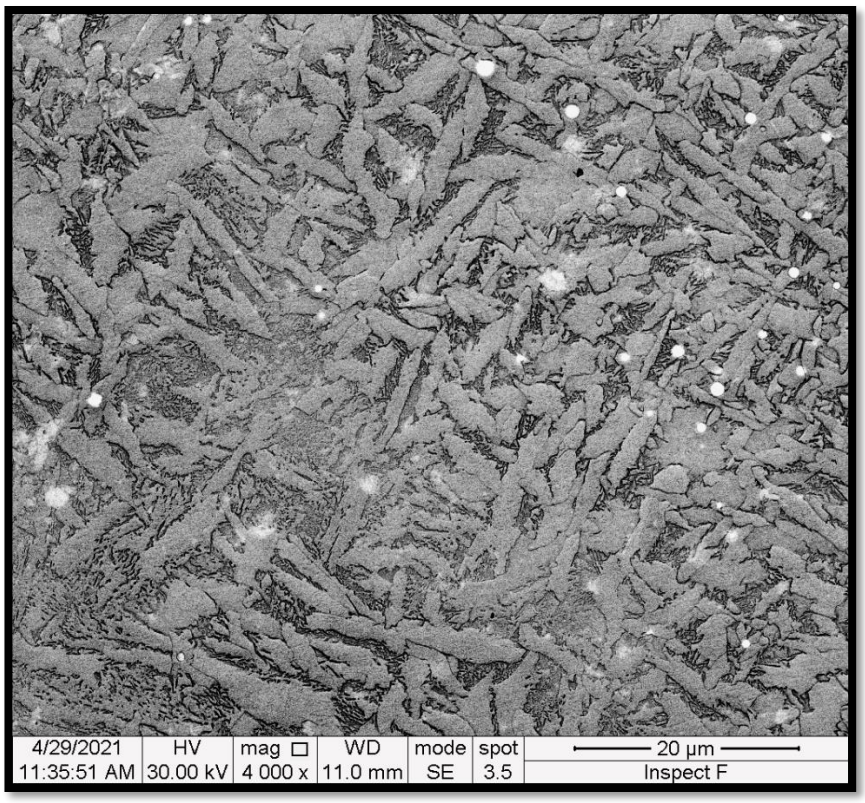

Figure (4.11): Microstructure of the weld center with a 10 wt.% Ni added to the flux using an SEM with two magnifications.

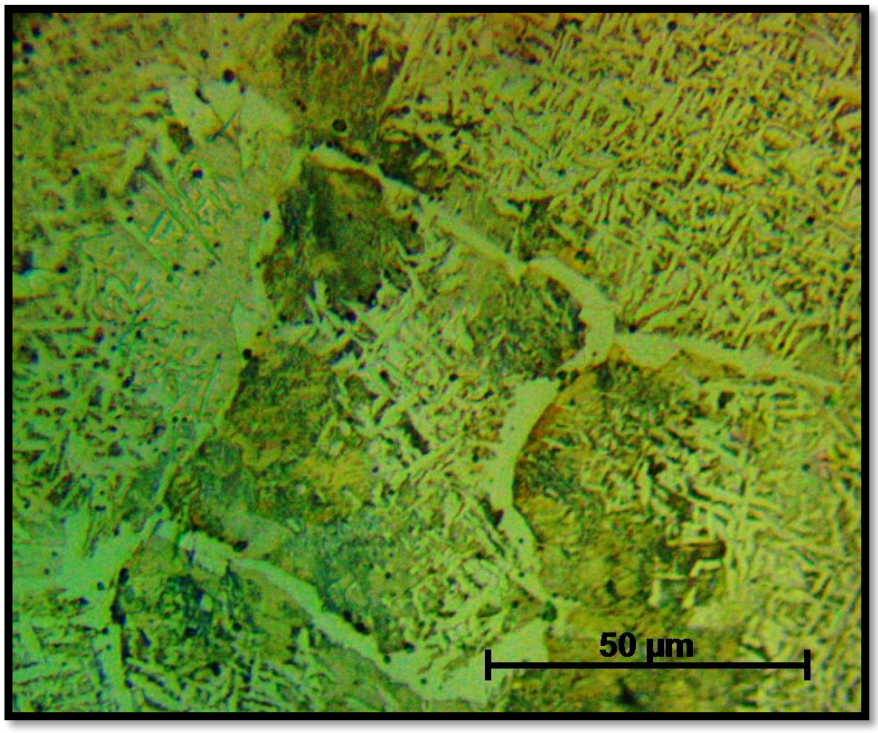

Figure (4.12): Micrography of the weld zone with a 10% wt.% Ni added to the flux.

As clearly observed in the last sample, microscopy of the 3rd sample welded with a 20 wt.% Ni powder added to the flux showed in the weld center acicular ferrite and pearlite colonies with ferrite at the grain boundaries. The acicular ferrite in this sample was however finer as shown in Figure (4.13a); this is in line with that obtained by Trindade et al. (2007). Figure (4.13b) presents the microstructure of this zone using the SEM.

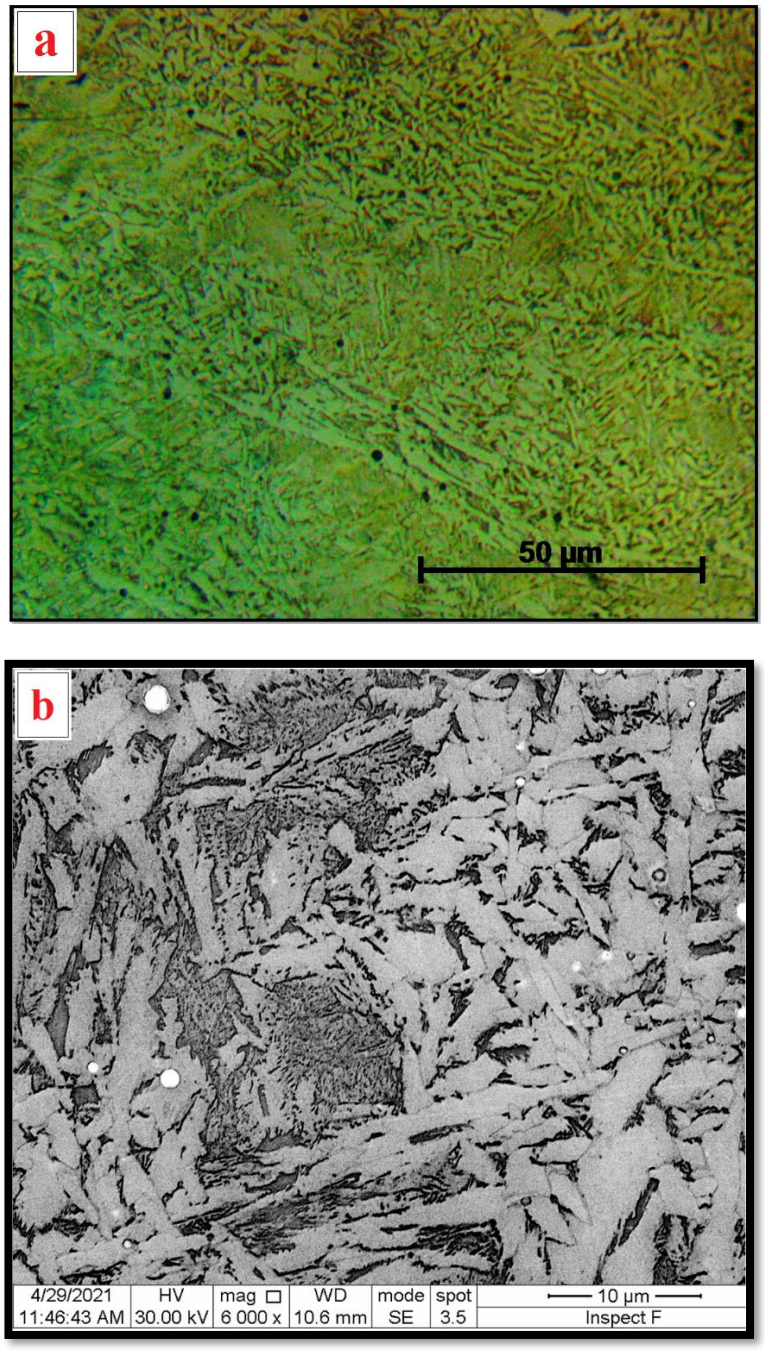

Figure (4.13): Micrography of the weld center with a 20% wt.% Ni added to the flux using an (a): OM and (b): SEM.

With an increase in the weight ratio of Ni powder added to the flux by 30%, the microstructure of the 4th sample showed a Ni structure at the expense of the proportion of acicular ferrite and pearlite colonies (Figure 4.14). The figure showed that increasing the weight ratio of Ni resulted in the refining of the acicular ferrite.

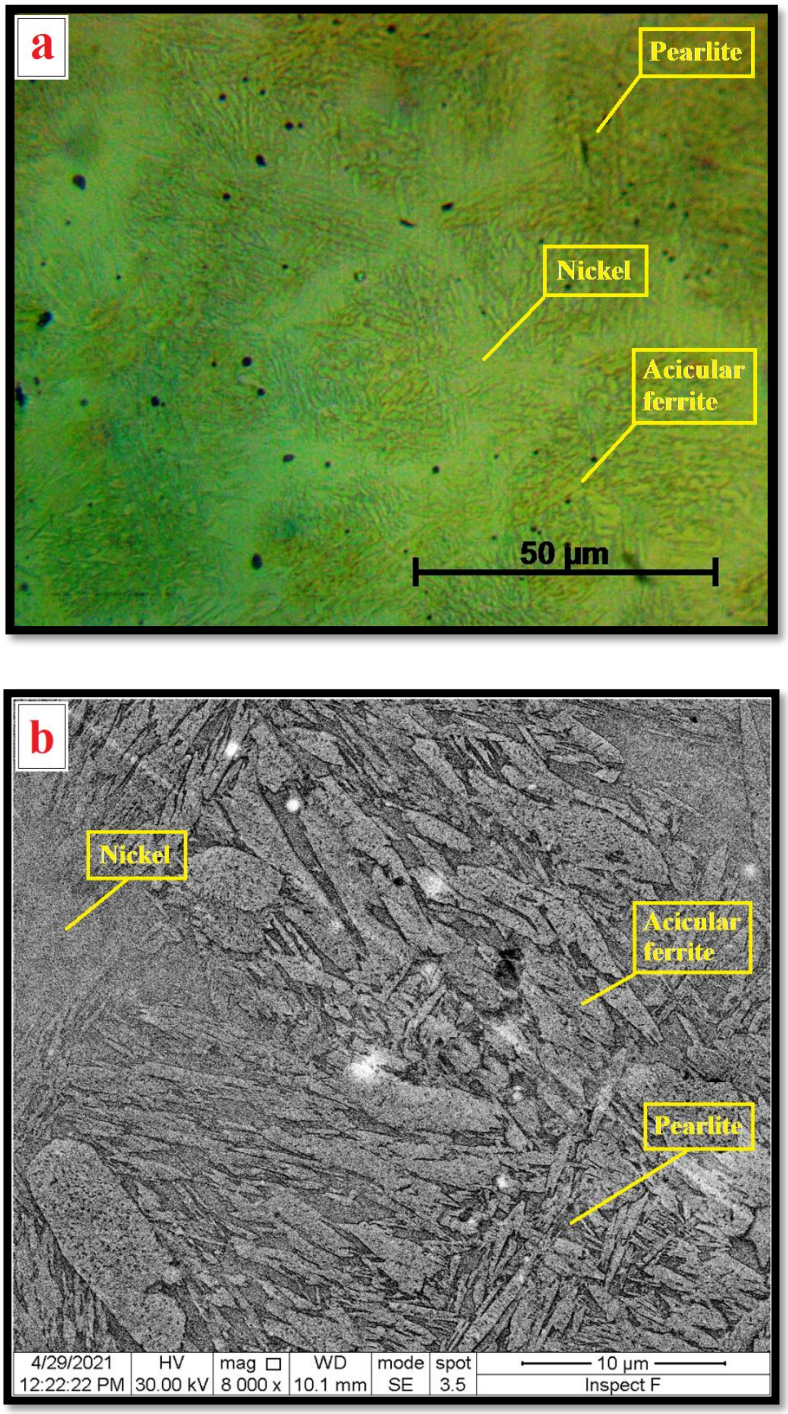

Figure (4.14): Micrography of the weld center with a 30% wt.% Ni added to the flux using an (a): OM and (b): SEM.

Microscopy of the 5th sample submerged arc welded with a 40 wt.% Ni powder added to the flux showed that the weld center is predominantly Ni structure (Figure 4.15). Through moving towards the HAZ, the microstructure of the weld zone looked like acicular ferrite and a very small amount of pearlite within a nickel matrix (Figure 4.16). However, the microstructure of the weld zone generally appeared to be only austenitic for the 6th sample welded with a 50 wt.% Ni powder added to the flux (Figure 4.17).

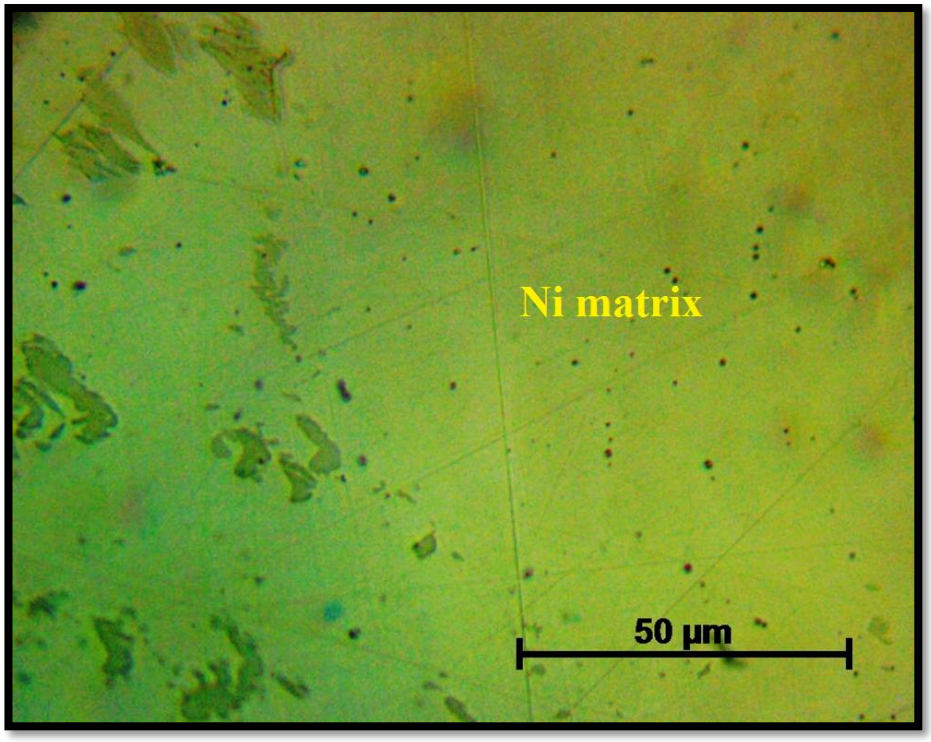

Figure (4.15): Optical microscopy of the weld center with a 40 wt.% Ni added to the flux.

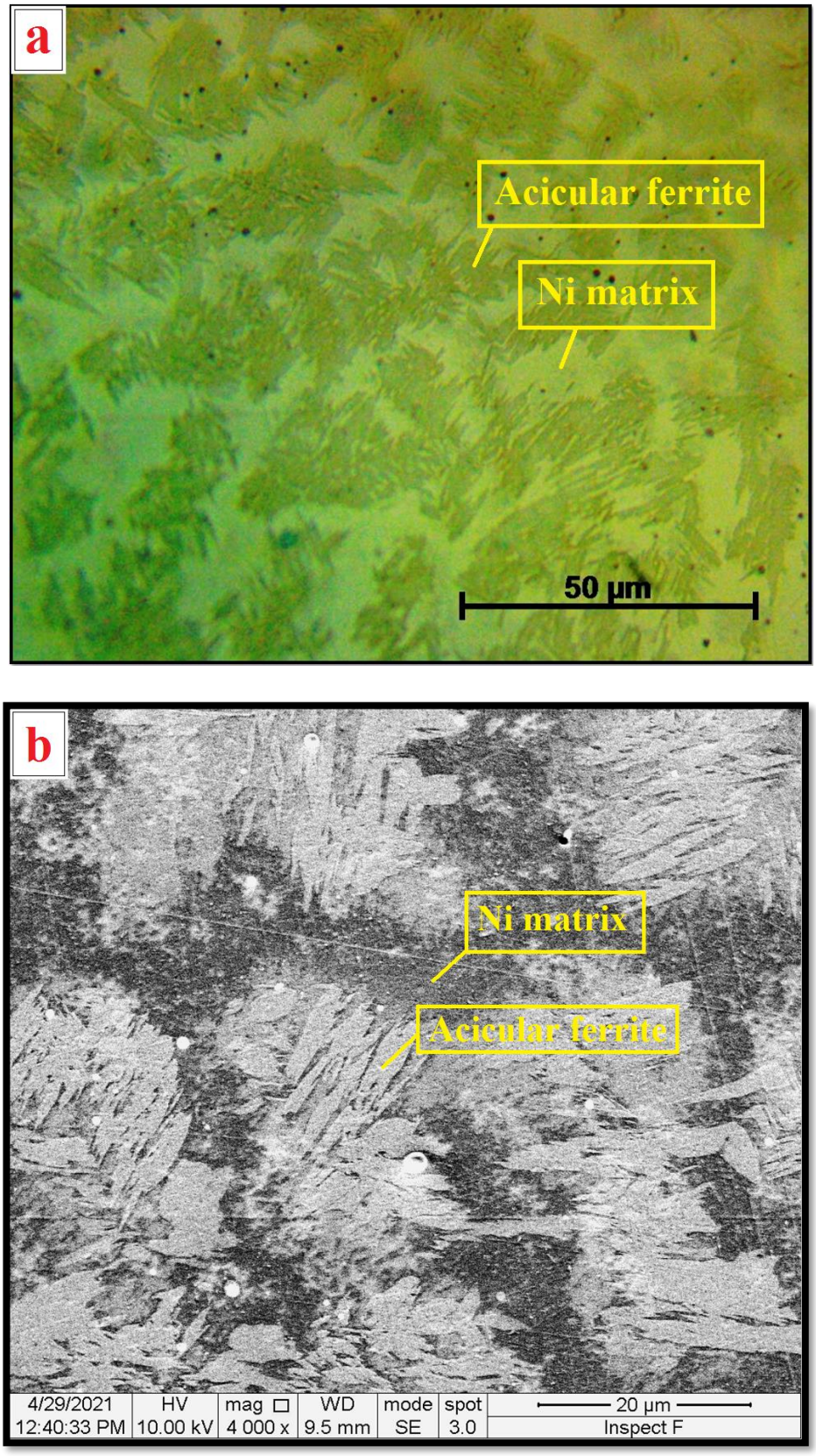

Figure (4.16): Micrography of the weld zone with a 40% wt.% Ni added to the flux using an (a): OM and (b): SEM.

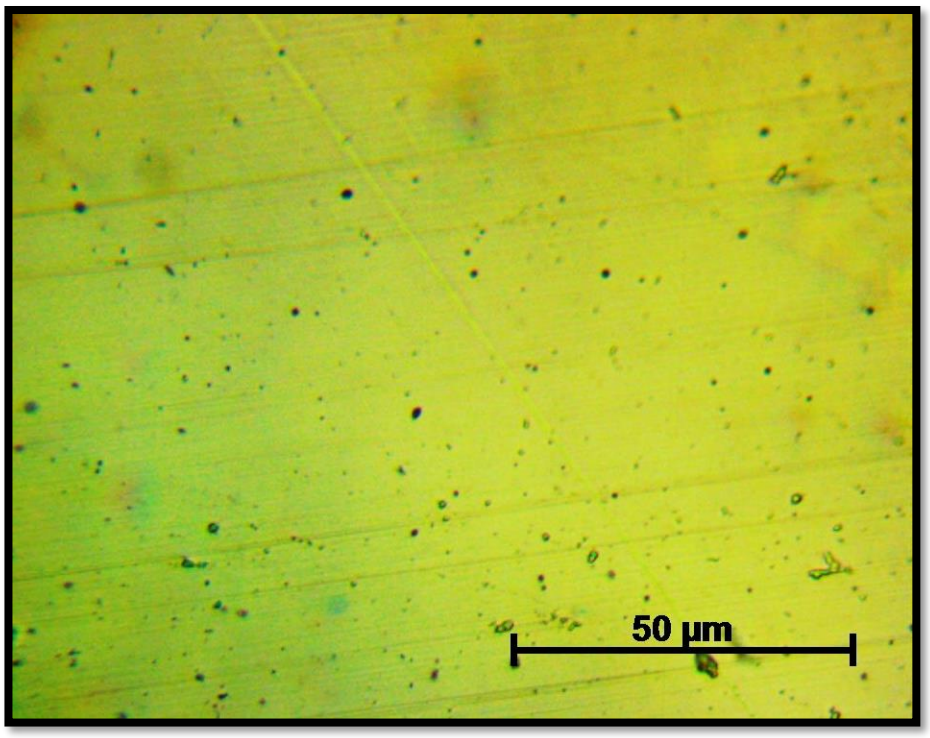

Figure (4.17): Optical microscopy of the weld zone with a 50 wt.% Ni added to the flux.

It is clearly observed from Figures (4.14a, 4.15, 4.16a and 4.17) that there are relatively densely diffuse porous defects in the weld zone of the fourth, fifth and sixth samples which were welded with adding nickel powder to the flux in weight ratios of 30, 40 and 50%, respectively. The possible reason behind this is that increasing the weight ratio of Ni powder at the expense of the flux will necessarily weaken the role of it; the most importance function of flux is to isolate the molten or hot weld zone from atmospheric contaminations causing porosity [17]. Another possible reason is that decreasing the weight ratio of the flux will definitely reduce the slag deposited on the weld metal, whose main benefit is to isolate the weld pool from the atmosphere, in addition to protect it from rapid cooling after welding [86]. Moreover, increasing the welding speed reduces the thermal input energy, and thus increases cooling rates. Rapid cooling rate typically causes insufficient time for the dissolved gas bubbles or those resulting from a reaction within the weld pool to exit into the atmosphere and thus remain trapped inside the solidified weld metal in the form of gaseous porosity [8].

This is likely to be obtained in the fifth and sixth samples due to the high welding speed (360 and 380 mm/min respectively). However, the fourth sample, in which the porous defects also appeared, had a relatively low cooling rate due to the use of the same welding speed utilized with the third sample (265 mm/min) with an increase in the current value to (400 A). So the first two reasons are the most likely to have these porous defects.

4.4.2.2 Heat Affected Zones

Welding parameters seem to affect not only the microstructure of the weld zone, but also that of the HAZ. Figure (4.18) shows the microstructure of the region adjacent to the weld zone for the second sample. The structure seems to be a troostitic pearlite with martensite, which is commonly known as primary troostite [45]. This structure appeared because the welding speed used with this sample was slower than in the first sample (Table 3.7). The SEM however revealed a small amount of structure similar to upper bianite. The microstructure of the same region in the third sample seems to be a mixture of troostitic pearlite, upper bianite and martensite structure more than that appeared in the second sample (Figure 4.19) as a result of the faster cooling rate associated with the higher welding speed used with this sample. In the fourth sample, the microstructure of this region revealed that the upper bianite structure increased at the expense of martensite (Figure 4.20). This could be attributed to a relatively low cooling rate compared to that of the third sample as mentioned previously. The martensitic structure increased significantly at the expense of the upper bianite structure in the same region for the fifth and sixth samples (Figures 4.21 and 4.22 respectively) even the structure of this region in the sixth sample appeared to be almost fully martensitic. The reason behind this is that cooling rates are higher than that in the fourth sample due to the significantly increased welding speed for these two samples with the use of the same current value.

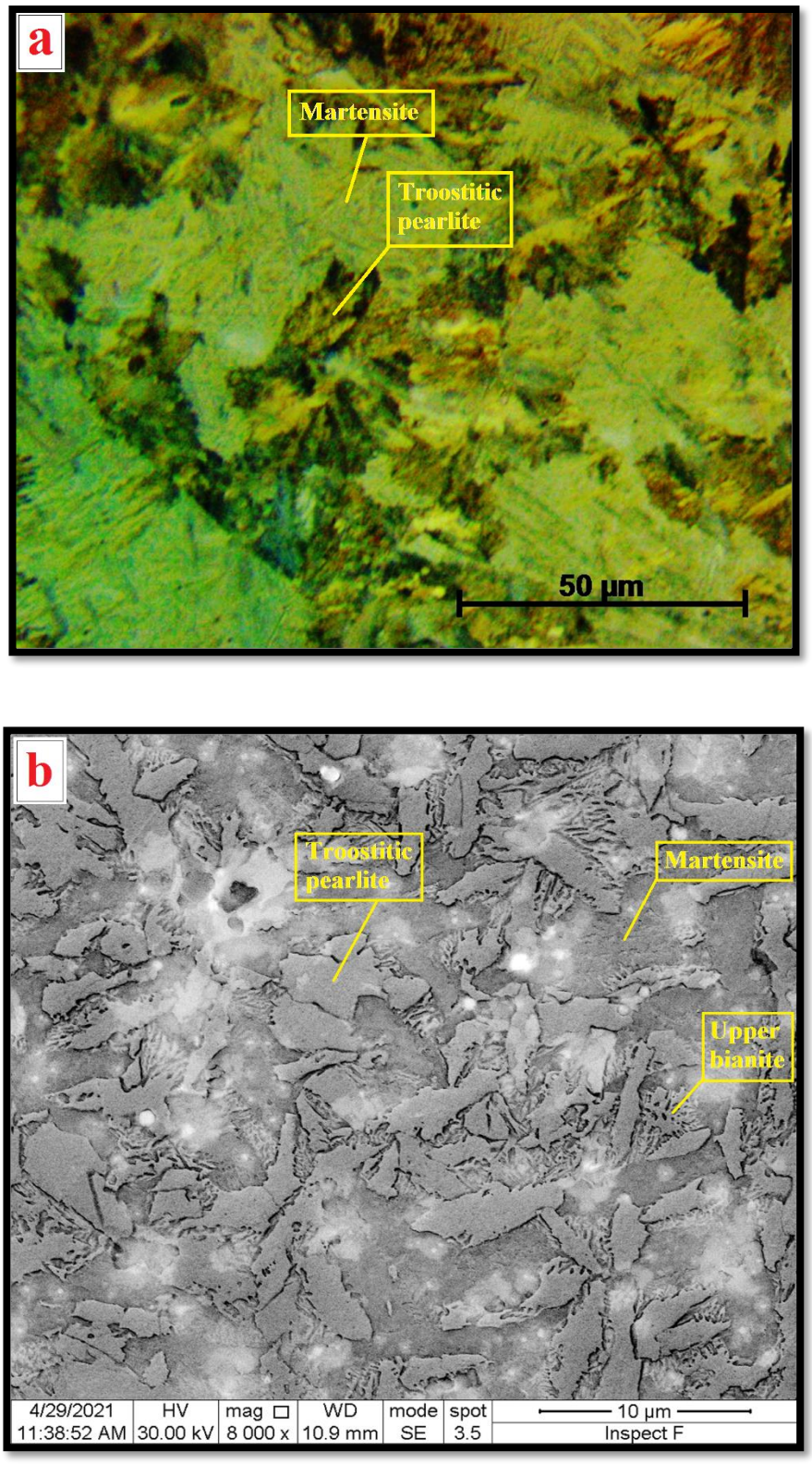

Figure (4.18): Micrography of the CGHAZ of the 2nd sample using an (a): OM and (b): SEM.

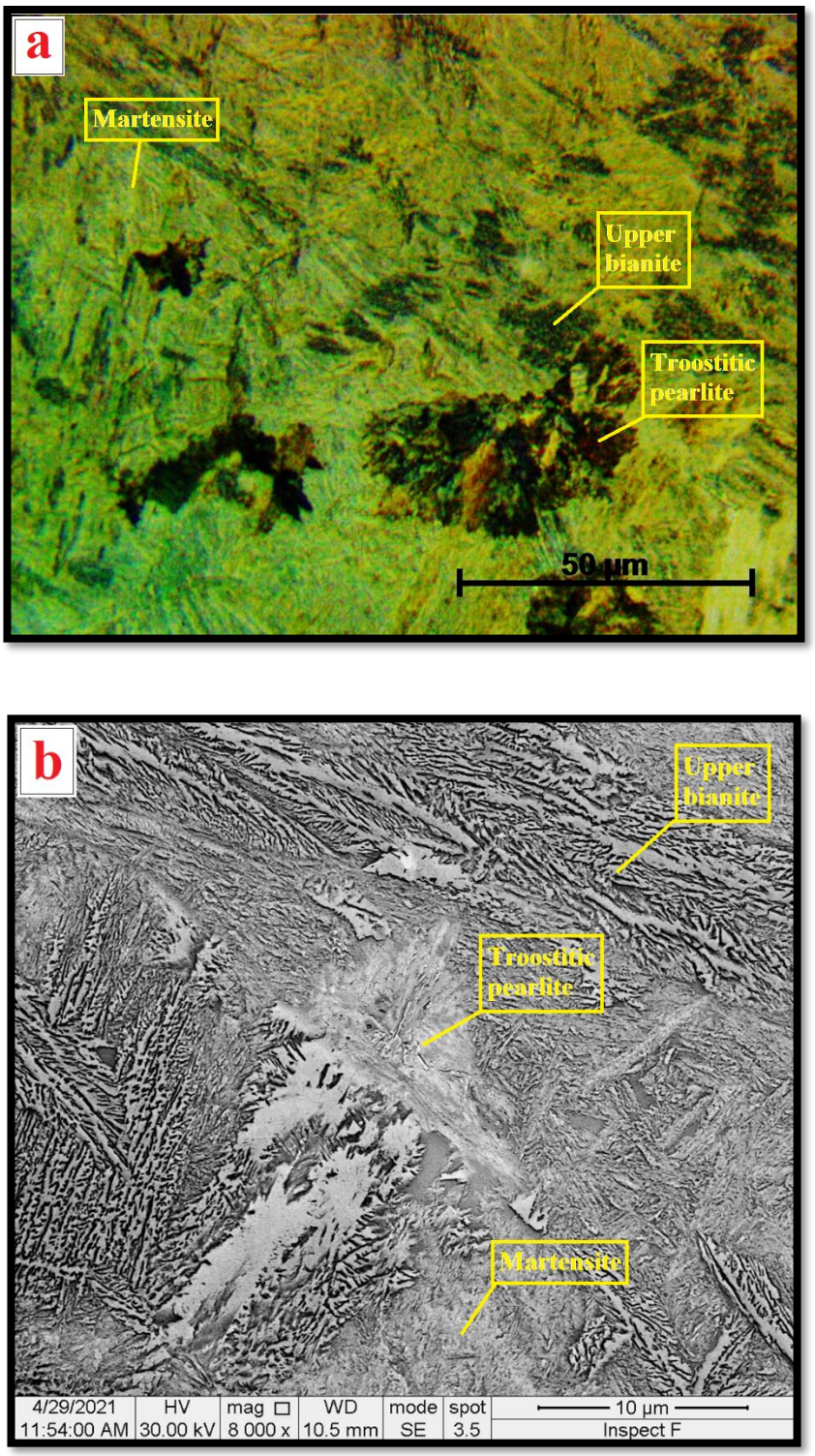

Figure (4.19): Micrography of the CGHAZ of the 3rd sample using an (a): OM and (b): SEM.

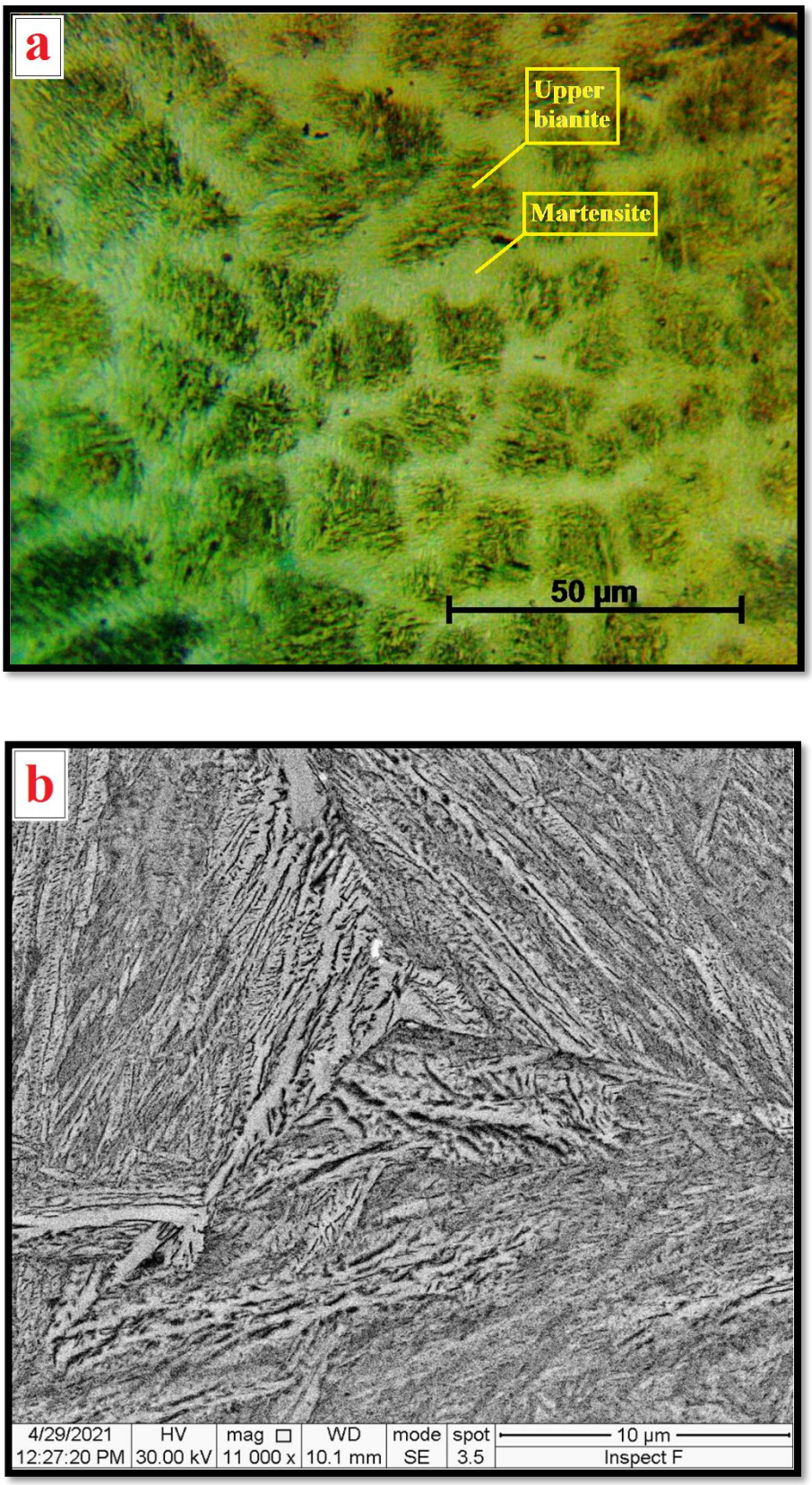

Figure (4.20): Micrography of the CGHAZ of the 4th sample using an (a): OM and (b): SEM.

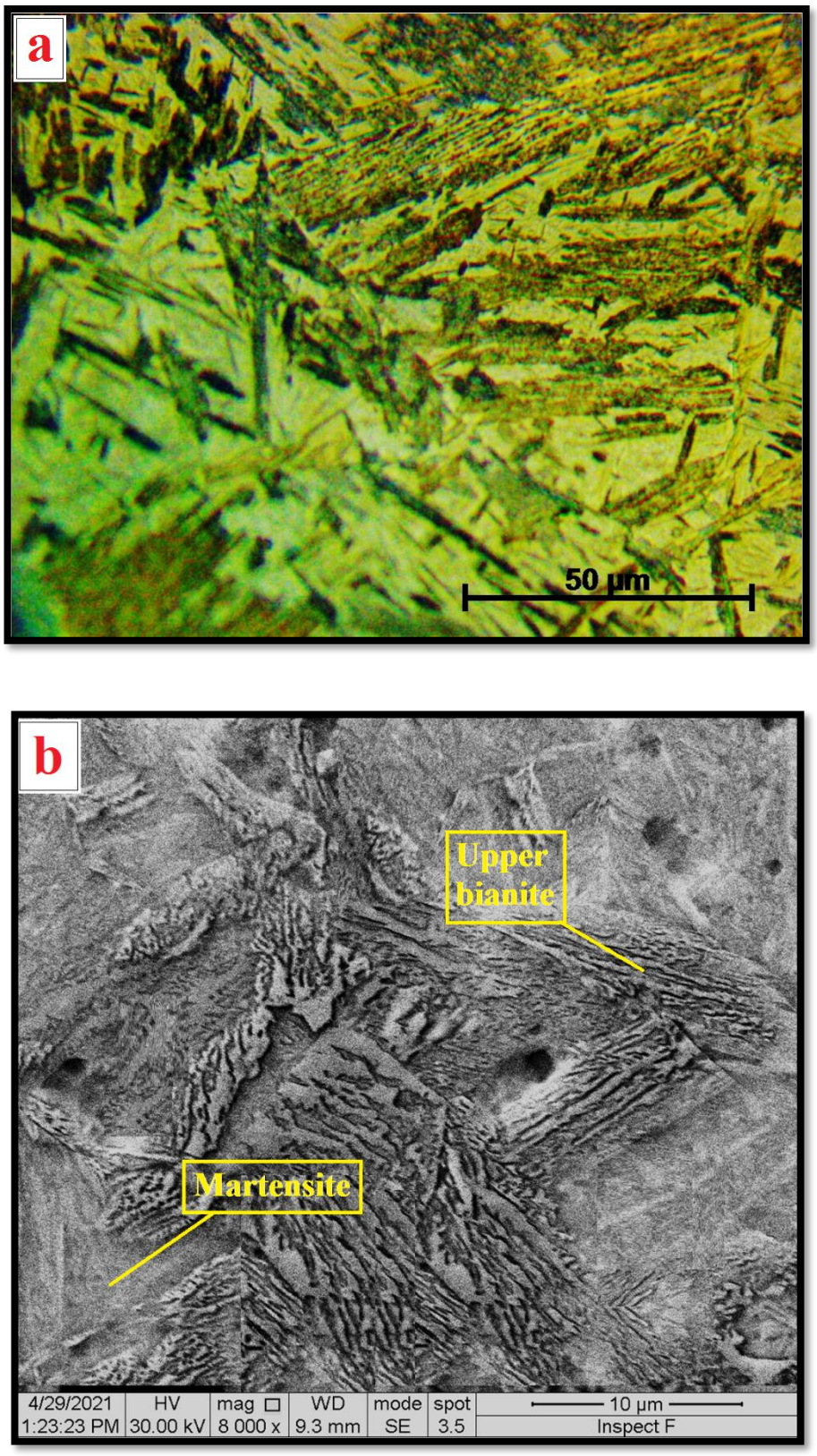

Figure (4.21): Micrography of the CGHAZ of the 5th sample using an (a): OM and (b): SEM.

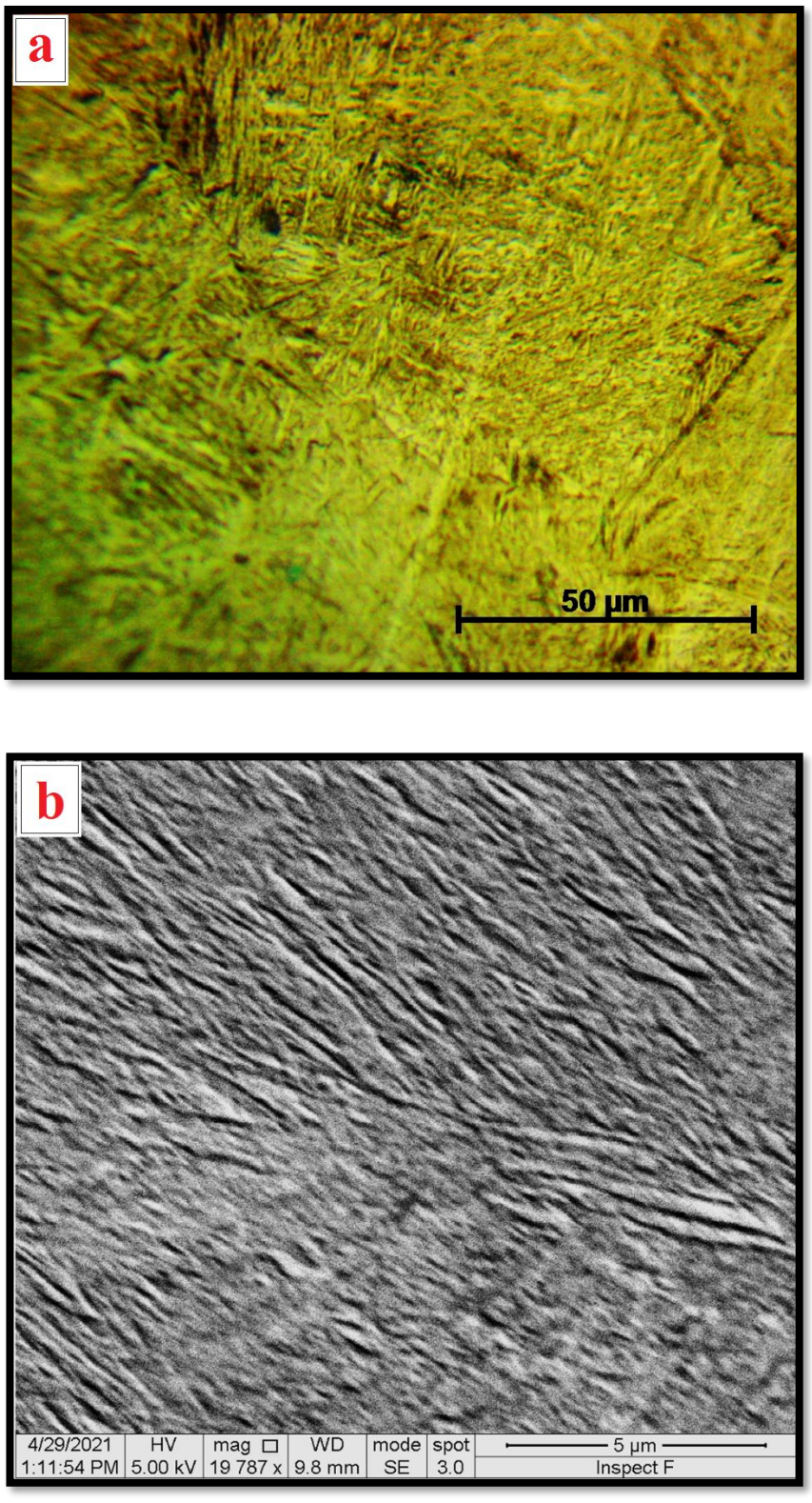

Figure (4.22): Micrography of the CGHAZ of the 6th sample using an (a): OM and (b): SEM.

Through advancing from the CGHAZ towards the unaffected parent metal, the structures become finer. This is because this region is exposed to temperatures just above A3, so that the suitable conditions are not available for the occurrence of the grain growth. Following the RGHAZ regions, the structure that appeared in all samples was partially spheroidized pearlite, where the finest grain size across the weld was (Figure 4.8).

4.5 Energy Dispersive Spectrometer

The SEM spectrums for energy dispersive spectrometer (EDS) of the 6^{th} sample examination and EDS results presented in Figures (4.23) and (4.24) the variation of nickel element wt. % across the submerged arc low alloy steel welds. In general, the nickel content slightly decreases through advancing from the weld center towards the HAZ, where it disappears. Some test points showed nickel slightly more than those in the weld centers. This might be due to the incomplete homogeneity in mixing the nickel powder with the flux. The results were consistent with those obtained by [5] despite the difference of the welding process used.

Spectrum: Acquisition

Nickel	Series	unn. C [wt.%]	norm. C [wt.%]	Atom. C [at.%]	Error (1 Sigma) [wt.%]
1	K-series	15.98	27.29	26.32	1.40
2	K-series	16.25	27.19	26.22	1.16
3	K-series	15.71	27.97	26.98	1.01
4	K-series	15.61	26.84	25.87	0.99
5	K-series	6.42	10.75	10.28	0.64

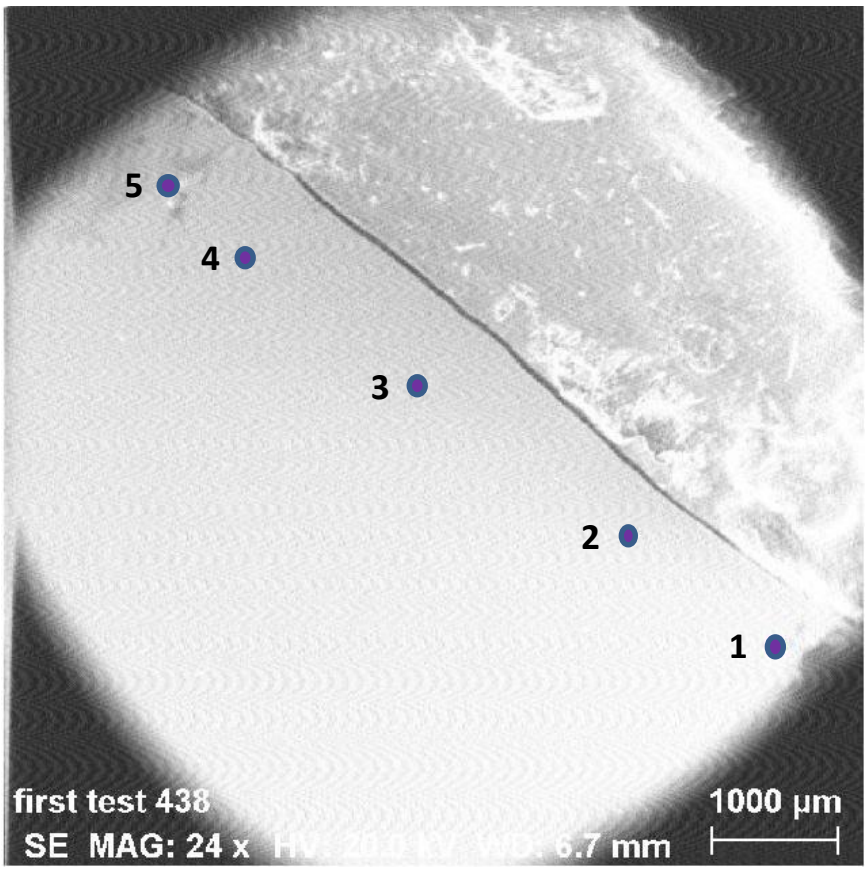

Figure (4.23): SEM spectrums for EDS of the 6th sample.

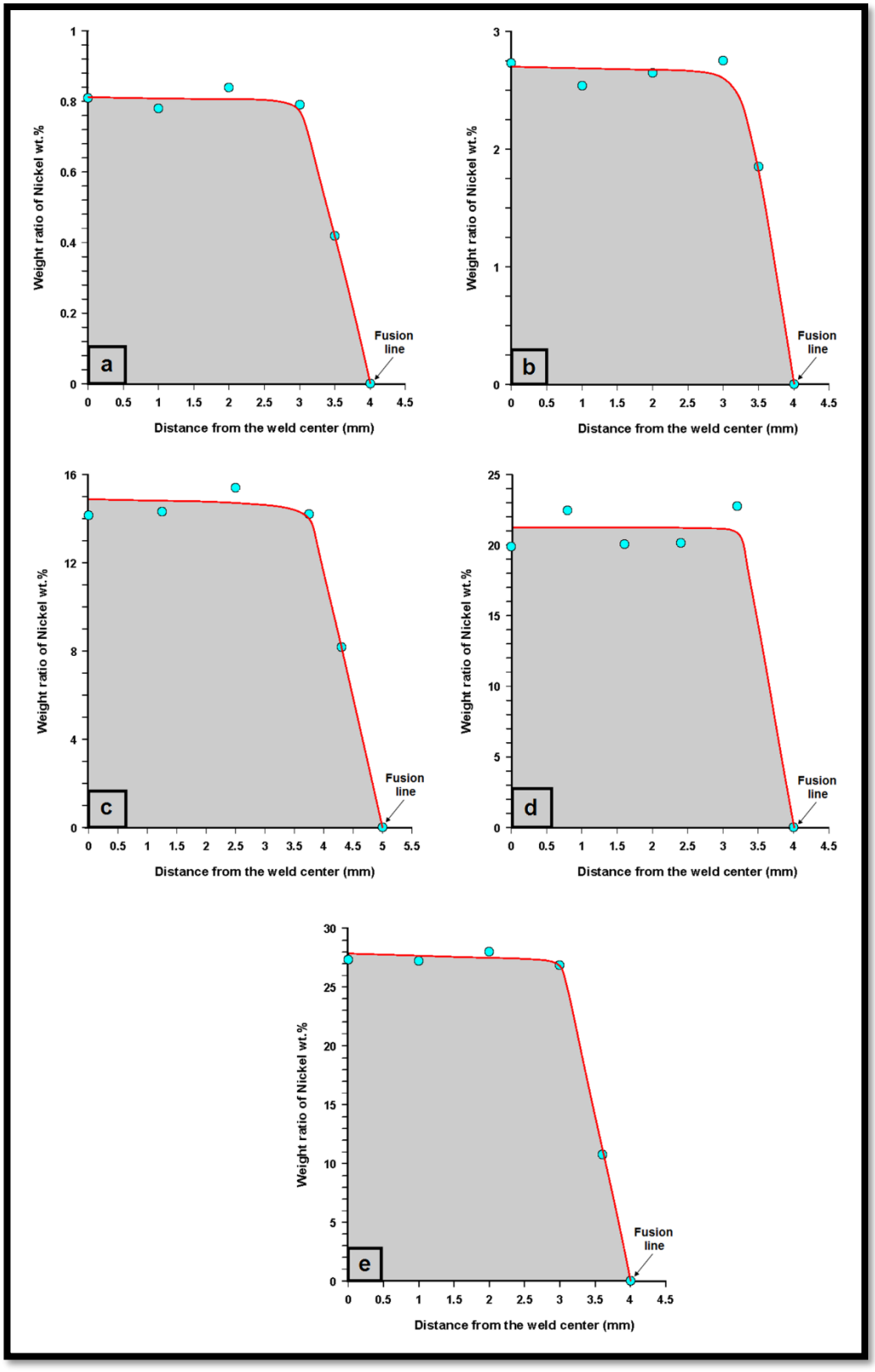

Figure (4.24): The variation of Ni element wt. % examined by the EDS across the submerged arc low alloy steel welds.(a), (b), (c), (d) and (e) for weldments joined with adding Ni powder of different wt.% (10, 20, 30, 40 and 50) respectively.

4.6 Microhardness Test

Due to a series of microstructural variations across the welds, the hardness was expected to vary as well. The hardness test is the easiest way to assess the quality of the weld and, accordingly, the weld performance. It is also important as a way to differentiate the different weld zones.

4.6.1 The First Sample

Figure (4.25) shows the hardness distribution across the AISI-5147 low alloy steel welds joined by SAW process with no Ni added to the flux. Hardness varies while advancing from the weld center (point 1) towards the parent metal (point 4). The hardness value sharply rises on slightly moving from the weld center (~225 HV) towards the parent metal up to the maximum value across the weld (~480 HV) at a 3 mm distance away from the weld center (point 2). Moving towards the parent metal, the hardness decreases to the minimum value across the weld (~193 HV) at a 13 mm distance away from the weld center (point 3). The hardness then increases to the parent metal hardness value (211 HV) at about 17 mm distance away from the weld center (point 4).

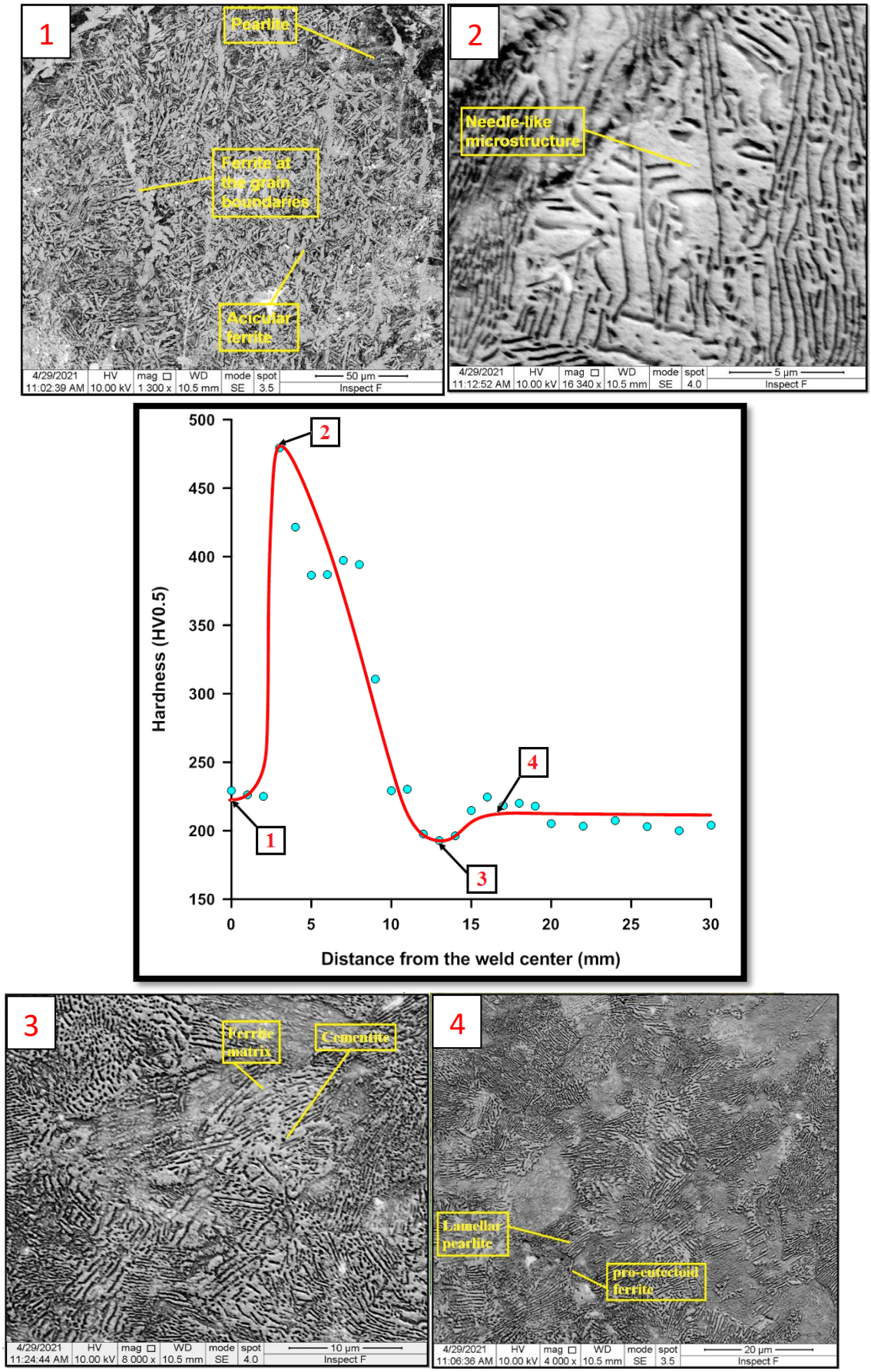

Figure (4.25): The hardness distribution across the AISI-5147 low alloy steel welds joined by SAW process with no Ni added to the flux.

The maximum hardness (~480 HV on average) across the weld is at a region 3 mm distance away from the weld centre. There are two possible reasons behind this sharp rise in hardness. The first one is the presence of very small amount of the soft ferrite phase in the microstructure of this region (Figure 4.25-2) compared to that in the weld center (Figure 4.25-1). The second reason is that the cooling rate in this region is generally higher than those in the other regions of the HAZ due to the severe thermal gradient from the higher temperature of this region to that of the cold parent metal causing a structure looks like martensite or lower bainite or a mixture of them. The hardness is therefore higher.

The minimum hardness (~193 HV on average) across the weld, which was observed in the inter-critical zone, could be attributed to the partially spheroidized pearlite structure in this region which consists of a partially spheroidised cementite in a soft ferrite matrix (Figure 4.25-3).

4.6.2 Samples with Different Nickel Contents

The Hardness distribution across the weld of the samples which submerged arc welded with adding pure nickel powder to the flux in various weight ratios (10, 20, 30, 40 and 50 wt.%) is shown in Figure (4.26).

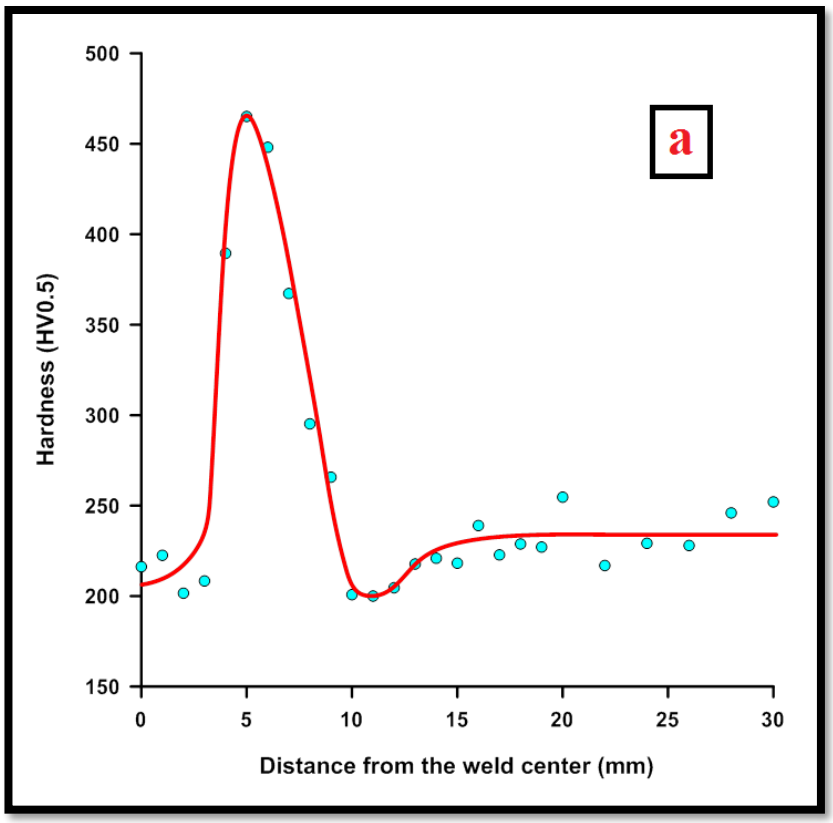
a
Hardness (HV0.5)
500
450
400
350
300
250
200
150
0
5
10
15
20
25
30
Distance from the weld center (mm)

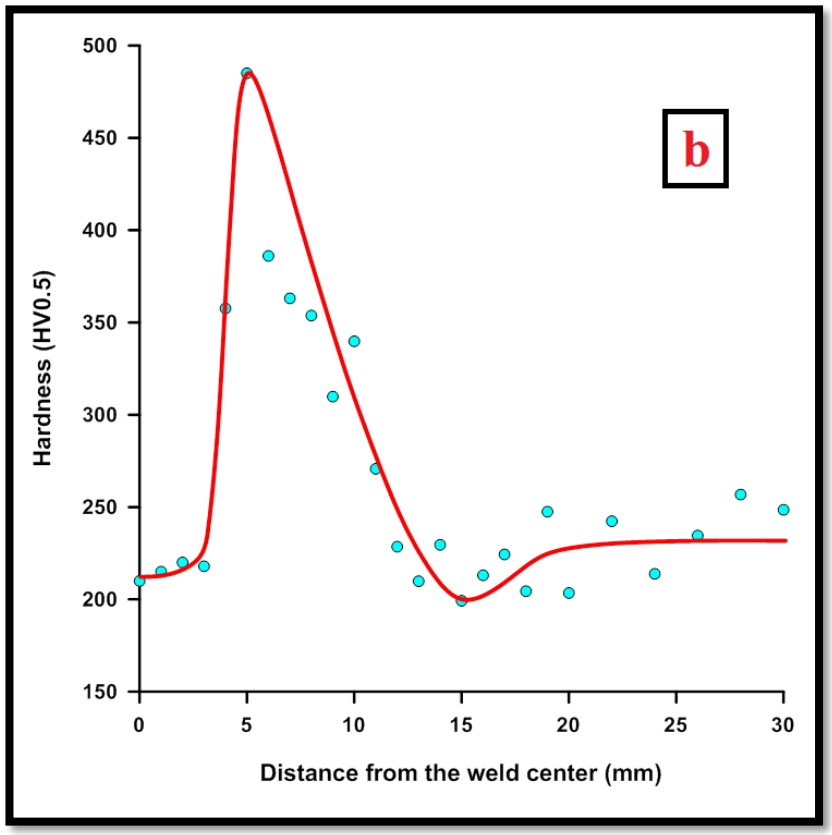
b
Hardness (HV0.5)
500
450
400
350
300
250
200
150
0
5
10
15
20
25
30
Distance from the weld center (mm)

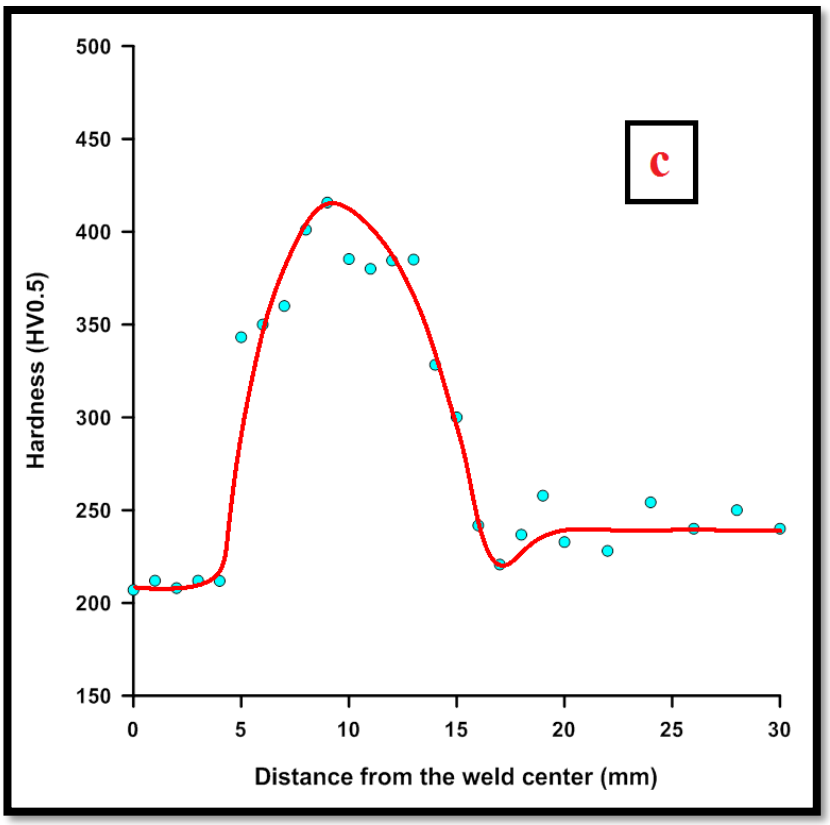
c
Hardness (HV0.5)
500
450
400
350
300
250
200
150
0
5
10
15
20
25
30
Distance from the weld center (mm)

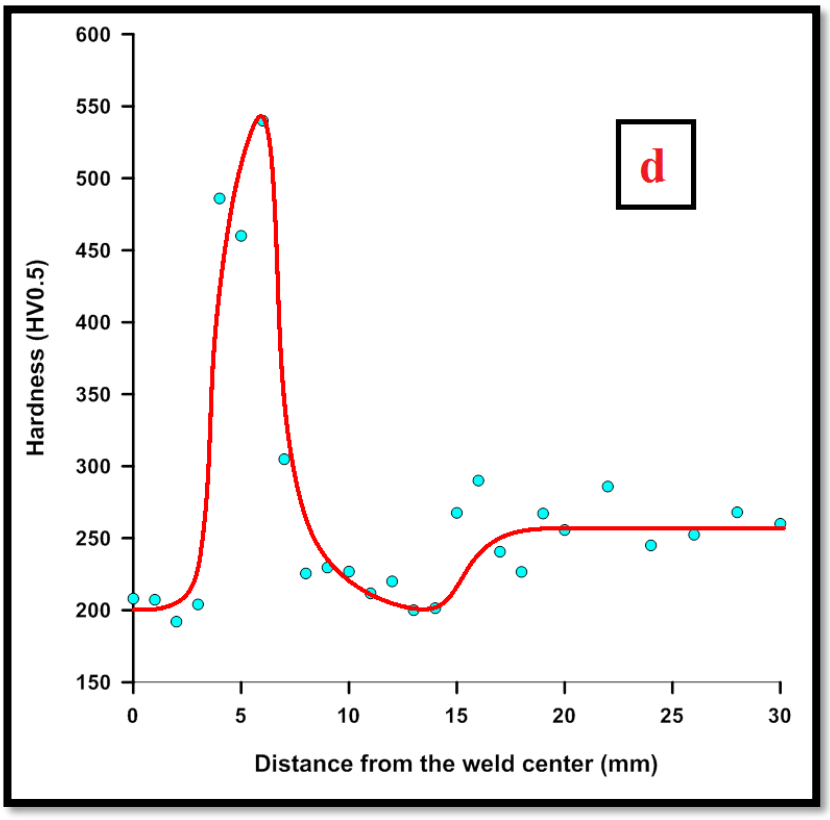
d
Hardness (HV0.5)
600
550
500
450
400
350
300
250
200
150
0
5
10
15
20
25
30
Distance from the weld center (mm)

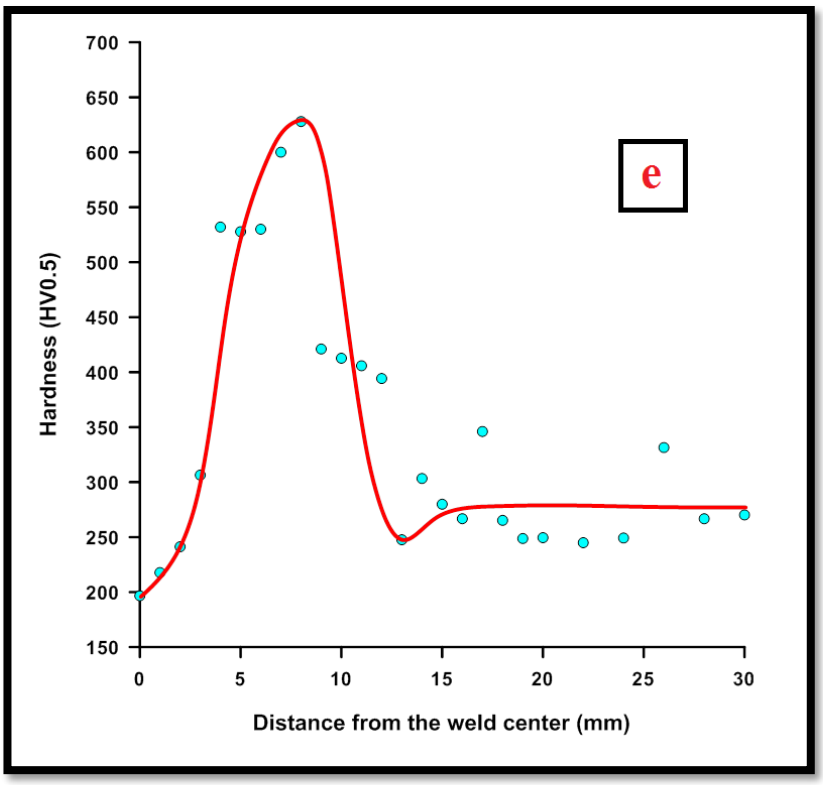

Figure (4.26): Hardness distribution across the welds. (a), (b), (c), (d) and (e) for weldments welded with different weight ratios (10, 20, 30, 40 and 50 % respectively) of Ni powder added to the flux.

It is observed from the Figure (4.26) that the hardness values at the weld center of these samples are slightly lower than that of the 1st sample. Figure (4.26a) shows that the hardness value at the weld center of the 2nd sample (~209 HV) was lower than that of the 1st sample due to the coarser structure of acicular ferrite (Figures 4.11 and 4.12). This might be attributed to the fact that the welding speed used with this sample was less than that used with the 1st sample (Table 3.7), which increases the amount of heat input and thus coarsens the structure. In the 3rd sample, the hardness value of the weld center (~213 HV) was slightly higher than that of the 2nd sample (Figure 4.26b). This could be attributed to the fact that an increase in the Ni ratio refines the acicular ferrite structure [74], which in turn increases the hardness values. Figure (4.26c) presents that the hardness value at the weld center of the 4th sample (~207 HV) was lower than that of the 3rd sample. There are two reasons behind this. The first one is the appearance of Ni structure at the

expense of the proportion of acicular ferrite and pearlite colonies (Figure 4.14); the hardness of nickel, predominantly deposited in the weld puddle, is less than the hardness of steels [87]. The second reason is that the welding speed has been fixed in this sample with increasing the value of the welding current to smelt the relatively high proportion of Ni powder added in this weld. The heat input therefore increases and thus decreases the cooling rate which in turn decreases the hardness values. Despite the fact that an increase of the Ni content in the weld refines the acicular ferrite structure [74], the hardness values in the weld center of the 5th and 6th samples notably decreased (~202 HV and ~197 HV respectively) as shown in figures (4.26d and 4.26e respectively). This could be attributed to that the structure in the weld center of these samples was predominantly Ni, even the structure of the 6th sample generally appeared to be only austenitic (Figures 4.16 and 4.18 respectively). Increasing the nickel content in the weld zone to a relatively large extent definitely increases the ductility of the weld metal and consequently decreases the hardness values.

The Figure (4.26a) also shows that the average hardness value at the CGHAZ of the 2ndsample (~465 HV) was lower than that of the 1st sample due to the apparent microstructures (primary troostite and small amount of upper bianite) in this sample (Figure 4.19) have lower hardness values than that appeared in the 1st sample. This is because the cooling rate in the 2nd sample was slower. The average hardness value at the same region for the 3rd sample (~485 HV) was higher than that of the 2nd sample (Figure 4.26b). The reason behind this is that the upper bianite and martensite structures appeared in this sample were more than that appeared in the 2nd sample (Figure 4.20) as a result of the faster cooling rate accompanied with the higher welding speed used with this sample. In the 4th sample, the figure (4.26c) shows that the hardness value at the CGHAZ (~416 HV) was much lower than that of the 3rd sample because of the upper bianite structure increased at the expense of

martensite (Figure 4.21). This could be attributed to a relatively low cooling rate compared to that of the 3rd sample as mentioned previously. For the same reason, the extension of the HAZ in this sample was more. The average hardness values in the same region of the 5th and 6th samples notably increased (~540 HV and ~628 HV) as shown in figures (4.26d and 4.26e respectively) because the martensitic structure increased significantly at the expense of the upper bianite structure (Figures 4.22 and 4.23 respectively), even the structure of this region in the 6th sample appeared to be almost fully martensitic. The reason behind this is that cooling rates were higher than that in the 4th sample due to the significantly increased welding speed for these two samples with the use of the same current value.

The minimum hardness across all the welds was observed in the inter-critical zone, where the pearlite was partially spheroidized (Figure 4.9) up to the hardness of the parent metal.

4.7 Fractography Examination

The visual inspection that included photographing the tensile specimens after fracture showed that the fracture in the first weld specimens (with no nickel added to the weld) was almost brittle (Figure 4.27a). The fracture behavior changed from brittle to ductile as a result of adding nickel powder to the flux with different weight percentages (Figure 4.27b-f).

Depending on the X-ray radiography, the tensile test specimens were extracted from regions free of defects such as porosity, cracks and/or slag inclusions.

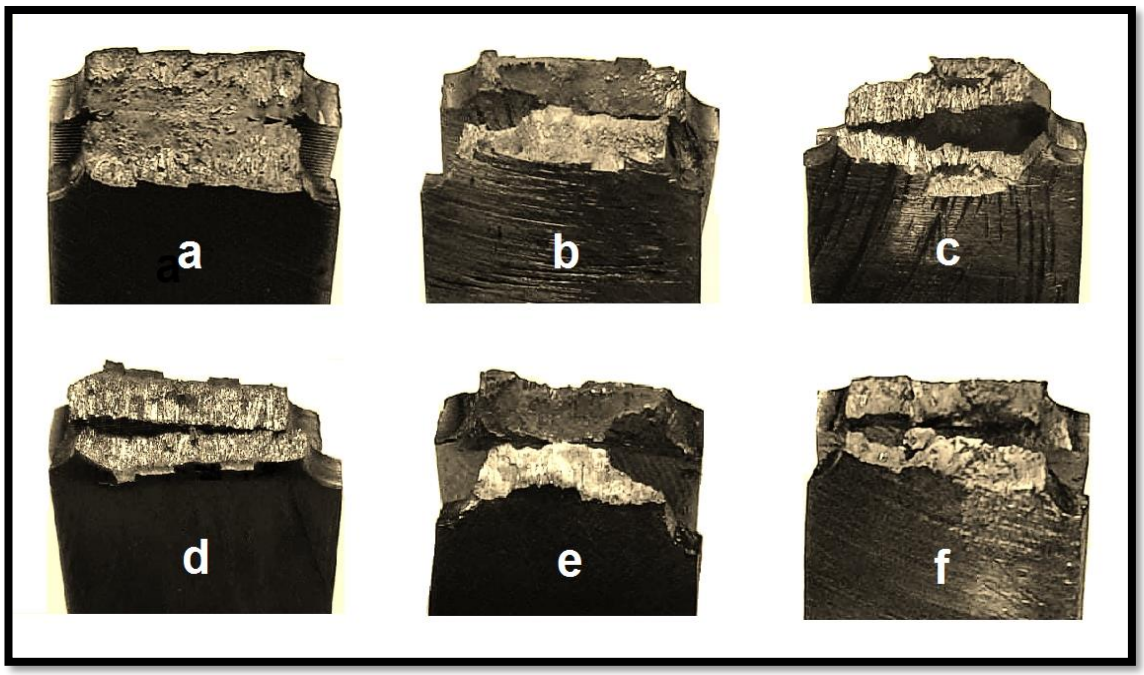

Figure (4.27): Tensile test specimens' visually inspected and photographed after fracture: (a) for submerged arc low alloy steel weld with no nickel powder added to the flux, (b), (c), (d), (e) and (f) for submerged arc low alloy steel welds with adding nickel powder of different wt.% (10, 20, 30, 40 and 50) respectively.

4.8 Tensile Test

The tensile test specimens were manufactured so that the weld center is in the mid of the specimen. One of the most important objectives of this study is to specify the tensile strength of the weld zones. To ensure that the fracture occurs in these zones, all test specimens were notched in the weld zone with a radius of 2.5 mm. Table (4.1) illustrates the average tensile strength of the submerged arc low alloy steel welds joined with and without nickel added to the flux. Since all tensile specimens were fractured from the weld zone, the tensile strength values illustrated in the tables (4.1) represent those of the weld metals. On the other hand, the tensile test result of the parent metal specimens was (754 MPa). Thus, the weld joint efficiency could be calculated for each weldment by using the following relationship [6]:

$$\textit{Weld joint efficiency (\%)} = \frac{\textit{Weld metal tensile strength}}{\textit{Base metal tensile strength}} * 100 \ldots\ldots\ldots \textbf{Eq. (2)}$$

Table (4.1): Average tensile strength and joint efficiency for the AISI-5147 steel welds.

Welding by the use of the	EM12K solid wire combined with the F7A5 powder flux	EM12K wire combined with mixed of F7A5 flux and pure Ni powder of percentages (%)				
		10	20	30	40	50
Average tensile strength (MPa)	697.4	823.6	844.6	423	582.6	603.8
Weld joint efficiency (%)	92.5	109.2	112	56.1	77.3	80.1

It is clearly noted from Table (4.1) that the average tensile strength of the submerged arc AISI-5147 steel weld with no nickel added to the flux was (697.4 MPa). This value is much more than the typical tensile strength of the weld metal aforementioned in Tables (3.4 and 3.5). Table (4.1) shows also that the efficiency of this weld joint is (92.5 %). The removal of oxides, rust, moisture, grease, oils and other contaminants from the surfaces of the steel plates being welded, in addition to appropriate fitting-up might be reasons for obtaining these high values. Pure nickel powder in different wt. % of (10, 20, 30, 40 and 50) was mixed with the F7A5 powder flux to be used in the SAW of AISI-5147 steel plates. The reason for these additives is that nickel is a ductile metal that may improve ductility and reduce brittleness of the weld metal and thus reducing the possibility of hot cracking while welding these types of steels [67]. Table (4.1) presents that the greatest tensile strength of the weld metals was (844.6 MPa) which is that of the weld metal deposited with the addition of 20 wt. % of nickel powder to the flux. The joint efficiency of this weld also reached (112 %).

The improvement in tensile strengths and thus weld joint efficiencies due to nickel additives could however be attributed to the grain size refinement. Nickel element may also inhibit the formation of brittle micro-constituents segregated at the grain boundaries in the weld zone [67]. The high ductility

of the Ni-based weld zone can play a crucial role in absorbing tensile stresses that initiate during welding. These can contribute to reducing susceptibility of the weld zone to hot cracks. In addition, the Ni-based weld zone has a greater affinity for sulfur and phosphorus. These can therefore enhance the weld zone's resistance to hot cracking [5], and thus improving tensile strengths. Moreover, the presence of slag inclusions and cracks in the weld zone might play a significant role in decreasing the tensile strength values of the welds (Figure 4.1). Increasing the nickel content in the weld zone to a relatively large extent increases the ductility of the weld metal to a great extent too, resulting in a decrease in the yield and tensile strengths of the weld zone. This was evident in the fracture region of the fifth and sixth welds, where a large elongation occurred in the weld zone prior the fracture (Figure 4.27e and f respectively).

In comparison with another study [77], despite the fact that it was on the ASTM A36 mild steel as a parent metal, there was good agreement in broad trend with the results of this study. The best tensile strength was as a result of adding 20% weight ratio of nickel powder to the flux. The tensile strength of the weld metal was more than that of the parent metal as well, and the weld joint efficiency was very close (115%).

CHAPTER FIVE:

CONCLUSIONS & RECOMMENDATIONS

CHAPTER FIVE: CONCLUSIONS & RECOMMENDATIONS

5.1 Conclusions

The most important results of this research can be concluded as follows:

1. The highest values of average tensile strength and weld joint efficiency were (845 MPa) and (112 %) respectively for the weld joined by adding 20 wt. % of nickel powder to the flux (2.65 wt.% Ni deposited in the weld), where the microstructure was a fine acicular ferrite.

2. The maximum hardness across the welds was at the CGHAZ, where the microstructure varied among lamellar pearlite, troostitic pearlite, bianite and/or martensite.

3. The minimum hardness was observed in the inter-critical zone, where the pearlite was partially spheroidized.

4. The hardness of the weld center generally decreased with increasing the Ni content in the weld.

5. With an increase of Ni content in the weld, fractography showed that the fracture behavior changed from brittle to ductile.

6. Microscopy and X-ray radiography showed that the greater the wt.% of Ni powder added to the flux, the more porosity and inclusions (with associated cracks sometimes) defects.

5.2 Recommendations

Lessons learned from this study can be taken into account in studies on welding of other steel grades, and some fields covered in this study can be further improved. The following is a summary of recommendations for further work.

1. The impact toughness test can be carried out for low alloy steel welds.

2. Other welding processes which use shielding gases such as the MIG and TIG can be used with filler wires having different Ni contents to add the Ni element to the weld.

3. The flux-cored arc welding process with metal-cored wires having different weight ratios of Ni powder could be used to add Ni to the weld.

References

1. Purohit R. K. (2005), *Material Science and Processes*, Scientific Publishers Journals Dept., INDIA.
2. Hashmi M. S. J. (2017), *Comprehensive Materials Finishing: Finish Machining and Net-shape Forming*, Vol 1, IRELAND.
3. Timings R. (2008), *Fabrication and Welding Engineering*, Elsevier Ltd, Hungary.
4. Higgins R. A. and Bolton W. (2010), *Materials for Engineers and Technicians*, 5th ed. UK.
5. Talib H. M. (2020), *Investigating the Effect of Nickel Content on Low Alloy High Strength Steel Welds*, M.sc Dissertation, Metallurgical Engineering-Babylon University.
6. Khanna O. P. (1980), *Welding Technology: A textbook for Engineering Students*, Dhanpat Rai and Sons, 1st ed, Delhi.
7. Weman K. and Liber AB (2012), *welding processes handbook*, 2nd ed., Stockholm.
8. د. عبد السميع جاسم عبد الزهرة (2000) *السيطرة على عيوب و تشوهات لحام الصلب الكاربوني*، رسالة ماجستير، كلية هندسة المواد جامعة بابل.
9. Colas R. and Totten G. E. (2016), *Encyclopedia of Iron, Steel, and Their Alloys*, Vol 1, CRC press.
10. Totten G. E. (2006), *Steel heat treatment: metallurgy and technologies*, CRC press.
11. Steels L. A. (2001), *High-Strength Low-Alloy Steels*.
12. Tuttle R. (2018), *Alloy Steels*, 1st ed., Saginaw Valley State University, USA.
13. Avner S. H. (1974), *Introduction to physical metallurgy*, Vol. 2, pp.481-497, New York: McGraw-Hill.
14. Tisza M. (2001), *Physical Metallurgy for Engineers*, ASM International and Freund Publishing House Ltd.
15. SINGH B., KHAN Z. A., SIDDIQUEE A. N., MAHESWARI S. and SHARMA S. K. (2016), *Effect of Flux Composition on the Percentage Elongation and Tensile Strength of Welds in Submerged Arc Welding*, New Delhi, India.
16. Creese R. C. (1999), *Introduction to Manufacturing Processes and Materials*, CRC Press.
17. Kumara V., Mohanb N. and Khambaa J. S. (2009), *development of agglomerated acidic flux for submerged arc welding*, Production

Engineering Faculty, Punjab Engineering College, 160012 Chandigarh, India.
18. Singh J., Singh C. D. and Sing R. (2018), *Influence of welding parameters on bead geometry in SAW*.
19. Murugan N. and Gunaraj V. (2005), *Prediction and control of weld bead geometry and shape relationships in submerged arc welding of pipes*, Journal of Materials Processing Technology,168(3):478–487.
20. Kiran D. V. and Joona S. (2014), *Experimental Studies on Submerged Arc Welding Process*, Journal of Welding and Joining (Vol. 32, No. 3).
21. Vendan S. A, Gao L. , Garg A. , Kavitha P. , Dhivyasri G. and Rahul SG (2019), *Interdisciplinary Treatment to Arc Welding Power Source*, Springer Nature Singapore, Pte, Ltd.
22. Svensson L. E. (1994), *Control of Microstructures and Properties in Steel Arc Welds*, Esab AB, Gothenburg, Sweden, CRC Press.
23. Narayana K. L., Rmana S. V. and Krishna P. V. (2010), *Production Technology*, 2nd ed., I.K. International Publishing House Pvt. Ltd.
24. Radhakrishnan V. M. (2008), *Welding Technology and Design*, New Age International Pvt. Ltd. Publishers.
25. Layus P. (2017), *Usability of the Submerged Arc Welding (SAW) Process for Thick High Strength Steel Plates for Arctic Shipbuilding Application*, PhD Thesis, Lappeenranta University of Technology.
26. Jeffus L. and Bower L. (2010), *Welding Skills, Processes and Practices for Entry-Level Welders*, 1st ed, Cengage Learning.
27. Gil O. (2016), *Welding Engineering*, Research World, New York.
28. KOBELCO (2015), *Arc Welding of Specific Steels and Cast Irons*, Kobe steel ltd.
29. Lippold J. C. (2015), *Welding Metallurgy and Weldability*, John Wiley & Sons, Inc.
30. American Welding Society (AWS) (2007), *Specification for Low-Alloy Steel Electrodes and Fluxes for Submerged Arc Welding*, 5th ed.
31. ESAB (2001), *Submerged Arc Welding*, Product catalog.
32. ESAB (2001), *Welding Handbook*, Consumable for manual and automatic welding, 6th ed.
33. KAUSHISH J. P. (2010), *MANUFACTURING PROCESSES*, 2nd ed., PHI Learning Private Limited, New Delhi.
34. Gandy D. (2007), *Carbon Steel Handbook*, EPRI Project Manager.
35. Mandal S. K. (2014), *Steel Metallurgy*, McGraw-Hill Education(India) Private Limited.

36. Talas S. (2010), *The assessment of carbon equivalent formulas in predicting the properties of steel weld metals*, Kocatepe University, Technical Education Faculty, Afyonkarahisar, Turkey. Elsevier Ltd.
37. Jeffus L. (2011), *Metal Fabrication Technology for Agriculture*, 2nd ed., Cengage Learning.
38. Rajput R. K. (2005), *Comprehensive Workshop Practice*, LAXMI PUBLICATIONS(P)LTD, New Delhi.
39. Gizejowski M. A., Marcinowski J., Kozlowski A. and Ziółko J. (2016), *Recent Progress in Steel and Composite Structures*, CRC Press.
40. Swift P. and Murray J. (2009), *Welding, FCS L3*, Person Education, South Africa.
41. KOBELCO (2015), *The ABC's of Arc Welding and Inspecsion*, Kobe Steel Ltd.
42. Kuppan T. (2000), *Heat Exchanger Design Handbook*, Marcel Dekker, Inc.
43. Kim I. S., Son J. S., Park C. E., Kim I. J. and Kim H. H. (2005), *An investigation into an intelligent system for predicting bead geometry in GMA welding process*, Journal of Materials Processing Technology,159(1), 113-118.
44. د.قحطان خلف الخزرجي و عبد الجواد محمد محمد احمد الشريف (1988)، *تكنلوجيا اللحام*، جامعة بغداد.
45. Baily F. W. J (1972), *Fundamentals of engineering metallurgy and Materials*, 5th ed. London.
46. Lancaster J. F. (1980), *Metallurgy of Welding*, 3rd ed. (Allen and Unwin, London UK).
47. Jefferson, T. B., & Woods, G. (1966), *Metals and How to Weld Them*, James F. Lincoln Arc Welding Foundation 2nd ed., Cleveland.
48. Technical committee, Indian institute of Welding, Bangalore branch. (Dec., 1977) *Welding Metallurgy, technology and quality assurance*, Venue: Bangalore.
49. Amani J. (2011), *Effect of Submerged Arc Welding Parameters on the Microstructure of SA516 and A709 Steel Welds*.
50. د. عبد الرزاق اسماعيل خضر و د.نوفل محمد حسين (1993)، *تكنولوجيا اللحام*، الجامعة التكنولوجية.
51. Houldcroft P T and John R (2004), *Welding and Cutting: A Guide to Fusion Welding and Associated Cutting Processes*, Woodhead Publishing Limited.
52. Bohnart E. R. (2017), *Welding Principles and Practices*, McGraw-Hill Education.
53. Gray, T. G. F. and Spence, J (1982), *Rational welding design*, Butterworth-Heinemann.

54. Boyer H. E. (1975), Metal Handbook, *Failure Analysis and Prevention*, 8th ed., American society for metals.
55. ASM, Metals Handbook (1975), *Welding and Brazing*, 8th ed.
56. Sacks R. J. (1981), *Welding, principles and practices*.
57. Burgess, N. T. (Ed.) (1989), *Quality assurance of welded construction*, 2nd ed., CRC Press.
58. Kou S. (2002), *Welding Metallurgy*, 2nd ed., John Wiley and Sons, Inc.
59. Zhang Y. (2008), *Real-Time Weld Process Monitoring*, Woodhead Publishing Limited and CRC Press LLC.
60. SYAMAL M. (2011), *Metal Fabrication Technology*, PHI Learning Private Limited, New Delhi.
61. Singh R. (2009), *Weld Cracking in Ferrous Alloys*, Woodhead Publishing Limited and CRC Press LLC.
62. Jeffus L. (2015), *Welding: Principals and Application*, 8th ed., Cengage Learning.
63. Bolton W. and Higgins R.A. (2015), *Materials for Engineers and Technicians*. 6th ed., Taylor & Francis Group.
64. Rampaul H. (2003), *Pipe Welding Procedure*, 2nd ed., Industrial Press, New York.
65. Bhandari V. B. (2013), *Introduction to Machine Design*, 2nd ed., McGraw Hill Education (India) Private Limited, New Delhi.
66. د.عبدالواحد كاظم راجح (2016)، *الميتالورجيا الهندسية والمواد المتقدمة*، جامعة بابل.
67. Pascual M., Cembrero J., Salas F., and Martínez M. P (2008), *Analysis of the weldability of ductile iron*, Materials Letters, 62(8-9),1359-1362.
68. Setiyanto N. A., Oktadinata H. and Winarto W. (2019), *Effect of Nickel on the Microstructure, Hardness and Impact Toughness of SM570-TMC Weld Metals,* Department of Metallurgy and Materials Engineering, Universitas Indonesia, Indonesia.
69. Gülich J. F. (2010), *Centrifugal Pumps*. 2nd ed., Springer.
70. kang B. Y., KIM H. J. and HWANG S. K. (2000), *Effect of Mn and Ni on the Variation of the Microstructure and Mechanical Properties of Low-carbon Weld Metals,* Korea Institute of Industrial Technology, ChonAnSi, 330-825 Korea.
71. Eroglu M. and Aksoy M. (2002), *Effect of nickel on microstructure and mechanical properties of heat affected zone of low carbon steel*, Materials Science and Technology, 18:1, 35-40.
72. Bhole S. D., Nemade J. B., Collins L. and Liu Cheng (2006), *Effect of nickel and molybdenum additions on weld metal toughness in a submerged arc*

welded HSLA line-pipe steel, Elsevier, Journal of Materials Processing Technology 173, 92–100.

73. Trindade V. B., Payão J.D.C., Souza L.F.G. and Paranhos R.D.R. (2007), *The role of addition of Ni on the microstructure and mechanical behavior of C-Mn weld metals*, Exacta, São Paulo, v. 5, n. 1, p. 177-183.
74. Sham K. L. (2014), *Advanced Characterization Techniques in Understanding the Roles of Nickel in Enhancing Strength and Toughness of Submerged Arc Welding High Strength Low Alloy Steel Multiple Pass Welds in the As-welded Condition*, PhD Thesis, Metallurgical and Materials Engineering- Colorado School of Mines.
75. Sharma Er. K. (2014), *Enrichment of Flux by Nickel to Improve Impact Strength in Submerged Arc Welding*, IJITKM Special Issue (ICFTEM-2014) May 2014 pp. 238-244 (ISSN 0973-4414).
76. Lijun Y., Huichao W., Zhi Z., Jin Z., Xianqun M., Shiming H. and Qiuyi B. (2015), *Effect of Mn and Ni on Microstructure and Impact Toughness of Submerged Arc Weld Metals*, Tianjin University and Springer-Verlag Berlin Heidelberg.
77. Verma D., Garg M. and Sing R. P. (2015), *Effect of Performance Parameters with Different Flux Composition on Weld Bead Geometry During Submerged Arc Welding (SAW) of Steel*, IJESRT.
78. WU D., HAN X., TIAN H., LIAO B., and XIAO F. (2015), *Microstructural Characterization and Mechanical Properties Analysis of Weld Metals with Two Ni Contents During Post-Weld Heat Treatments*, The Minerals, Metals & Materials Society and ASM International.
79. Mei L., Zhang J., Huang Y., Yu Y., Jiang Y., Liu Q., Zhang X. and Gu Y. (2017), *Ivestigation on Deposited Metal Properties of Homemade Nickel & Nickel-free Electrodes and Fluxes for Submerged Arc Welding of SA-508 GR.3 CL.1*, ICONE25-66331.
80. Wang Z. Q., Wang X. L., Nana Y.R., Shang C. J., Wang X. M., Liu K. and Chen B. (2018), *Effect of Ni content on the microstructure and mechanical properties of weld metal with both-side submerged arc welding technique*, Elsevier, Inc.
81. Mao G., Cao R., Cayron C., Loge R., Guo X., Jiang Y. and Chen J. (2018), *Microstructural evolution and mechanical property development with nickel addition in low-carbon weld butt joints*, Journal of Materials Processing Technology.
82. Jilabi A. J. A. and Talib H. M. (2020), *Studying the effect of nickel on properties of low alloy high strength steel welds by using an economical technique*, Collage of Materials Engineering/University of Babylon.

83. http://bbnsteelplate.com/news/astm-a36-steel-equivalent-indian-standard-is-is2062_928.html.
84. https://www.esabna.com/us/en/education/blog/choosing-the-right-filler-metal-for-a513-hsla-70-steel.cfm.
85. Oerlikon Metco (2017), *Material Product Data Sheet.*
86. Khan M. I. (2007), *Welding science and technology*. New Age International.
87. Jordan L. and Swanger W. H. (1980), *The properties of pure nickel*, Bureau of standards. J Res. doi, 10, 6028.
88. Rajesh K. R. (2016), *Basics of Mechanical Engineering*, 2nd ed., Juthis Puplishers, India.
89. KAUSHISH J. P. (2010), *MANUFACTURING PROCESSES*, 2nd ed., PHI Learning Private Limiting, New Delhi.

ملخص البحث

يستخدم الفولاذ منخفض السبائكية بشكل بارز في تصنيع العديد من المنتجات الهندسية مثل صهاريج تخزين الوقود وخطوط أنابيب النفط والغاز والمعدات الصناعية والعديد من أجزاء الآلات الزراعية وآلات البناء التي قد تفشل اثناء الخدمة، مما قد يتطلب إصلاحها من خلال عمليات اللحام. ويعتبر لحام القوس الكهربائي المغمور أحد أكثر العمليات استخدامًا للحام الصناعات الهندسية المختلفة. ومع ذلك، يرافق لحام الفولاذ منخفض السبائكية بطريقة القوس الكهربائي المغمور بعض العيوب، كما تعتبر التشققات الساخنة عادة أكثر هذه العيوب أهمية وخطورة. ويتم تحديد قابلية اللحام للفولاذ من خلال قابلية تعرضه للتشققات والتي يمكن الحد منها باستخدام إجراءات لحام معينة، والتي غالبًا ما تكون مكلفة وصعبة الاستخدام. تم لحام الفولاذ منخفض السبائكية (AISI 5147) بطريقة القوس الكهربائي المغمور، أولاً بدون إضافات نيكلية، ثم بإضافة مسحوق نيكل نقي إلى الصهيرة بنسب وزنية مختلفة (10، 20، 30، 40 و 50٪). تهدف الدراسة أساسا إلى معرفة تأثير محتوى النيكل على خصائص ملحومات الفولاذ منخفض السبائكية بطريقة لحام القوس الكهربائي المغمور. كما تهدف أيضاً إلى دراسة تأثير النيكل في تقليل التشققات الساخنة في هذه الملحومات وبالتالي زيادة كفاءة وصلات اللحام. تم إجراء العديد من الفحوصات لتقييم الملحومات الناتجة بما في ذلك الفحص الشعاعي بالأشعة السينية وتصوير مناطق الكسر والفحص المجهري والفحص بمطياف تشتت الطاقة والاختبارات الميكانيكية. أظهرت النتائج أن مقاومة الشد وكفاءة وصلة اللحام بلـــغت (845 MPa) و (112٪) على التوالي للملحومة الناتجة عن إضافة مسحوق نيكل بنسبة وزنية مقدارها 20٪ الى الصهيرة، حيث كانت البنية المجهرية عبارة عن فرايت ابري دقيق. وكان الحد الأقصى للصلادة عبر اللحامات هي في منطقة النمو الحبيبي من المنطقة المتأثرة بالحرارة، بينما لوحظ الحد الأدنى للصلادة في المنطقة الحرجة، حيث تم تكوير البرلايت جزئيًا. كما بيّن الفحص

الشعاعي بالأشعة السينية والفحص المجهري أنه كلما زادت النسبة الوزنية لمسحوق النيكل المضاف إلى الصهيرة زادت عيوب الشوائب الدخيلة والمسامية، في حين أظهر تصوير مناطق الكسر أن سلوك الكسر يتغير من هش إلى مطيلي، حيث تبدو بنية مركز اللحام عمومًا وكأنها اوستنايتية فقط، وذلك في الملحومة الناتجة عن إضافة مسحوق نيكل بنسبة وزنية مقدارها 50٪ الى الصهيرة.

وزارة التعليم العالي والبحث العلمي
جـــــامـــعـــة بـــابـــــل
كـــلـــيـــة هـــنـــدســة الـمـواد
قـسـم هـــنـــدســة الـــمـعـادن

تأثير إضافات النيكل على صهيرة ملحومات الصلب AISI 5147 بالقوس الكهربائي المغمور

رسالة مقدمة إلى

قسم هندسة المعادن في كلية هندسة المواد/جامعة بابل وهي
جزء من متطلبات نيل شهادة الماجستير في هندسة المواد/هندسة المعادن

من قبل

دعاء كامل يوسف حمادي

بإشـــــراف

أ.م. د .عبد السميع جاسم عبد الزهرة الكلابي

1442 هـ 2021 م